DISS. ETH NO. 25495

MICROFLUIDIC STRATEGIES FOR STUDYING COMMUNICATION BETWEEN CELLS AND TISSUES

A thesis submitted to attain the degree of
DOCTOR OF SCIENCES of ETH ZURICH
(Dr. sc. ETH Zurich)
presented by

ALICIA JANE KÄSTLI

M.Sc. Biotechnology, ETH Zurich
B.Sc. Biological Engineering, Massachusetts Institute of Technology

born on 25.09.1989
citizen of
St. Margrethen/SG & United States of America

accepted on the recommendation of
Prof. Andreas Hierlemann
Prof. Timm Schroeder
Dr. Olivier Frey

2018

Table of Contents

Abstract

Understanding communication between cells and tissues is critical for treating human diseases, as communication is key for a coordinated response of many single cells into a population-wide response. Oscillations of signaling molecules, known as cytokines, can transform a heterogeneous population into an entrained population with the goal of, for example, organizing the response of the immune system against an infection. Further, including communication in multi-tissue models is critical in accurately predicting the pharmacokinetics and pharmacodynamics of drugs in patients. Multi-tissue models are needed to better understand how a drug interacts with a patient, from absorption into the body and hepatic activation into a drug's active form, until a drug's final excretion from the patient's body.

Microfluidics is a powerful technology that can be used to gain a better understanding of communication dynamics at the scale of single cells and up to microtissues. In this thesis, two types of microfluidics technology were used for studying communication between small populations of cells and microtissues: (1) valve-based microfluidics with high spatiotemporal resolution, and (2) tilting-based microfluidics with easy-to-use hardware. The objective of each platform is described below:

1. *Interrogation of cytokine secretion dynamics:* The goal of this platform was to understand how immune cells respond to dynamic inputs. A valve-based microfluidic platform was designed that can be used to automatically (1) pattern an immunoassay, (2) culture cells, and (3) expose and measure the response of cells to dynamic inputs. This is the first microfluidic platform developed with the ability to integrate these three tasks inside of the same chip. As a proof of concept experiment, the device was used to measure how a macrophage cell line responses to a dynamic stimulus of lipopolysaccharide (LPS) by quantifying transcription factor NF-κB activity and cytokine TNF secretion. The chip was able to confirm previous findings that a high stimulus of LPS results in a single peak in both NF-κB activity and TNF secretion.
2. *Prediction of drug efficacy on patient-derived samples:* A tilting-based microfluidic "leukemia-on-a-chip" device was developed with the objective of measuring the effect of both, standard drugs and prodrugs, the latter of which require hepatic bio-activation, on patient-derived leukemia samples. A key component of the leukemia-on-a-chip platform is a metabolic compartment to culture liver microtissues. In contrast to standard well plate experimental setups lacking a metabolic compartment, the

leukemia-on-a-chip platform was able to measure the effect of a prodrug on patient derived leukemia samples. The simplicity of the leukemia-on-a-chip devices gives it the potential to be used directly in the clinic to advise treatment decisions.

The overarching goal of both platforms was to improve patient outcomes in the clinic. For instance, the cytokine secretion dynamics platform can be used to screen the potential of novel drugs to cause cytokine storms, characterized by uncontrolled cytokine secretion, which can result in organ failure, and, in some cases, death. Further, the objective of the leukemia-on-a-chip device is to predict the efficacy of prodrugs in high-risk leukemia patients. Increased throughput is critical for transforming each device from a proof-of-concept platform into a platform that can be used to advise clinical decisions. Through increased throughput, the devices will be able to achieve increased statistical confidence needed to inform decisions and make a patient-specific impact in the clinic.

Zusammenfassung

Das Verständnis von Zell- und Gewebe-Kommunikation ist für die Erforschung neuer Therapieansätze gegen menschliche Krankheiten von grosser Bedeutung. Die Kommunikation zwischen Einzelzellen ist grundlegend für die Entwicklung einer koordinierten Reaktion. Oszillationen von Signalmolekülen - sogenannten Zytokinen - können eine heterogene Zellpopulation in eine koordinierte Zellgruppe umwandeln, welche die Reaktion des Immunsystems auf eine Infektion organisiert. Darüberhinaus ist die Erforschung der Kommunikation zwischen mehreren Gewebemodellen (multi-tissue models) von entscheidender Bedeutung für die genaue Vorhersage der Pharmakokinetik und -dynamik von Arzneimitteln. Modelle mit mehreren implementierten Geweben sind notwendig, um besser zu verstehen, wie ein Medikament mit einem Organismus interagiert, von der Aufnahme in den Körper, über eine mögliche hepatische Aktivierung in eine aktive Form bis hin zur endgültigen Ausscheidung.

Die Mikrofluidik ist eine leistungsfähige Technologie, welche für die Erforschung der Kommunikation auf Einzelzell- und Mikrogewebe-Ebene eingesetzt werden kann. In dieser Dissertation werden zwei Arten von Mikrofluidik-Plattformen für die Untersuchung dieser Kommunikation verwendet: (1) Ventilbasierte Mikrofluidik, welche eine hohe räumlich-zeitliche Auflösung aufweist und (2) Kippbasierte Mikrofluidik, die sich durch ihre einfach zu bedienende Hardware auszeichnet. Die Ziele der einzelnen Plattformen werden im Folgenden beschrieben:

1. *Untersuchung der Sekretionsdynamik von Zytokinen*: Ziel dieser Plattform ist es, die Antwort von Immunzellen auf dynamische Inputs zu erforschen. Es wurde eine ventilbasierte Mikrofluidik-Plattform entwickelt, mit der automatisiert (1) ein Immun-Assay erstellt werden kann, (2) Zellen kultiviert, und (3) die Zellen gegenüber dynamischen Inputs exponiert und deren Antwort gemessen werden können. Es handelt sich hierbei um die erste entwickelte Mikrofluidik-Plattform, welche diese drei Aufgaben in einem System integriert. Im Rahmen einer Machbarkeitsstudie wurde die Antwort von Makrophagen auf dynamische Stimulationen durch Lipopolysaccharid (LPS) untersucht. Dabei wurde die Aktivität des Transkriptionsfaktors NF-κB und die Sekretion des Zytokins TNF quantifiziert. Die Plattform wurde ferner dazu verwendet, frühere experimentelle

Studien zu bestätigen, welche aufzeigten, dass ein hoher LPS-Stimulus sowohl zur Erhöhung der NF-κB-Aktivität als auch der TNF-Sekretion führt.

2. *Untersuchung der Arzneimittelwirksamkeit an Patientenproben*: Eine kippbasierte Mikrofluidikplattform - genannt "Leukemia-on-a-chip" - wurde entwickelt, um die Wirkung von Standardmedikamenten und Medikamentenvorläufer-substanzen, bei welchen eine hepatische Bioaktivierung erforderlich ist, mit Leukämieproben von Patienten zu testen. Eine Schlüsselkomponente der entwickelten Mikrofluidikplattform ist dabei eine Kammer, welche die Kultivierung von Lebermikrogeweben ermöglicht. Im Gegensatz zu herkömmlichen, statischen Ansätzen ohne Stoffwechselkompartiment, konnte mit der "Leukemia-on-a-chip"-Plattform die Wirkung einer Medikamentenvorläufersubstanz auf Leukämie-Proben gemessen werden. Durch die Einfachheit und Benutzerfreundlichkeit hat diese Technologie zudem das Potential, direkt in ein klinisches Labor integriert zu werden und bei klinischen Therapieentscheidungen eine Rolle zu spielen.

Übergeordnetes Ziel beider Plattformen ist letztlich den Erfolg ärztlicher Behandlungen zu verbessern. So kann beispielsweise mit der Plattform zur Untersuchung der Sekretionsdynamik von Zytokinen das Potential neuartiger Medikamente untersucht werden, welche einen Zytokinsturm auslösen können, der sich durch eine unkontrollierte Zytokinsekretion auszeichnet. Diese Arzneimittelnebenwirkung kann zu Multi-organversagen und in einigen Fällen zum Tode führen. Darüberhinaus war es das Ziel des "Leukemia-on-a-chip"-Projekts die Wirksamkeit von Medikamentenvorläufersubstanzen bei Hochrisikopatienten mit Leukämie vorherzusagen.

Die Erhöhung des Durchsatzes ist entscheidend für die Weiterentwicklung beider Plattformen von Machbarkeitsstudien zu Geräten, die zu klinischen Entscheidungen beitragen können. Durch eine Erhöhung des Durchsatzes können die mit den Plattformen gewonnene Messdaten eine höhere statistische Sicherheit erreichen, welche für Therapieentscheidungen für individuelle Patienten in der Klinik erforderlich ist.

1 Introduction

Communication is critical for coordinating complex activity between single cells and tissues. In a healthy patient, communication through dynamic cytokine secretion gradients is key for both, directing immune cells to the site of infection and synchronizing the immune response among many heterogeneous single cells[1–3]. On a larger scale, interactions between different tissue types are essential for predicting a drug's efficacy in patients. Modeling a patient-specific drug response requires knowledge of the absorption of the compound into the body (e.g., through the gastrointestinal tract), the distribution of the drug (e.g., via blood flow), the metabolism of the drug (e.g., oxidation through liver enzymes), elimination of the drug (e.g. through the kidney), and lastly knowledge of any tissue-specific drug toxicity[4].

Miscommunication between single cells or organs can be fatal. For instance, uncontrolled overproduction of cytokines can lead to a cytokine storm, whereby there is massive activation of immune cells that further leads to the production of cytokines in a positive feedback mechanism[5]. Moreover, incorrect modeling of a patient's specific liver metabolic activity can lead to an unintentional drug overdose[6]. Consequently, it is important understand what are the healthy levels of cell and tissue communication in patients, and how to bring a disrupted system back to healthy levels.

In order to study communication at single-cell up to multi-organ level, a modular technology is needed that has the potential to integrate sensors to measure various communication parameters and related signaling-molecule concentrations. Microfluidics fits this requirement and has been successfully used over the past 20 years to construct devices for studying both, single-cell and multi-tissue interactions[4]. In this thesis, two different types of microfluidic devices were developed in order to understand (1) how populations of immune cells respond to dynamic stimuli, and (2) how patient-derived tissue samples respond to real-time metabolized drugs.

1.1 INTRODUCTION TO TYPES OF BIOLOGICAL COMMUNICATION

1.1.1 Communication between single cells

Cellular communication is critical in order to maintain healthy homeostasis in the human body. Communication occurs through the diffusion of signaling molecules between cells[7]. Between single cells, two major forms of communication exist: (1) autocrine signaling, by which a cell releases signaling molecules that bind to a receptor on the same cell, and (2) paracrine signaling, by which a cell releases signaling molecules that bind to a receptor on a different cell[7]. In both types of signaling, the binding of a signaling molecule to a cell can stimulate a response, such as the up-or down-regulation of signaling pathways. In the immune system, tight control of communication is essential. Healthy immune cell communication results in the directed migration of immune cells. For instance, waves of cytokine secretion across a tissue are hypothesized to coordinate the movement of neutrophils towards the site of infection[1]. Simultaneously, neutrophils direct $CD8^+$ T cells to the site of infection through a "bread crumb" strategy of leaving small pieces of CXCL12 cytokine-enriched membranes behind during migration[2]. Inadequate communication dynamics in the immune system can cause adverse health conditions, such as autoimmune diseases and cytokine storms. In autoimmune diseases, such as multiple sclerosis and rheumatoid arthritis, one of the pathology mechanics is the false identification of innate molecules as foreign. This can subsequently lead to auto-inflammation, whereby neutrophils accumulate locally[1]. In a cytokine storm, the massive release of cytokines results in a life-threatening level of inflammation[5]. Clearly, cellular communication is essential in maintaining a robust immune system.

1.1.2 Communication between tissues

Communication between tissues is also critical for maintaining a healthy homeostasis. For example, coordinated interaction between the liver, pancreas, muscle, and fat through endocrine hormones is important for maintaining stable glucose levels[8]. Additionally, communication between the liver, bloodstream, and a solid tumor is important in modeling the response of the tumor to prodrugs[9]. Prodrugs are drugs that require biotransformation into an active state by liver enzymes in order to maximize efficacy against a target[6]. Biotransformation of prodrugs is typically executed by cytochrome P450 (CYP) enzymes[6]. However, there is high variability in CYP activity in the population. This high variability can result in a drug being undermetabolized, and thus underdosed and inefficacious in one patient population, and the same drug being excessively metabolized, and thus toxically overdosed in a different patient

population[6]. Clearly, correct communication between tissues is essential for an efficacious response to prodrugs.

In order to study drug interactions in a clinically-relevant system, adsorption, distribution, metabolism, elimination and toxicity (ADMET) should be modeled. When studying ADMET processes, it is important to include liver tissue to model both the metabolism and elimination of various pharmaceutical compounds[4]. For instance, in cancer treatment, epipodophyllotoxins and cyclophosphamide are prodrugs that require CYP450 enzyme activation; whereas, glucocorticoids and vincristine require CYP450 enzyme inactivation. As a result, multi-tissue systems are important for physiological *in vitro* modeling of complex clinical diseases, such as cancer.

1.1.2.1 Improved in vitro systems are needed for studying multitissue interactions

There is currently great interest in developing improved multi-tissue *in vitro* systems in order to better model human physiology without using animal models[4,9]. The current approach to predict and investigate potential compounds and therapies includes animal studies and 2D *in vitro* assays with the cell types of interest. It is known that simple cell-line based *in vitro* assays do not fully represent the situation in the body because they (1) mostly lack organotypic physiology, (2) often are not suitable for long term culture and (3) lack the level of complexity to model drug-tissue-immune system interactions[10–12]. Laboratory animal studies, on the other hand, may not be applicable due to lack of cross-reactivity of highly specific antibody drugs and, in case that surrogate markers, specific for a given pre-clinical species, are designed, often show significantly altered immune responses compared to humans, which renders the interpretation and translation of data difficult[13]. Therefore, more predictive human cell culture systems are needed, including organotypic cell systems in a realistic physiological environment. These sophisticated *in vitro* systems will also provide an alternative to animal testing, which is in accordance with efforts to reduce, refine or replace animal experimentation in the near future (3R)[14].

1.2 INTRODUCTION TO MICROFLUIDICS

Microfluidics is a powerful technology that can be used to study cellular systems at various spatiotemporal scales[15,16]. Microfluidic technology is based on the precise movement of fluidics through small channels with dimensions on the order of micrometers to millimeters[17,18]. The key to the high predictability of fluid flow through a microfluidic system is its low Reynolds number[18]. The Reynolds number is a dimensionless number that relates inertial forces to viscous forces[4,18]. When a Reynolds number is low, it indicates that the viscous forces dominate fluid flow, and, as a result, fluid flow is laminar[18]. Laminar flow is achieved typically when a channel diameter is less than 1 mm[4]. With laminar flow, well-defined physical and chemical gradients can be established in microfluidic chips[4,15,16]. For instance, it is possible to expose cells to oscillating concentrations of signaling molecules[19], or to direct migration of immune cells through the establishment of a static gradient[15,16,20]. Exposing cells to well-defined signals is increasingly important, as it was found that immune cells can become entrained in response to oscillating concentrations of signaling molecules[3]. Another key feature of microfluidic devices is their low volume. Typical chambers in microfluidic devices are about 1 nL[4]. The small volume of microfluidic devices permits the use of less reagents than required for standard biochemical assays, while also increasing the sensitivity of included biosensing devices[4,18,21,22] Lastly, microfluidic devices are commonly produced via soft-lithography from poly-dimethylsiloxane (PDMS)[4,17,23]. The major advantages of PDMS microfluidic devices are the ability to rapidly and affordably iterate through many designs and to do imaging in PDMS devices due to the transparent nature of the material and its low autofluorescence[17,22]. Two major types of microfluidic techniques were used in this thesis: integrated valved microfluidic devices with pneumatic layer and liquid-flow layer and tilting microfluidic devices.

1.2.1 Using valved microfluidics to study populations of cells at high spatiotemporal resolution

Valved microfluidics is a method used for precise spatiotemporal control in microfluidic devices[17]. Valved microfluidic devices are usually made of at least two PDMS layers, a pneumatic layer with air-filled channels and a second layer underneath that accommodates the liquid channels; they feature pressure-driven flow[17,18]. The respective microfluidic valves are typically connected to a solenoid valve through tubing[23]. In turn, a solenoid valve is connected to an external pressure source. Microfluidics valves are closed upon application of pressure when the solenoid valve is open. In contrast, when a solenoid valve is closed, a microfluidic valve is not exposed to an external pressure source, and the microfluidic valve is open[17]. A

microfluidic chip can be constructed with just one or up to thousands of microfluidic valves[3,17,24,25]. Moreover, microfluidic valves can be used to control the speed of fluid flow through channels via peristaltic pumps[3,15–17,20,25–27]. Furthermore, a small number of solenoid valves can be used to control complex fluid flows through multiplexing[3,15–17,20,25–27]. Nevertheless, the high spatiotemporal resolution achieved with valved microfluidic devices comes at the cost of complexity and expertise needed to run experiments (Figure 1).

1.2.2 Using tilting microfluidics to study interactions between multiphysiological systems

Tilting microfluidics is a user-friendly method that can be used to study multi-tissue interactions[28–30]. Tilting microfluidic devices have gravity-driven flow that is controlled by the height difference between two reservoirs connected by a channel[28–30]. The main characteristics of a tilting chip are two reservoirs that are, in most cases, exposed to atmospheric pressure, and a tilting stage. The equations that are used to describe the flow in a tilting device are given in the supplementary materials and methods section of chapter 2. The nature of the devices makes high-spatiotemporal-resolution drug stimulation experiments impossible, as, e.g., concentration changes in the system are not instantaneous. Nevertheless, the simplicity of the devices allows the technology to more easily be transferred into clinical settings.

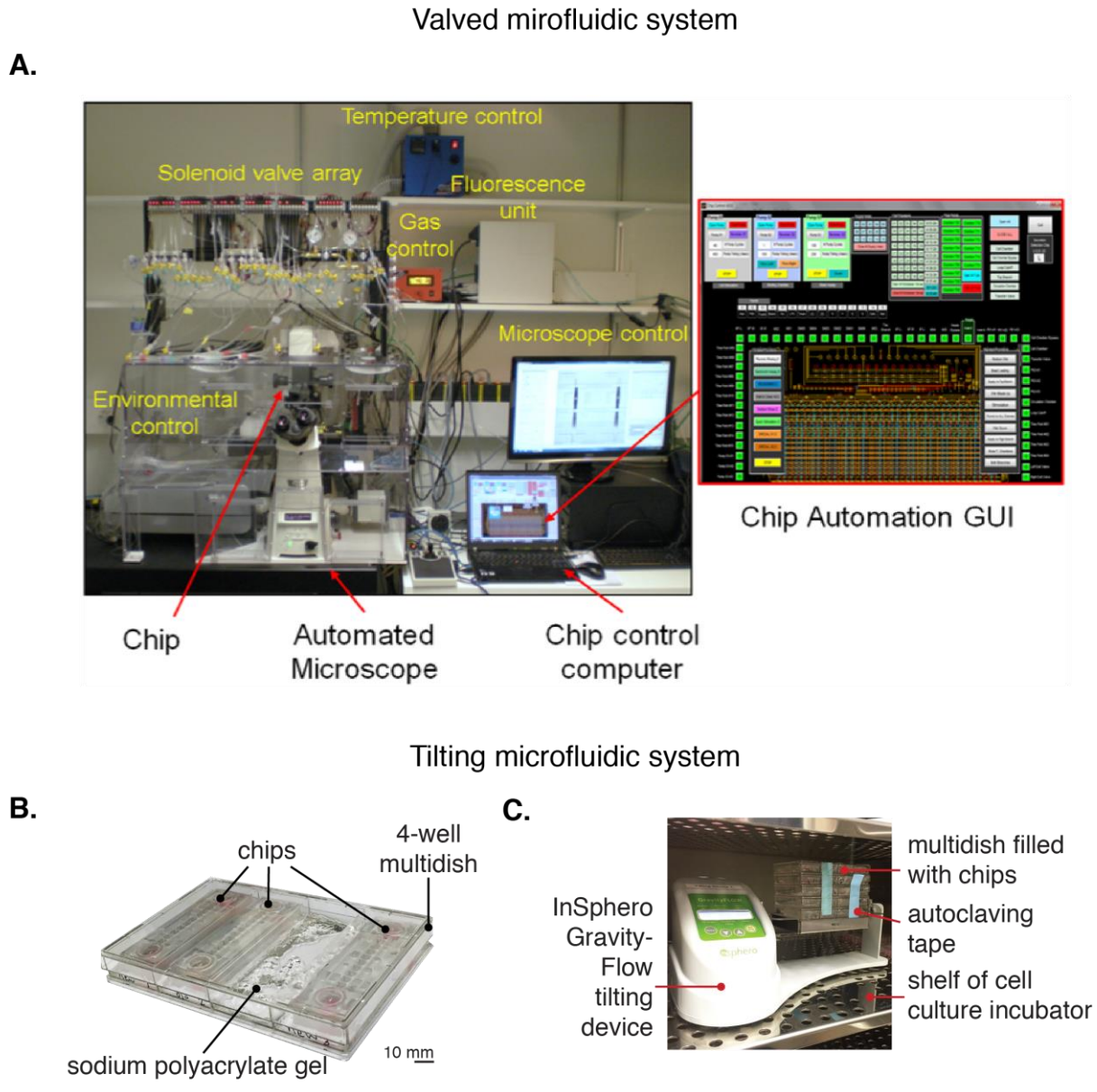

Figure 1: *Valved microfluidic devices require more equipment to run experiments than tilting microfluidic devices. (A) Valved microfluidic devices require: temperature control, pneumatic pressure control, an environmental control container, an automated microscope, a microscope control computer and software, a microfluidic chip control computer and software, and the microfluidic chip. The image in (A) was previously published* [25]*. (B, C) Tilting microfluidic systems require: a microfluidic chip, a multi-well dish, a tilting stage, and a cell-culture incubator.*

1.3 SCOPE AND STRUCTURE OF THIS THESIS

The focus of this thesis is on the development of microfluidic devices to study the interaction between cells and tissues. In Chapter 2, an automated microfluidic device is described that has the ability to measure communication dynamics between small populations of cells. In Chapter 3, a different microfluidic platform is described that is used to test the susceptibility of patient-derived leukemia cells to various drugs.

1.4 SUMMARY OF RESULTS AND MAJOR FINDINGS

This thesis includes three publications. The author contributions are listed for each publication of the thesis in the corresponding chapter.

1. Michael Junkin, **Alicia J. Kaestli**, Zheng Cheng, Christian Jordi, Cem Albayrak, Alexander Hoffmann, and Savaş. Tay. "High-content quantification of single-cell immune dynamics." Cell Reports, 15: 411-422 (2016). DOI: 10.1016/j.celrep.2016.03.033
2. **Alicia J. Kaestli**, Michael Junkin, Savaş Tay. "Integrated Platform for Cell Culture and Dynamic Quantification of Cell Secretion." Lab on a Chip, 17: 4124-4133 (2017). DOI: 10.1039/C7LC00839B
3. **Alicia J. Kaestli** [*], Martina A. de Geus [*], Brice Mouttet, Christian Lohasz, Nassim Rousset, Flavio Bonanini, Yun Huang, Jean-Pierre Bourquin, Beat Bornhauser, Andreas Hierlemann, Kasper Renggli. "Leukemia-on-a-Chip: A Flow-and Metabolism-Based Drug Screening Platform for Patient-Derived Leukemia Samples." In preparation for submission.

1.4.1 Integrated platform for cell culture and dynamic quantification of cell secretion

To investigate the dynamic profile of cytokines released from both, single and small populations of cells, we developed an automated microfluidic chip that is able to reconstruct secretion profiles from small populations of cells (Fig. 1). The device can dynamically stimulate cells with multiple inputs and measure the secretion in each cell chamber. We cultured 16 populations of cells in nanoliter-sized chambers for over three days. The chip has the ability to work with rare cell types – such as lymphocytes T-cells in cerebral spinal fluid – by seeding cells at concentrations lower than 10,000 cells/mL.

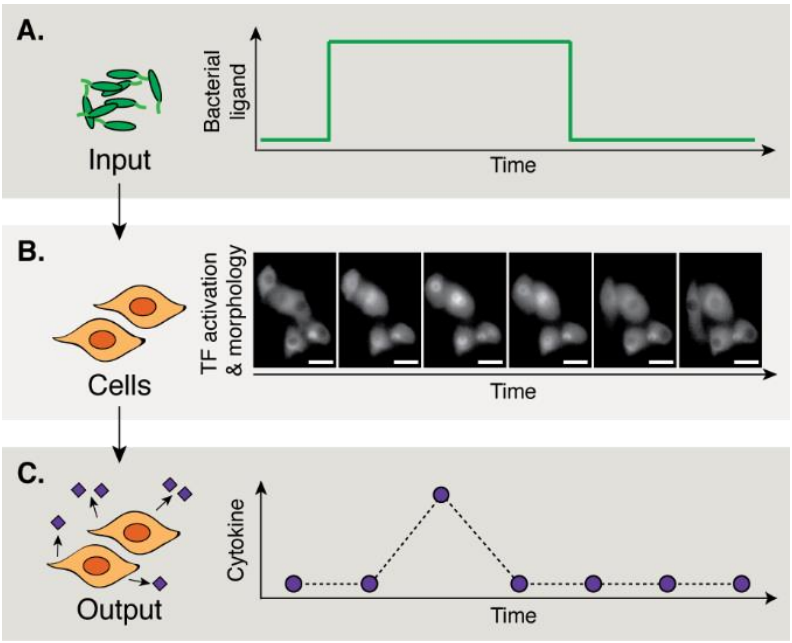

Figure 2. *The developed platform can dynamically stimulate cells, culture cells, and quantify cytokine secretion. (A) The dynamic cell secretion chip can expose cells to a dynamic input. Cells are stimulated with a bacterial ligand to stimulate an infection. (B) Simultaneously, the transcription factor (TF) activation and morphology of the cells can be imaged every 5 minutes. Scale bar is 20 μm. (C) The cytokine secretion is measured every two hours.*

1.4.2 Measurement of the effect of dynamic stimuli on immune cell cytokine secretion

The dynamic secretion chip was used to measure the response of small populations of macrophages to two different stimuli – a single lipopolysaccharide (LPS) pulse and an LPS ramp. Specifically, both the transcription factor NF-κB activity and cytokine TNF activity of the populations were measured. Macrophages responded to a high concentration of LPS with a single peak in both NF-κB and TNF activity (Fig. 2).

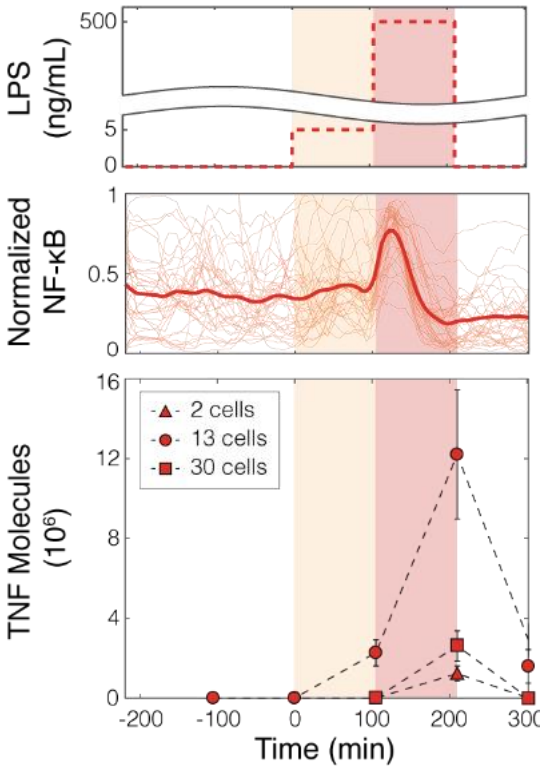

Figure 3: *The response of populations of macrophages to a dynamic LPS stimulus.*

1.4.3 Leukemia-on-a-chip: A flow-and metabolism-based drug screening platform for patient-derived leukemia samples

We developed an easy-to-use and tubing-free microfluidic device to combine patient derived leukemia cells with primary liver microtissues. Perfusion of media by tilting enables parallelization and scaling up of experiments, without requiring complex equipment. The device was optimized for culturing acute lymphoblastic leukemia (ALL) patient-derived xenograph (PDX) samples, on top of a mesenchymal stromal cell (MSC) feeder layer. Liver spheroids were cultured in cell traps. With the developed device, we have been able to measure to response of ALL PDX samples to both non-metabolized drugs as well as prodrugs that require hepatic bio-activation.

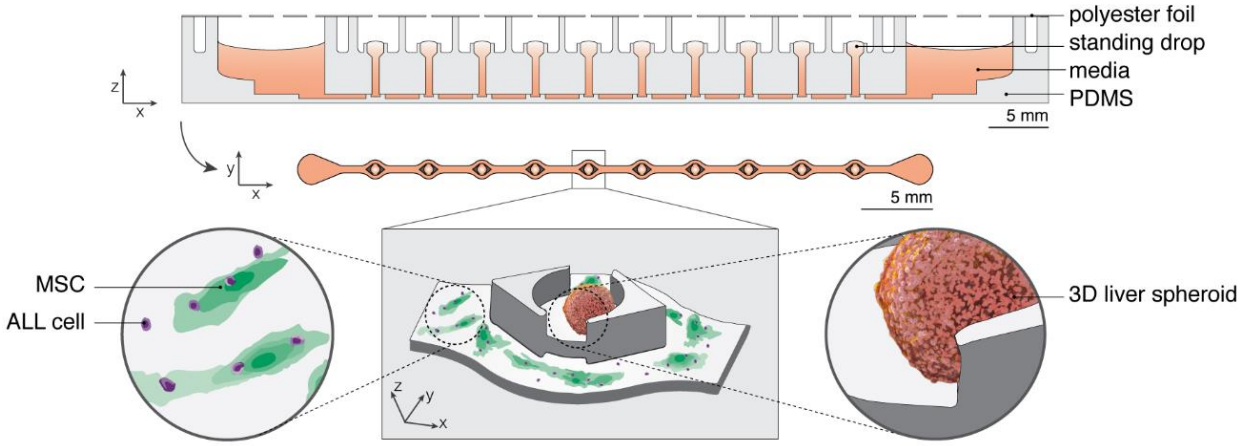

***Figure 4**: The leukemia-on-a-chip platform viewed from various sliced angles. A close up of an elevated trap is illustrated. 3D liver spheroids are cultured on top of the elevated trap platform, whereas MSCs and PDX ALL cells are cultured directly on the bottom of the channel, below the elevated trap platform.*

1.4.4 Measurement of the effect of a prodrug on a patient-derived leukemia sample

The leukemia-on-a-chip device was used to measure the effect of a prodrug on a patient-derived xenograph (PDX) leukemia sample. The prodrug cyclophosphamide was tested. PDX cells were exposed to a total of four conditions both in the leukemia-on-a-chip platform and in a standard well plate. The four conditions tested were: (1) media, (2) media with cyclophosphamide, (3) media with liver tissue, and (4) media with cyclophosphamide and liver tissue. In the static well-plate experiment, no significant difference between the conditions was measured. In contrast, in the leukemia-on-a-chip experiments, PDX cells tended to have reduced viability when cultured in the presence of both, the prodrug cyclophosphamide and liver tissues.

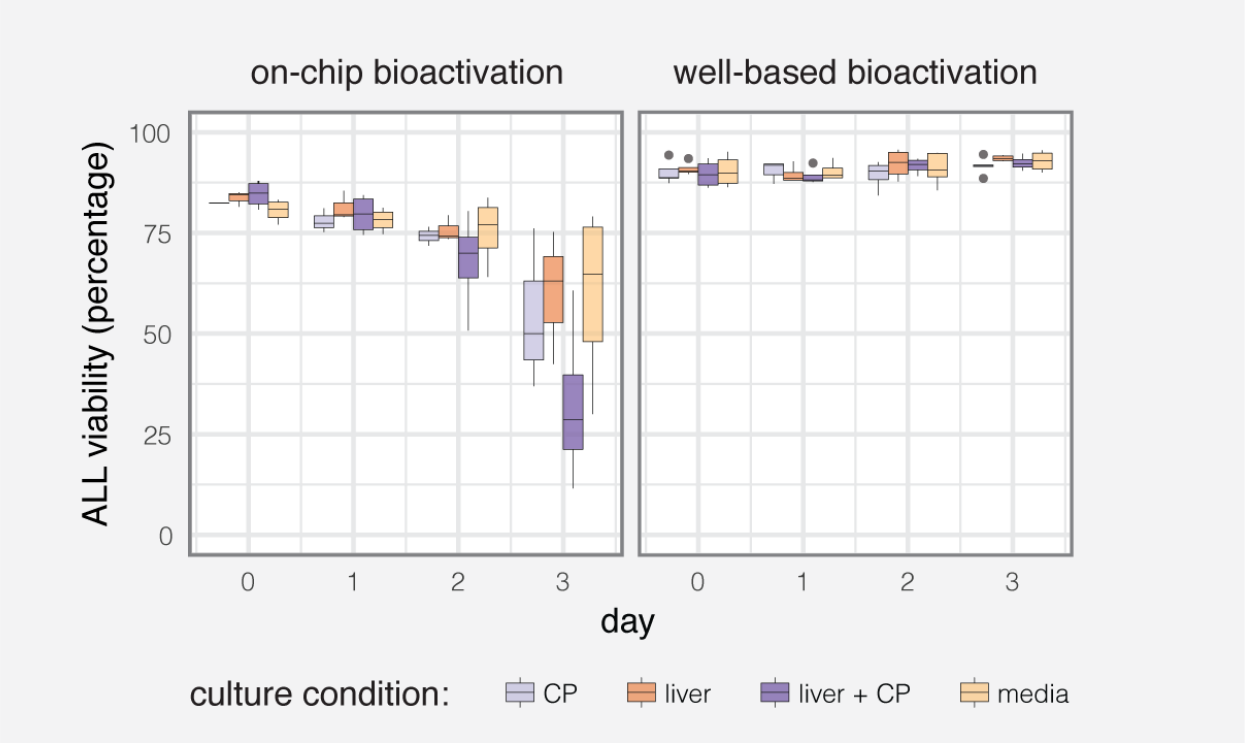

Figure 5: *The effect of cyclophosphamide (CP) on the viability of a PDX ALL sample the leukemia-on-a-chip platform and a well plate.*

1.5 REFERENCES

1. Yde, P., Mengel, B., Jensen, M. H., Krishna, S. & Trusina, A. Modeling the NF-kB mediated inflammatory response predicts cytokine waves in tissue. *BMC Syst. Biol.* **5,** 115 (2011).

2. Lim, K. *et al.* Neutrophil trails guide influenzaspecific CD8+ T cells in the airways. *Science (80-.).* **349,** (2015).

3. Kellogg, R. A. & Tay, S. Noise facilitates transcriptional control under dynamic inputs. *Cell* **160,** 381–392 (2015).

4. Bhatia, S. N. & Ingber, D. E. Microfluidic organs-on-chips. *Nat. Biotechnol.* **32,** 760–772 (2014).

5. Ward, S. *et al.* Cytokine Storm in a Phase 1 Trial of the Anti-CD28 Monoclonal Antibody TGN1412 Ganesh. *N. Engl. J. Med.* 1018–1028 (2006).

6. Zanger, U. M. & Schwab, M. Pharmacology & Therapeutics Cytochrome P450 enzymes in drug metabolism : Regulation of gene expression , enzyme activities , and impact of genetic variation. *Pharmacol. Ther.* **138,** 103–141 (2013).

7. Doğaner, B. A., Yan, L. K. Q. & Youk, H. Autocrine Signaling and Quorum Sensing: Extreme Ends of a Common Spectrum. *Trends Cell Biol.* **26,** 262–271 (2016).

8. Röder, P. V., Wu, B., Liu, Y. & Han, W. Pancreatic regulation of glucose homeostasis. *Exp. Mol. Med.* **48,** e219 (2016).

9. Frey, O., Misun, P. M., Fluri, D. A., Hengstler, J. G. & Hierlemann, A. Reconfigurable microfluidic hanging drop network for multi-tissue interaction and analysis. *Nat. Commun.* **5,** 1–11 (2014).

10. Pampaloni, F. & Stelzer, E. H. K. Three-Dimensional Cell Cultures in Toxicology. *Biotechnol. Genet. Eng. Rev.* **26,** 117–137 (2010).

11. Edmondson, R., Broglie, J. J., Adcock, A. F. & Yang, L. Three-Dimensional Cell Culture Systems and Their Applications in Drug Discovery and Cell-Based Biosensors. *Assay Drug Dev. Technol.* **12,** 207–218 (2014).

12. Antoni, D., Burckel, H., Josset, E. & Noel, G. Three-Dimensional Cell Culture: A Breakthrough in Vivo. *International Journal of Molecular Sciences* **16,** (2015).

13. Mestas, J. & Hughes, C. C. W. Of Mice and Not Men: Differences between Mouse and

Human Immunology. *J. Immunol.* **172,** (2004).

14. Flecknell, P. Replacement, reduction and refinement. *ALTEX* **19,** 73–8 (2002).

15. Frank, T. & Tay, S. Automated co-culture system for spatiotemporal analysis of cell-to-cell communication. *Lab Chip* **15,** 2192–2200 (2015).

16. Mehling, M., Frank, T., Albayrak, C. & Tay, S. Real-time tracking, retrieval and gene expression analysis of migrating human T cells. *Lab Chip* **15,** 1276–1283 (2015).

17. Melin, J. & Quake, S. R. Microfluidic Large-Scale Integration : The Evolution of Design Rules for Biological Automation. (2007). doi:10.1146/annurev.biophys.36.040306.132646

18. Squires, Todd M; Quake, S. R. Microfluidics : Fluid physics at the nanoliter scale. **77,** (2005).

19. Piehler, A., Ghorashian, N., Zhang, C. & Tay, S. Universal signal generator for dynamic cell stimulation. *Lab Chip* 2218–2224 (2017). doi:10.1039/c7lc00531h

20. Frank, T. & Tay, S. Flow-switching allows independently programmable, extremely stable, high-throughput diffusion-based gradients. *Lab Chip* (2013). doi:10.1039/c3lc41076e

21. Squires, T. M., Messinger, R. J. & Manalis, S. R. Making it stick : convection , reaction and diffusion in surface-based biosensors. **26,** 417–426 (2008).

22. Mehling, M. & Tay, S. Microfluidic cell culture. *Curr. Opin. Biotechnol.* **25,** 95–102 (2014).

23. Kellogg, R. A., Gómez-sjöberg, R., Leyrat, A. A. & Tay, S. High-throughput microfluidic single-cell analysis pipeline for studies of signaling dynamics. **9,** 1713–1726 (2014).

24. Yazdi, S. R. *et al.* Microfluidic Hanging-Drop Platform for Parallel Closed-Loop Multi-Tissue Experiments. 535–538 (2015). doi:10.1109/MEMSYS.2015.7051010

25. Junkin, M. *et al.* High-Content Quantification of Single-Cell Immune Dynamics. *Cell Rep.* **15,** (2016).

26. Kaestli, A. J., Junkin, M. & Tay, S. Integrated platform for cell culture and dynamic quantification of cell secretion. *Lab Chip* 4124–4133 (2017). doi:10.1039/C7LC00839B

27. Dettinger, P. *et al.* Automated Micro fl uidic System for Dynamic Stimulation and Tracking of Single Cells. (2018). doi:10.1021/acs.analchem.8b00312

28. Kim, J.-Y. *et al.* 3D spherical microtissues and microfluidic technology for multi-tissue experiments and analysis. *J. Biotechnol.* **205,** 24–35 (2015).

29. Kim, J.-Y., Fluri, D. A., Kelm, J. M., Hierlemann, A. & Frey, O. 96-Well Format-Based Microfluidic Platform for Parallel Interconnection of Multiple Multicellular Spheroids. *J. Lab. Autom.* **20,** 274–282 (2015).

30. Park, T. H. & Shuler, M. L. Integration of cell culture and microfabrication technology. *Biotechnol. Prog.* **19,** 243–253 (2003).

31. Frismantas, V. *et al.* Ex vivo drug response pro fi ling detects recurrent sensitivity patterns in drug-resistant acute lymphoblastic leukemia. *Blood* **129,** e26–e38 (2017).

2 Integrated platform for cell culture and dynamic quantification of cell secretion

Alicia J. Kaestli,[a] Michael Junkin[a,b,c] and Savaş Tay[a,b,c]

a. Department of Biosystems Science and Engineering, ETH Zürich, Mattenstrasse 26, 4058 Basel, Switzerland
b. Institute for Molecular Engineering, University of Chicago, Chicago, IL 60637, USA
c. Institute for Genomics and Systems Biology, University of Chicago, Chicago, IL 60637, USA

Published in *Lab on a Chip*

DOI: 10.1039/C7LC00839B 2017

2.1 AUTHOR CONTRIBUTIONS

AJK designed the chip, ran the experiments, analyzed the data, and wrote the manuscript.

MJ assisted in the design of the chip, experimental advice, and wrote the manuscript.

ST wrote the manuscript.

2.2 ABSTRACT

We developed an automated microfluidic chip that can measure dynamic cytokine secretion and transcription factor activation from cells responding to time-varying stimuli. Our chip patterns antibodies, exposes cells to time-varying inputs, measures cell secretion dynamics, and quantifies secretion all in the same platform. Secretion dynamics are measured using micrometer-sized immunoassays patterned directly inside the chip. All processes are automated, so that no user input is needed for conducting a complete cycle of device preparation, cell experiments, and secretion quantification. Using this system, we simulated an immune response by exposing cells to stimuli indicative of chronic and increasing inflammation. Specifically, we quantified how macrophages respond to changing levels of the bacterial ligand LPS, in terms of transcription factor NF-κB activity and TNF cytokine secretion. The integration of assay preparation with experimental automation of our system simplifies protocols for measuring cell responses to dynamic and physiologically relevant conditions and enables simpler and more error free means of microfluidic cellular investigations.

2.3 INTRODUCTION

Cells continuously receive and respond to a wide variety of inputs. For instance, when immune cells are activated by pathogen sensing receptors, cytokines are produced and secreted to induce inflammation and activate the body's innate immune response.[1] Precise control of cytokine concentration is critical because abnormally high or low secretion of cytokines can result in inflammatory conditions, such as sepsis, or increased susceptibility to infection, respectively.[2] Prolonged inflammation can lead to other debilitating conditions, such as asthma, rheumatoid arthritis, multiple sclerosis, and cancer.[3] Tight regulation of cytokine secretion is thus essential for a healthy immune response.

The dynamics of cytokine secretion are important for tuning a cell's response in a larger population response.[3,4] For instance, it is predicted that neutrophils are recruited to the site of infection by propagating cytokine waves across tissue cells.[3] Moreover, pulsing a cytokine over a population of cells transforms unsynchronized transcription factor oscillations into entrained and synchronized oscillations.[4] Furthermore, an activated macrophage is able to transmit a wave of transcription factor activation across a population of fibroblast cells through cytokine secretion.[5] Undoubtedly, the dynamics of cytokines received and released from cells are important in understanding how populations of cells communicate with each other, and more specifically, how the immune system is coordinated. Nevertheless, due to technical challenges, the dynamics of cytokines released from cells given a dynamic input are not well understood. Even clonal populations of cells have heterogeneity in response to an immune stimulus.[6,7] This heterogeneity is an essential component in understanding how cells process biological noise to ultimately produce a robust response to infection.

Techniques exist to measure dynamic cytokine secretion from cells. However, these methods lack an all-in-one device to run dynamic cell experiments and immunoassays on the same platform. For instance, microengraving is a technique where cells are cultured in nanowells on a polydimethylsiloxane (PDMS) slab.[8-11] The PDMS slab is reversibly attached to an antibody-patterned glass slide used to measure secretion. Microengraving requires complex manual manipulation of (1) off-chip patterning of glass slides, and (2) detachment and replacement of a new glass slide for both changing media and measuring secretion for each time point. Furthermore, the final quantification of secretion using detection antibodies is completed separately off-chip. Single-cell barcode chips can also be used to measure dynamic cytokine secretion. In barcode chips, secretion is measured by seeding cells in nanowells on a PDMS slab, and successively replacing antibody coated glass slides on the top of nanowells

for each secretion time point. However, this device is not an all-in-one device, in that the DNA-encoded antibody libraries need to be patterned using an additional microfluidic device.[12-14] This limits the duration and feasibility of experiments and requires substantial manual involvement. We recently published a microfluidic chip that measures dynamic secretion from cells without the need to manually intervene to conduct immunoassays.[7]

In the current work, we improve on our prior design, by easing the chip set up to eliminate all off chip-steps necessary for experimentation. To use our previous chip, antibodies had to be attached to beads in additional off-chip processes. Subsequently, the beads had to be manually and sequentially loaded into the chip. By using an on-chip antibody patterning protocol, we cut down on many hours of manual labor needed to conduct experiments.[15-18] As a result, our new dynamic cell secretion chip saves researchers significant manual work and is more robust to errors as it does not require manual intervention in assay processes. The chip presented here is, to our knowledge, the first device that incorporates a full immunoassay, from antibody patterning to secretion quantification, of a cell culture exposed to dynamic stimuli. An all-in-one integrated and automated device is essential to simplify protocols, reduce operator time and errors, conduct long-term, complex, and multiday assays, and ultimately bring devices out of engineering labs and into the clinic and biology-focused labs.

Here, we present an integrated and automated platform that can expose cells to a dynamic input, track the cellular inflammatory transcription factor response, and measure the resulting cytokine secretion over time (Figure 1). To test the platform, we studied how macrophages respond to infection. Specifically, we measured how RAW 264.7 macrophages respond to lipopolysaccharide (LPS), an inflammatory molecule found on the cell wall of gram-negative bacteria. We measured the response by tracking NF-κB transcription factor activation, and TNF cytokine release. NF-κB is a major transcription factor in inflammation, which is known to control TNF secretion.2 The platform improves on existing techniques by being able to precisely pattern micrometer-sized immunoassays, culture cells, and perform surface-based immunoassay quantification all in the same device. Furthermore, the device is adaptable in that immunoassay patterning, cell experiments, and immunoassay quantification are each automated, with no further manual manipulation needed after the reagents are connected to the device. The ease of operation of our current chip will facilitate further microfluidic exploration into how cells respond to dynamic inputs.

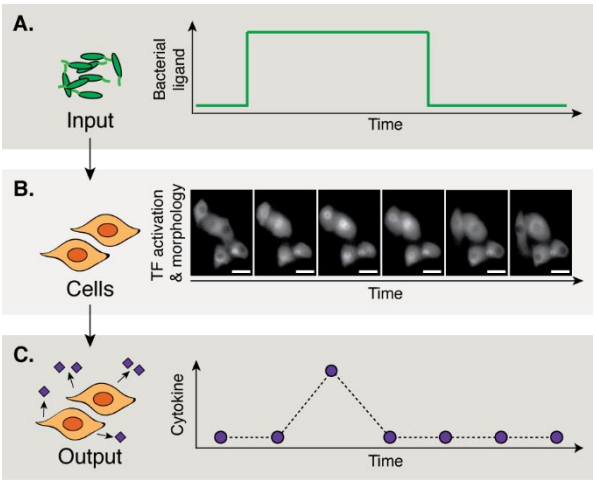

Figure 1. *Quantifying cell response to dynamic inputs. (A) The dynamic cell secretion chip can expose cells to a dynamic input. Cells are stimulated with a bacterial ligand to stimulate an infection. (B) Simultaneously, the transcription factor (TF) activation and morphology of the cells can be imaged every 5 minutes. Scale bar is 20 μm. (C) The cytokine secretion is measured every two hours.*

2.4 MATERIALS AND METHODS

2.4.1 Chip control and operation

The device design and fabrication protocol was previously described in detail,[19] and further described in our supplementary materials and methods. The control channels of the dynamic secretion chip were selectively pressurized in order to control the movement of fluids in flow channels (Figure 2, Figure S1). To operate the device, the control channels were filled with diH_2O and pressurized at 30 psi. The flow lines were operated at 5 psi, and valve switching was controlled with a custom MATLAB program. We developed a GUI with a corresponding library of scripts in order to implement automation in the device (available on request).[20] We extensively developed and built upon the simple open and close valve commands that comprised the basis of the control to fully automate chip assay functions.[20] An automated script works by timing the flow of various fluids through different parts of the chip.

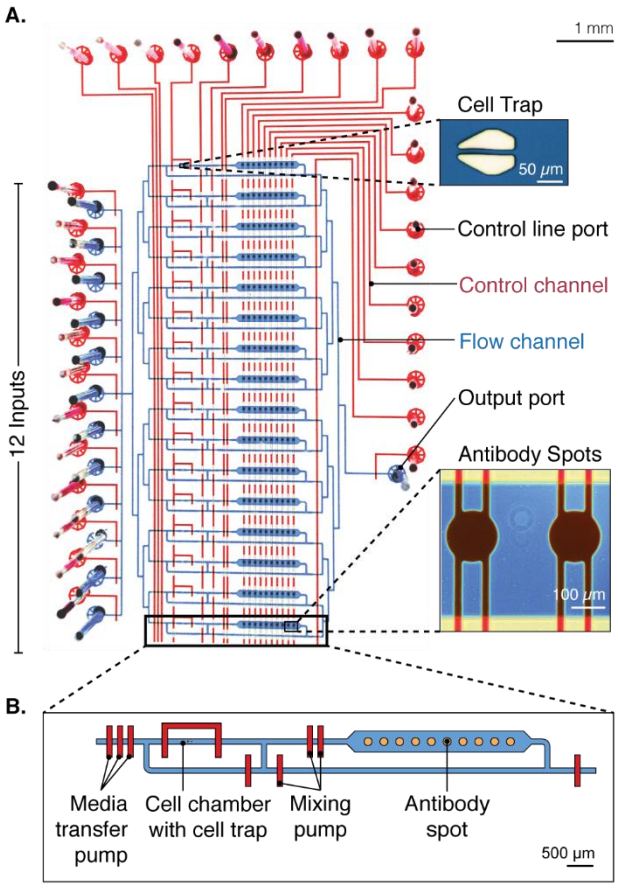

Figure 2: *Overview of dynamic cell secretion chip. (A) The chip has 16 units, 12 inputs, and 1 output. The control layer, marked in red, modulates the flow of fluids in the flow layer, marked in blue, where cells are cultured and the immunoassay is performed. (B) Each unit consists of a cell culture chamber, with a media transfer pump to feed cells, and an antibody spot chamber with 10 capture antibody spots used to measure the amount of cytokine in the cell culture supernatant. A separate mixing pump is used to mix the supernatant over the immunoassay (Movie S1). Each cell culture chamber contains a cell trap.*

2.4.2 Chip preparation

Preparation of a chip begins with purifying reagents, all of which were filtered through a 0.2 μm sterile filter before being added to the device. Air inside fluidic lines was then removed by debubbling the chip with PBS for 5 minutes. PBS was flowed into the chip, with a closed exit, until all bubbles were pushed out of the flow channels through the air-permeable PDMS. Then, cell chambers and button valves were closed, and 10 mg/mL pluronic (Pluronic F-127, Life Technologies) dissolved in water was flowed through the antibody spot chambers of the chip (Figure 3bi). This rendered all surfaces besides the cell chamber and antibody spotting regions non-adhesive. After pluronic treatment, the antibody spot chambers were extensively washed

with PBS for 4 hours. Next, the cell chambers were coated with fibronectin to render the surface adhesive for cells.[19] 200 µg/mL fibronectin (FC010, Milipore, Zug, Switzerland) dissolved in PBS was flowed into the cell chambers, and incubated for the duration of the antibody patterning protocol (12 hours).

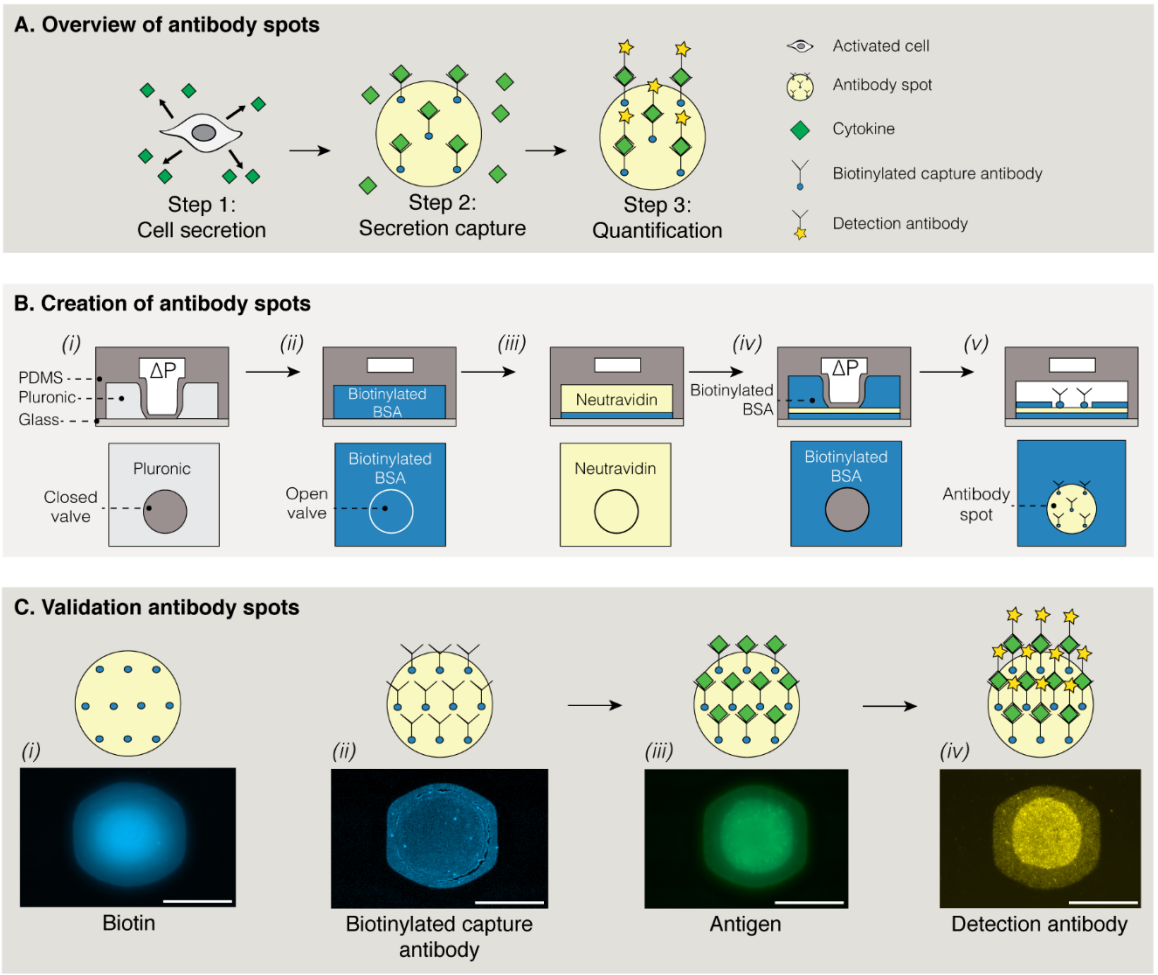

Figure 3. *On-chip patterned antibody spots for cytokine secretion quantification. (A) Overview of antibody spots. A cell secretes cytokines (step 1). Secreted cytokines are captured on antibody-coated spots (step 2). The number of cytokines bound to each spot is measured using a fluorescently labelled antibody (step 3). (B) Creation of antibody spots. The top images are representative of a cross section of the chip. The bottom images are from a birds-eye-view. The channel is initially passivated with pluronic (i) to create a non-adhesive surface outside the antibody spots. The antibody spots are then patterned by flowing biotinylated BSA (ii), and then neutravidin (iii) through antibody spot channels with open buttons valves. Next, the buttons valves are pressurized, and biotinylated BSA (iv) is flowed through the channel. This creates a neutravidin spot underneath the button valve. Lastly, the buttons valves are opened,*

and biotinylated anti-TNF antibodies (v) are flowed through the chip. The antibody spots are now patterned (v). (C) Validation of the antibody spots. The neutravidin spot patterned in (B.iv) is confirmed by flowing a fluorescent biotin solution through the chip. Fluorescent biotin binds robustly to the neutravidin spot. The existence of the initial biotinylated antibody spot was confirmed by using a fluorescent antibody against the antibody spot (ii), and using a labelled eGFP antigen (iii). A picture of a completed immunoassay on the spot is also shown (iv). Scale bar is 50 μm.

2.4.3 Antibody spot patterning

Patterning of the antibody-based cytokine detecting spots was fully automated, and required no operator input after the reagents were connected to the device. The antibody patterning protocol was adopted from previous work.[15-18] In order to pattern an antibody, the antibody must only be biotinylated. To start the patterning protocol, the button valves were closed, and pluronic was flowed through the chip (Figure 3bi) as mentioned above. Next, the button valves were opened and 2 mg/mL biotinylated bovine serum albumin (BSA) (29130, Thermo Fisher Scientific) dissolved in distilled water (Figure 3bii), followed by 1 mg/mL neutravidin (3100, Thermo Fisher Scientific) dissolved in PBS (Figure 3biii), were flowed into the chip. The button valves were then closed, and biotinylated BSA was again flowed into the chip in order to bind to and passivate exposed neutravidin molecules surrounding the button valves (Figure 3biv). After this step, there is a neutravidin spot directly underneath the button valves. This specificity of patterning was confirmed by a fluorophore-tagged biotin molecule (Figure 3ci). Next, 7.5 μg/mL biotinylated anti-TNF (T9160-14, US Biological, USA) dissolved in PBS was added to the channels (Figure 3bv). Because of the neutravidin spot underneath the button valves, the antibodies were precisely patterned onto only to this spot, and the antibody spotting protocol was completed (Figure 3cii). The density consistency of capture antibodies was verified, and no significant difference in density was found between different buttons and rows (Figure S2). The integrity of remaining parts of the immunoassay, both the antigen and detection antibody addition, were also confirmed in Figure 3ciii and Figure 3civ, respectively. Specific details of the patterning are described further in the supplementary materials and methods.

2.4.4 Addition of cells to device

After the antibody spots were patterned, the previously applied fibronectin was washed out of the cell chambers with fresh media. A cell suspension was then flowed through the chamber to seed cells before the start of the experiment. Cells were captured with a cell trap.[7] Cells were

typically seeded at a concentration of 10^5 cells/mL, though cell populations as low as $5x10^4$ cells/mL could also be successfully seeded, albeit this results in a lower density of cells per chamber. The cell seeding protocol is explained in detail in the supplementary materials and methods.

2.4.5 NF-κB measurement and analysis

We used RAW macrophages $p65^{-/-}$ with a p65-GFP reporter gene and H2B-dsRed nuclear marker to track cellular NF-κB activity.[2] In order to culture cells while maintaining simultaneous imaging capabilities, chips were operated on a Nikon Eclipse Ti inverted microscope inside of an enclosure with a fixed temperature of 37°C with 95% humidity and 5% CO_2 (Life Imaging Services Basel, Switzerland). The cells were imaged using bright field and epifluorescence every 5 minutes during experiments. The NF-κB fluorescence of each cell was quantified by measuring the average fluorescent intensity in the cellular nucleus. Background fluorescence due to autofluoresence in the media was subtracted from cellular NF-κB measurements. Similar to our previous device, the NF-κB fluorescence of each cell was determined manually, and further downstream analysis was automated in MATLAB.[7] The background corrected measurements were normalized to the minimum and maximum fluorescence per cell during an experiment. Lastly, normalized measurements were smoothed using a moving average.

2.4.6 Secretion from cell

After connecting reagents to the chip, the secretion measurements were conducted with a fully automated script implemented in MATLAB. The script controls both the location and the timing of reagents in the chip. To quantify secretion, cellular supernatant was periodically moved from the cell chamber into the antibody spot chamber (Figure 4a). First, PBS was flowed into the top part of the antibody chamber (Figure 4a) for 5 minutes. Next, fresh media was flowed around the cell chamber and the bottom part of the antibody chamber (Figure 4ai). This step was necessary to periodically replace the media in the cell chamber. When providing a cellular stimulus, a solution of LPS (L4524, Sigma-Aldrich Chemie GmbH, Switzerland) in media was instead flowed around the cell chamber. Next, the cellular supernatant was transferred to the antibody spot chamber. Specifically, the cell chamber was opened, and a peristaltic pump transferred the supernatant into the antibody spot chamber, and at the same time, transferred new media or media with stimulus into the cell chamber (Figure 4aii and S3). Next, a button valve was opened, revealing an antibody spot, and the valves surrounding the antibody spot chamber were closed. One antibody spot was used per measurement time

interval. A peristaltic pump was then used to mix the cell supernatant over the antibody spot (Movie S1). The solution was mixed until adequate cytokine binding was achieved (Figure 4d). After 90 minutes, the button valves were closed, and the antibody spot chamber was washed for 5 minutes with PBS. The process was repeated for each time point of cellular cytokine secretion.

2.4.7 Secretion calibration

Following cell experiments, a calibration with known amounts of TNF diluted into media was completed on chip (Figure 4b-c). Specifically, the same protocol was used as for cellular measurements, except that solutions with known concentrations of TNF (PMC3014, Thermo Fisher Scientific, USA) dissolved in media were first flowed into the cell chamber. This process was repeated for each TNF concentration tested. Using these calibration points, the amount of cytokine secreted by the cells was quantified. The limit of detection (LOD) is defined as the mean fluorescence intensity of media plus 3 times the standard deviation. The LOD of the dynamic secretion chip is ~155,000 molecules (10^{-19} moles) of soluble TNF. All calibrations were completed under identical conditions as cellular cultures; humidity, temperature, and surface coatings were all maintained.

2.4.8 Quantifying secretion

Two antibodies were used to quantify the amount of TNF captured on the antibody spots during measurements. The quantification process began by first washing out the antibody spot chambers with 0.05% PBS Tween (P7949, Sigma-Aldrich Chemie GmbH, Switzerland) for 20 minutes to remove unbound cytokines and other components from the assay chamber. Next, 7.6 μg/mL of rabbit anti-TNF antibody (GWB-489500, GenWay Biotech, USA) in PBS was added with the button valves open. The anti-TNF antibody was flowed through antibody spot chambers for 5 minutes, and then incubated in the chambers for 10 minutes. This flow and incubation cycle was repeated twice, for a total of 30 minutes. The antibody chambers were then washed with 0.05% PBS Tween for 20 minutes.

Next, 3.3 μg/mL of fluorescent Cy3 labeled anti-rabbit IgG (I1903-12H, US Biological, USA) in PBS was flowed through the antibody spot chambers in order to visualize and quantify the amount of TNF bound to the spots. Specifically, the antibody was flowed through the channels for 5 minutes, followed by a 10 minute incubation. This process was repeated twice for a total of 30 minutes. Next, the antibody chambers were washed with 0.05% PBS Tween for 20 minutes, followed by PBS for 20 minutes. The antibody spots were then imaged using a

Nikon Eclipse Ti inverted microscope. To quantify the fluorescence signal of each antibody spot, the mean fluorescence of each spot was measured using ImageJ. The spots were then normalized by subtracting the mean background signal next to each antibody spot from the measured mean fluorescence intensity of each spot.[21] The method for converting a measurement of fluorescence intensity to the number of TNF molecules is described further in the supplementary methods and Figure S4.

2.5 RESULTS AND DISCUSSION

2.5.1 Device design

We designed an automated microfluidic chip that can expose cells to a dynamic input, quantify the cellular inflammatory transcription factor response, and finally measure the resulting cytokine secretion all in the same platform (Figure 1). The microfluidic chip is composed of PDMS control and flow layers bonded to a glass slide in a push-down configuration (Figure 2a). In this configuration, the cells were cultured and assays were performed directly on the glass surface. All protocols were automated with a MATLAB control software and corresponding GUI.[19,22]

The chip is capable of measuring the inflammatory transcription factor and cytokine secretion response of up to 16 groups of cells via parallelized units. Each unit consists of a nanoliter-sized cell chamber (920 pL), and an on-chip peristaltic media transfer pump to control the replacement of media in the cell chamber (Figures 2b). Each cell chamber contains a cell trap in order to capture cells from a cell suspension for on-chip culture.[7] Furthermore, each unit contains 10 patterned antibody spots, which are used to measure cytokine secretion at 10 different time intervals, and an on-chip peristaltic mixing pump in order to increase the cytokine capture efficiency of the antibody spots (Figure 2b).[7,23] In total, the device can measure 160 time points of cytokine secretion.

Cell secretion was measured with an immunoassay using on-chip patterned antibody spots (Figure 3). Antibody spots were patterned with a capture antibody specific to a cytokine of interest. Later, cell supernatant was incubated over these spots, and secreted cytokines were captured on the spot (Figure 3a). The amount of cytokine bound to each spot was quantified by a double sandwich immunoassay. All of these steps, from the initial patterning of antibodies, to the cell culture and secretion experiments, and to the final quantification of secretion using

detection antibodies, were completed on-chip with fully automated control, meaning that no operator time or input was needed after the reagents were connected.

2.5.2 Capture antibody spots are patterned on-chip

Antibody spots were patterned on-chip using an adaptation of the mechanically induced trapping of molecular interaction (MITOMI) method.[15-18] This protocol uses button valves to selectively pattern antibodies directly underneath the valves. Unlike the traditional pneumatic microfluidic valves, which completely close a rounded flow channel, button valves are both narrower than the flow channel and are placed above a rectangular flow channel, and thus do not fully block the flow channel when closed (Figure S1). Button valves only block a small surface below the valve from exposure to external reagents, while allowing the rest of the flow channel to be exposed to a given solution (Figure S1b). Button valves are essential to the operation of the dynamic secretion chip by saving valuable functional chip area and allowing multiple antibody spots to be patterned adjacent to the cell chamber. Patterning in this way is additionally highly flexible in that the only requirement for placement of antibodies is that the antibodies are functionalized with biotin.

Two changes were made to the established MITOMI antibody patterning protocol.[15-18] First, instead of bonding the device to an epoxy coated glass slide, the PDMS chips were bonding directly to an uncoated glass slide Patterning on epoxy slides, unlike glass slides, results in covalent attachment of antibodies.[15-18] Nevertheless, we patterned antibodies on glass slides in order to maintain good cell viability in our system. Second, the first reagent used for antibody patterning was pluronic (Pluronic F-127, Life Technologies), in order to make the flow channel surfaces, apart from the antibody spot regions, non-adhesive to proteins and other components within the medium. Pluronic was also necessary to make the antibody spot chamber non-stick for cell seeding into the cell chamber.

The antibody patterning protocol was run in an automated fashion. After the reagents were connected to the chip, a MATLAB script controlled the antibody patterning protocol and the protocol ran automatically for 12 hours. This is a significant improvement over our previously published method for dynamic cell secretion quantification[7], which required up to 8 hours of manual loading of antibody beads. Moreover, this is also in contrast to the microengraving and barcoding methods, that require manual slide processing in order to coat antibodies onto glass slides.[8-10,12-14] The automation of antibody patterning described in our

dynamic cell secretion chip is a strong advantage of our technique due to manual time saved setting up the device for an experiment.

2.5.3 Cellular secretion profile measurement using antibody spots

The secretion profile of cells was measured using an on-chip sandwich immunoassay over the patterned antibody spots. Each antibody spot can be used for one-time point measurement. To measure secretion dynamically, cell supernatant was periodically moved from the cell chamber to the antibody spot chamber (Figure 4a), where one spot per time point is opened for the assay. By closing the button valve after each measurement, each antibody spot was mechanically blocked from further supernatant exposure. As a result, every antibody spot operated independently of one another, and multiple measurements could be performed in the same chamber by using a different antibody spot for each measurement.

We ensured no cytokine molecules were lost in this process by preventing diffusion losses by pumping cell supernatant directly into the antibody spot chamber (Figure 4a). The cell chamber and antibody spot chambers are separated by a single valve, ensuring there was no loss of cytokines upon solution transfer. Moreover, the volume of the antibody spot chamber was ~23 times larger than the cell chamber. By pumping the supernatant into the middle of the antibody spot chamber, we further ensured that all of the supernatant reached the antibody spot chamber by continued pumping until new media behind the supernatant was also pumped into the antibody spot chamber (Figure 4aii and S3).

Cells were exposed to dynamic inputs by changing the solution that flowed into the cell chamber (Figure 4a) at each medium replenishment step. By having programmable and automated valves at input ports, it was possible to change the stimulus in the cell chamber within 5 seconds (Movie S2). As a result, it is possible to use our device to expose cells to a wide range of possible input conditions, from short input pulses, to longer stimulations. By making use of all available input ports, it is possible to expose cells to up to 12 different stimuli.

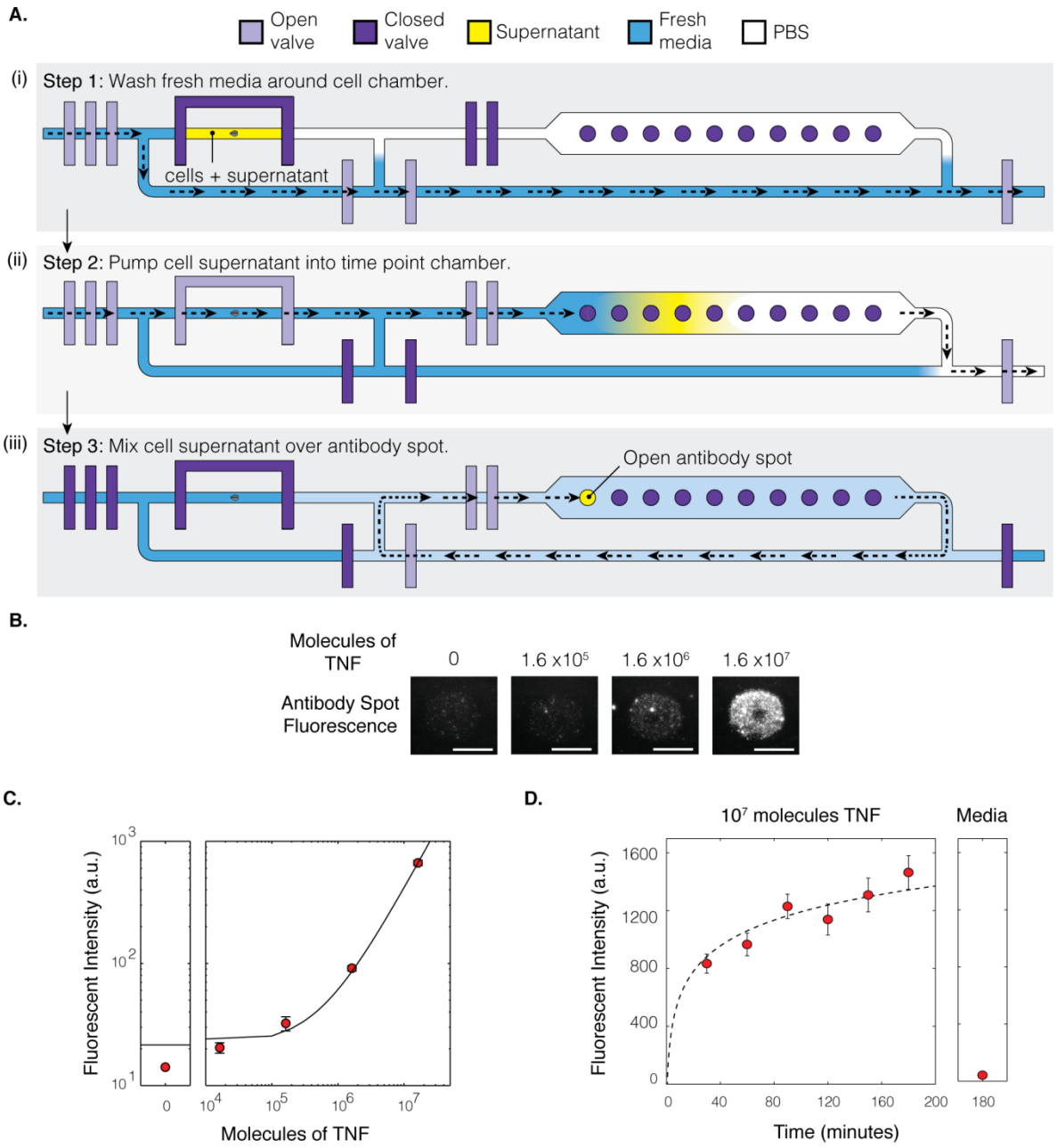

Figure 4. *The secretion profile is measured using an immunoassay. (A) (i) First, the cells are cultured in the cell chamber (yellow). New media (blue) is washed around the cell chamber. The antibody spot chamber is filled with PBS (white). (ii) After an incubation, new media (blue) is pumped into the cell chamber, and the cell supernatant (yellow) is pumped into the antibody spot chamber. The pumping parameters for successful transfer of supernatant from the cell chamber to the time point chamber are described further in Figure S3. (iii) In the antibody spot chamber, the cell supernatant is mixed over an exposed antibody spot, and the amount of TNF secreted by the cells is measured. A video of the mixing of a solution over an antibody spot is shown in Movie S1. (B) Representative examples of antibody spots bound with varying amounts of TNF. Scale bar is 50 μm. (C) A calibration curve for TNF on the antibody spots. Error bars*

are the standard error of the mean. The limit of detection is ~155,000 molecules. (D) Dependence of antibody spot signal with mixing time. The time 10^7 molecules of TNF were circulated inside the chip was varied from 30 to 180 minutes. With increasing mixing time, the fluorescent intensity measured increased. As a control, media was mixed for 180 minutes over an open antibody spot. Error bars represent standard deviation. The dashed line is the line of best fit to a logarithmic curve.

2.5.4 Dynamic quantification of cellular NF-κB and TNF secretion response to LPS time courses

The dynamic secretion chip was used to expose cells to a dynamic input, track the cellular transcription factor response every 5 minutes, and track the resulting cytokine secretion every 2-3 hours. It is meaningful to observe the secretion patterns of small populations of cells, as paracrine signaling is important to recapitulate a strong response to LPS in macrophages.[14,24] Specifically, we studied how cells process a LPS input through the NF-κB transcription factor, and finally to a TNF cytokine output (Figure 5a). Activation of NF-κB leads to the secretion of proinflamatory cytokines. For instance, NF-κB is known to control TNF secretion[2], and TNF is one of the first proinflamatory cytokines secreted by macrophages in response to a pathogen.[25]

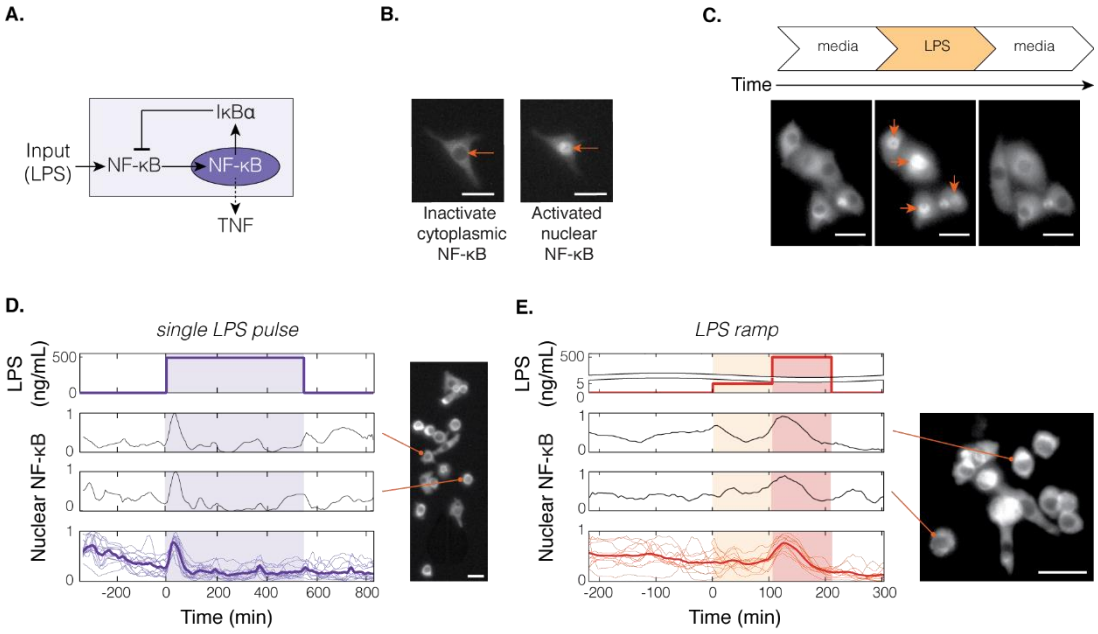

Figure 5. *The dynamic secretion chip tracking of the cellular NF-κB response to a variable input. (A) Exposure to LPS causes NF-κB activation and TNF secretion. When activated by LPS, NF-κB translocates from the cytoplasm (light purple) to the nucleus (dark purple). (B) Raw 264.7 macrophages with a p65-GFP reporter gene were used for experiments. During the*

cellular resting state, NF-κB is inactive and located in the cytoplasm. When NF-κB is activated, the transcription factor moves from the cytoplasm into the nucleus. (C) The dynamic secretion chip can be used to apply a dynamic stimulus to cells, and track the cellular NF-κB activation over time. When exposed to LPS, NF-κB translocates into the nucleus, as indicated with arrows. (D) The NF-κB response of 18 cells to a single pulse of LPS. Specifically, cells were exposed to 6 hours of media, 9 hours of LPS, and 3 hours of media. The media and LPS inputs are represented as a white and purple background, respectively. (E) The NF-κB response of 13 cells to an LPS ramp consisting of 4 hours media, 2 hours 5 ng/mL LPS, 2 hours 500 ng/mL LPS, and 3 hours media. The white, light orange and dark orange backgrounds indicates when media, 5 ng/mL LPS, and 500 ng/mL LPS, respectively, were in the cell chamber. In panels (D) and (E), the stimulus input is shown in the top graph, the trace of two cells from the population is shown in the middle two graphs, and the average cellular response shown by the bolded line in the bottom graph. The thin lines in the bottom graph are the NF-κB responses of all cells in the chamber. Scale bar is 20 μm.

The cellular NF-κB response was tracked by using RAW 264.7 macrophages labeled with a p65 GFP marker.[2] An example time course of a media stimulus, followed by a 500 ng/mL LPS, and then a media stimulus is shown in Figure 5c. Note how during the media stimulations, NF-κB is mainly found in the cytoplasm, and how the NF-κB translocated to the nucleus during the LPS stimulation. The first NF-κB and secretion measurements were always done under baseline conditions, with fresh media. This was necessary to understand the initial cellular state before stimulus addition. Examples of two stimulus patterns given to cells are shown in Figures 5d and 5e. First, we exposed cells to a time course that mimics a strong, chronic inflammatory state (Figure 5d). We exposed cells to media, 9 hours of high concentration LPS, and lastly media. We were able to track NF-κB dynamics on a single cell level with 5-minute resolution over 20 hours. Additionally, we exposed cells to increasing inflammation, by exposing cells to media, a low concentration of LPS, a high concentration of LPS, and finally media (Figure 5e). In the increasing stimulus condition, macrophages only had a NF-κB peak response to the high concentration of LPS.

We observed that the cellular NF-κB response to a strong and chronic inflammation was similar to the cellular response to an increasing ramp of LPS exposure. In both conditions, no difference was observed in the peak response to the high 500 ng/mL LPS stimulus. The single cell response to a strong and chronic stimulus resulted in a NF-κB peak 22 ± 1.4 minutes after stimulation, and similarly the increasing inflammation condition had a peak 20.5 ± 1.6

minutes after stimulation. The peak timing of NF-κB in response to LPS closely matched published results, where NF-κB activation was observed 24 minutes after stimulation of RAW 264.7 macrophages with LPS.[2]

Variability in macrophage activity was also studied through the standard deviation of the cellular NF-κB response (Figure S5). Variability in macrophage NF-κB activity decreased after exposure to the high dose of LPS in both the chronic and increasing inflammation conditions. Variation in NF-κB activity was highest during the first media stimulus (Figure 5d-e and S5). This is likely due to stress on the cells after seeding. For this reason, stimulation experiments with LPS always started at least 3 hours after cell seeding.

On the same set of cells, we were also able to measure TNF secretion (Figure 6). Both stimulation conditions resulted in a single peak of TNF secretion following LPS exposure (Figure 6). A single high peak in response to LPS stimulation matches previous results[7], and we hypothesize that we only observed one TNF peak because upon cellular activation, the cellular TNF mRNA stockpile is rapidly translated, transported to the cellular membrane, enzymatically cut and rapidly secreted from cells.[26] After the peak in TNF secretion, cellular NF-κB relocated from the nucleus back to the cytoplasm. Deactivation of cellular NF-κB has been suggested to decrease levels of proinflamatory cytokine expression, such as TNF.[2] In one experiment of the increasing inflammation condition, we observed a gradual release of TNF (Figure 6b). This may be a result of the lack of cellular NF-κB activation during the low concentration of LPS exposure, and subsequent peak of activation after stimulation with the high concentration of LPS. We thus observed that only after NF-κB peak activation, is there a maximum peak in TNF secretion.

These results show that we are able to use the dynamic secretion chip to track cellular response to dynamic stimuli via coupled NF-κB activation and TNF secretion. We were able run cell experiments in a fully automated fashion over 20 hours with a resolution of 5 minutes for NF-κB signaling and 2-3 hours for cytokine secretion measurements.

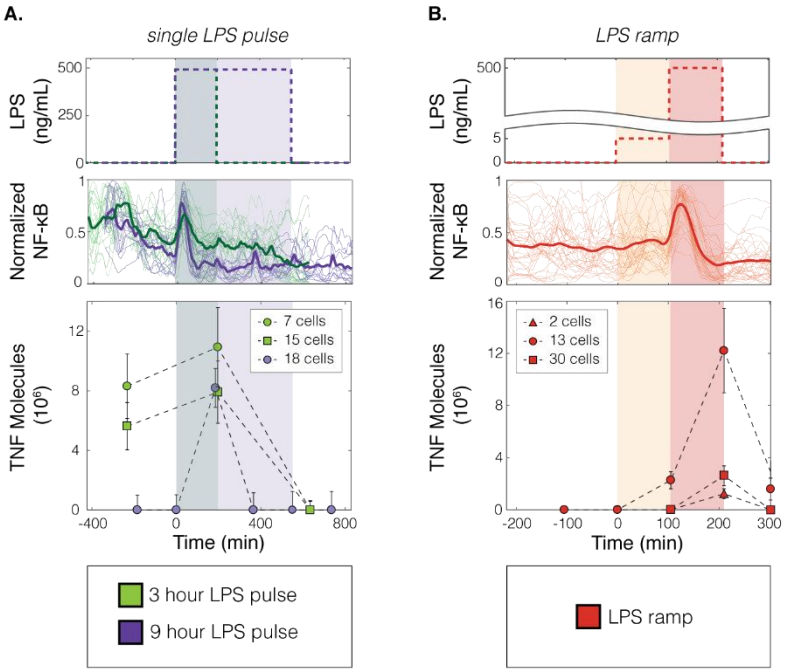

Figure 6. *Coupled cytokine secretion and transcription factor response of cells to a dynamic LPS input. Cells were simulated with an LPS time course, indicated by the top graphs. The middle panel shows the NF-κB response of all cells. The thin lines represent the single cell traces. The bold lines are the average cellular response. The cellular TNF secretion response is shown in the bottom graph of both panels. Time zero indicates the start of the LPS pulse. The top, middle, and bottom graphs all have the same time course, as indicated by the time course in the bottom graph. (A) 40 cells were stimulated with a single pulse of 500 ng/mL of LPS. Cells were exposed to an LPS pulse of either 3 hours (green) or 9 hours (purple). Cells were exposed to media preceding and following the LPS pulse. The media, 3 hour LPS, and 9 hour LPS inputs are indicated by a white, green, and purple background, respectively. The TNF secretion of cells from 3 experiments is shown in the bottom panel. (B) 45 cells were stimulated with two doses of LPS (LPS ramp). Specifically, cells were stimulated with (1) media, (2) a dose of 5 ng/mL LPS, (3) a dose of 500 ng/mL LPS, and (4) media. The media, 5 ng/mL LPS and 500 ng/mL LPS inputs were represented by a white, light orange and dark orange background, respectively. The TNF secretion of cells from 3 experiments is shown. In the bottom graph of both panels, the error bars represent the standard error of the maximum likelihood that a certain fluorescence value equals a value of TNF secretion. This is described further in Supplementary Figure S4.*

2.6 CONCLUSIONS

We developed an integrated device that is able to expose cells to dynamic inputs, study the cellular transcription factor activity, and track the resulting cytokine secretion over time. To our knowledge, this is the first platform that has full automation of immunoassay preparation, cell secretion experiments, and secretion quantification all in the same device. Unlike microengraving, barcode-based chips, and our previously published chip, here, total immunoassay preparation, experimentation, and readouts are conducted automatically on chip, without the need for complex manual manipulations.[7-10,12-14] We used this integrated platform to measure how cells respond to two different stimuli, an extended and high concentration of LPS, representing a chronic infection, and an increasing ramp of LPS, representing increasing inflammation. This showed, quantitatively, how cells sensed and differentiated dynamic inputs. Moreover, our device has the potential to work with rare cell populations, such as circulating tumor cells and rare stem cells as even low concentrations of cells can be seeded into the device.

Our device will allow further deciphering of how cells control cytokine secretion in response to dynamic stimuli. Precise control of cytokine secretion is essential in order to further study how cells communicate with each other to coordinate a robust response to infection. This is especially important considering that the latest breakthroughs in immunological therapies, such as engineered T cell therapy, rely on understanding how immune cells compose a potent attack specifically against cancer cells.[27] In response to such therapy, many patients have experienced a cytokine release syndrome side effect, characterized by uncontrolled cytokine secretion, that has resulted in organ failure, cardiotoxicity, and, in some cases, death.[27] Understanding the cytokine response of engineered immune cells is thus critical for further developing such new technologies. The integration and automation provided by our device makes it well suited for studying cellular responses to dynamic stimuli in the clinic or in traditional biology labs.

2.7 REFERENCES

1. K. Murphy, P. Travers, M. Walport, P. Walter and J. Theriot, *Janeway's Immunobiology*, Taylor & Francis Group, 8 edn. 2012.
2. E. A. Wall, J. R. Zavzavadjian, M. S. Chang, B. Randhawa, X. Zhu, R. C. Hsueh, J. Liu, A. Driver, X. R. Bao, P. C. Sternweis, M. I. Simon and I. D. C. Fraser, *Science Signaling*, 2009, **2**, ra28–ra28.
3. P. Yde, B. Mengel, M. H. Jensen, S. Krishna and A. Trusina, *BMC Syst Biol*, 2011, **5**, 115.
4. R. A. Kellogg and S. Tay, *Cell*, 2015, **160**, 381–392.
5. T. Frank and S. Tay, *Lab Chip*, 2015, **15**, 2192–2200.
6. S. Tay, J. J. Hughey, T. K. Lee, T. Lipniacki, S. R. Quake and M. W. Covert, *Nature*, 2010, **466**, 267–271.
7. M. Junkin, A. J. Kaestli, Z. Cheng, C. Jordi, C. Albayrak, A. Hoffmann and S. Tay, *Cell Rep*, 2016, **15**, 411–422.
8. J. C. Love, J. L. Ronan, G. M. Grotenbreg, A. G. van der Veen and H. L. Ploegh, *Nat Biotechnol*, 2006, **24**, 703–707.
9. Q. Han, N. Bagheri, E. M. Bradshaw, D. A. Hafler, D. A. Lauffenburger and J. C. Love, *Proc. Natl. Acad. Sci. U.S.A.*, 2012, **109**, 1607–1612.
10. Q. Han, E. M. Bradshaw, B. Nilsson, D. A. Hafler and J. C. Love, *Lab Chip*, 2010, **10**, 1391.
11. Y. Lu, Q. Xue, M. R. Eisele, E. S. Sulistijo, K. Brower, L. Han, E.-A. D. Amir, D. Pe'er, K. Miller-Jensen and R. Fan, *Proc Natl Acad Sci USA*, 2015, **112**, 201416756–E615.
12. R. C. Bailey, G. A. Kwong, C. G. Radu, O. N. Witte and J. R. Heath, *J. Am. Chem. Soc.*, 2007, **129**, 1959–1967.
13. R. Fan, O. Vermesh, A. Srivastava, B. K. H. Yen, L. Qin, H. Ahmad, G. A. Kwong, C.-C. Liu, J. Gould, L. Hood and J. R. Heath, *Nat Biotechnol*, 2008, **26**, 1373–1378.
14. C. Ma, R. Fan, H. Ahmad, Q. Shi, B. Comin-Anduix, T. Chodon, R. C. Koya, C.-C. Liu, G. A. Kwong, C. G. Radu, A. Ribas and J. R. Heath, *Nat Med*, 2011, **17**, 738–743.
15. J. L. Garcia-Cordero and S. J. Maerkl, *Lab Chip*, 2014, **14**, 2642–2650.
16. J. L. Garcia-Cordero, C. Nembrini, A. Stano, J. A. Hubbell and S. J. Maerkl, *Integr Biol (Camb)*, 2013, **5**, 650–658.
17. J. L. Garcia-Cordero and S. J. Maerkl, *Chem. Commun. (Camb.)*, 2013, **49**, 1264–1266.

18. S. J. Maerkl and S. R. Quake, *Science*, 2007, **315**, 233–237.
19. R. A. Kellogg, R. Gómez-Sjöberg, A. A. Leyrat and S. Tay, *Nat Protoc*, 2014, **9**, 1713–1726.
20. R. Gómez-Sjöberg. https://sites.google.com/site/rafaelsmicrofluidicspage/valve-controllers/usb-based-controller.
21. C. Zheng, J. Wang, Y. Pang, J. Wang, W. Li, Z. Ge and Y. Huang, *Lab Chip*, 2012, **12**, 2487–2490.
22. R. Gómez-Sjöberg, A. A. Leyrat, D. M. Pirone, C. S. Chen and S. R. Quake, *Anal. Chem.*, 2007, **79**, 8557–8563.
23. M. A. Unger, H. P. Chou, T. Thorsen, A. Scherer and S. R. Quake, *Science*, 2000, **288**, 113–116.

2.8 SUPPLEMENTARY MATERIALS AND METHODS

2.8.1 Device fabrication

The device design and fabrication protocol was previously described in detail (Kellogg et al., 2014). In brief, the chip was fabricated using standard multilayer soft lithography (Unger et al., 2000). The chips were designed in AutoCAD (Autodesk Inc., USA), and printed at 40,000 dpi onto transparencies (Fine Line Imaging, Minneapolis, USA). Photolithography was used to make the control and flow molds on 4-inch silicon wafers (Figure 2a). The control mold was made with SU-8 3025 (MicroChem, USA) spun at 3000 rpm to a height of 25 μm. The flow mold was made with AZ 50XT (MicroChem, USA) spun at 4500 rpm and then reflowed, and with SU8-3010 (MicroChem, USA) spun at 3000 rpm. The final height of the AZ 50XT and SU-8 3010 on the flow mold was 15 μm and 10 μm, respectively. The reflow process consisted of heating the wafer up to 200°C and maintaining the temperature for a total of 13 hours to hard bake the resist after reflow. This process caused the reflowing of AZ 50XT into rounded channels (Unger et al., 2000).

To produce polydimethylsiloxane (PDMS) chips from the silicon molds, the molds were first coated with chlorotrimethylsilane (92360, Sigma-Aldrich Chemie GmbH, Switzerland) for 15 minutes in a fume hood. This coating renders the molds non-stick to PDMS. Then, 69 g of a 10:1 mixture of PDMS (RTV-615, Momentive Specialty Chemicals Inc., USA) was cast onto the control layer and degassed. The flow mold was spun with 10:1 PDMS at 2800 rpm for 1 minute. Both layers were then baked at 80°C for 45 minutes. The control layer was peeled off the silicon mold, punched with a 710 μm inner diameter biopsy punch (CR0350255N20R4, Syneoco, USA), aligned, bonded to the flow layer via plasma treatment for 15 seconds at 45W (Femto #112296, Diener electronic GmbH + Co. KG, Germany), and baked for 2 hours at 80°C. The input and output holes on the aligned PDMS chip was then punched using the same 710 μm inner diameter biopsy punch. A glass slide (1100020, Biosystems Switzerland AG, Switzerland) was cleaned via a 5 minute sonication with ultra pure water. The aligned PDMS layers were bonded to glass via plasma treatment, and baked overnight at 80°C to strengthen bonding.

2.8.2 Antibody spot patterning

The antibody spot patterning protocol was fully automated. No operator input was needed after the reagents were connected to the device. The script run for the antibody patterning of the device is described below.

To begin patterning, biotinylated BSA (29130, Thermo Fisher Scientific) at a concentration of 2 mg/mL in distilled water was flowed through the antibody spot chambers (Figure 3bii). All button valves were opened, and the cell chambers were closed. Every 10 minutes, biotinylated BSA was flowed into all antibody spot chambers for 5 minutes. Next, flow was stopped, and the solution was incubated in the chambers for 5 minutes. This process was continued for a total of 90 minutes. All button valves were closed, and the antibody spot chambers were then washed with 0.05% PBS Tween (P7949, Sigma-Aldrich Chemie GmbH, Switzerland) for 20 minutes. Then, the same protocol was repeated with 1 mg/mL neutravidin (3100, Thermo Fisher Scientific) dissolved in PBS (Figure 3biii).

Next, the button valves were closed, and the surrounding neutravidin was passivated by flowing 2 mg/mL biotinylated BSA through the antibody spot chambers in the chip (Figure 3biv). Every 10 minutes, biotinylated BSA was flowed into all antibody spot chambers for 5 minutes. Next flow was stopped, and the solution was incubated in the chambers for 5 minutes. This process was continued for a total of 90 minutes. Afterwards, the antibody spot chambers were then washed with 0.05% PBS Tween for 20 minutes. After this step, there are now neutravidin spots specifically underneath the button valves. Next, the same protocol was repeated with starting block buffer (37578, Thermo Fisher Scientific, USA).

Subsequently, the antibodies were patterned onto the neutravidin spots (Figure 3bv). Here, it is possible to either stop the script, and connect a cold and freshly prepared antibody solution to the chip, or continue running the script with the antibody solution having been plugged into the chip at the beginning of the experiment. No difference was found in connecting freshly prepared solution or running the script antibody plugged into the chip from the start of the patterning protocol. Button valves were opened, and biotinylated anti-TNF (T9160-14, US Biological, USA) at a concentration of 7.5 μg/mL in PBS was flowed through the antibody spot chambers in the chip. Every 10 minutes, biotinylated-BSA was flowed into all antibody spot chambers for 5 minutes. Next, flow was stopped, and the solution was incubated in the chambers for 5 minutes. This process was continued for a total of 120 minutes. Then, all button valves were closed, and the antibody spot chambers were washed with 0.05% PBS Tween for 20 minutes. The antibody spots are now patterned underneath the button valves (Figure 3bvi).

As a final step, the antibody spots are blocked using starting block buffer. Specifically, starting block buffer was flowed through the antibody spot chambers in the chip. All button valves were opened, and the cell chambers were closed. Every 10 minutes, buffer was flowed into all antibody spot chambers for 5 minutes. Next, flow was stopped, and the solution was

incubated in the chambers for 5 minutes. This process was continued for a total of 90 minutes. All button valves were closed, and the antibody spot chambers were then washed with 0.05% PBS Tween for 20 minutes.

At the end of the antibody patterning protocol, the antibody chambers were additionally washed with PBS for 20 minutes. To prevent pressure buildup in the antibody spotting chamber from water diffusion through the PDMS (Garcia-Cordero et al., 2013), the valves adjacent to the antibody spotting chamber and waste port were opened every 90 minutes to relieve the built up pressure.

Step	**Reagent**	**Product Information**	**Button valve opened or closed**	**Total time in antibody spot chamber**
1	2 mg/mL Biotinylated BSA	29130, Thermo Fisher Scientific, USA	Open	90 minutes
2	1 mg/mL Neutravidin	3100, Thermo Fisher Scientific, USA	Open	90 minutes
3	2 mg/mL Biotinylated BSA	29130, Thermo Fisher Scientific, USA	Closed	90 minutes
4	Starting block buffer	37578, Thermo Fisher Scientific, USA	Closed	90 minutes
5	7.5 µg/mL Biotinylated anti-TNF	T9160-14, US Biological, USA	Open	120 minutes
6	Starting block buffer	37578, Thermo Fisher Scientific, USA	Open	90 minutes

Table S1. *Summary of antibody patterning protocol. There are 6 steps in the antibody spotting protocol. For each step, the reagent and product information are noted. Additionally, it is marked if the button valves were opened or closed during each step of the protocol. Finally, it is indicated for how long each reagent remained in the antibody spot chamber. During this time, flow of 5 minutes, and an incubation of 5 minutes were repeated for each reagent for the time indicated in the last column of the table.*

2.8.3 Antibody spot validation

To validate the neutravidin spot underneath button valves (Fig 3ci), steps 1 through 4 in Table 1 were implemented. Then, 2 µg/mL of atto 565-biotin (92636, Sigma-Aldrich Chemie GmbH, Switzerland) in PBS was incubated in the antibody spot chamber for 90 minutes. After incubation, all button valves were closed, and the antibody spot chambers were then washed with 0.05% PBS Tween for 20 minutes.

To validate the antibody spot underneath button valves (Fig 3cii), a fluorescently labeled antibody specific to the patterned anti-TNF antibody was added to the chamber. This allowed visualization of the location of the anti-TNF antibody spots. To accomplish this, steps 1 through 5 of Table 1 were first implemented. Next, to test if the biotinylated anti-TNF antibody was successfully patterned underneath the button valves, a fluorescent antibody against the patterned antibody was added to the antibody spot chambers. Specifically, 5 μg/mL of Alexa 488 Goat Anti-Rat IgG (H+L) (A-11006, Thermo Fischer Scientific, USA) in PBS was flowed into the antibody spot chambers for 5 minutes, and then mixed over a revealed antibody spot for 90 minutes. After the incubation, all button valves were closed, and the antibody spot chambers were then washed with 0.05% PBS Tween for 20 minutes. The fluorescence of the spots was now imaged to quantify the consistency of the anti-TNF antibody patterning.

To validate the binding of an antigen to an antibody (Fig 3ciii), steps 1 through 4 in Table 1 were implemented. Then, step 5 was completed using 2 μg/mL of biotinylated anti-GFP antibody (ab6658, Abcam, USA) in PBS. Next, 16 μg/mL of enhanced green fluorescent protein (eGFP) (4999-100, BioVision, USA) in PBS was incubated over the antibody spots, via 5 minutes flow followed by 5 minutes incubation, repeated for a total of 90 minutes. After, all button valves were closed, and the antibody spot chambers were washed with 0.05% PBS Tween for 20 minutes. The fluorescence of the spots was now imaged to quantify antigen binding to the pattered antibody spots.

2.8.4 Converting fluorescence intensity to TNF molecules

To convert the fluorescence intensity measured to a number of TNF molecules, the maximum likelihood function and variability for each fluorescent value was calculated (Fig S4). First, a normalized probability function was calculated using the mean and standard deviation of data points in the calibration curve (Fig. S4a). Next, the maximum likelihood and standard error for each fluorescent value in the normalized probability function was computed (Fig. S4b). Additionally, the limit of detection of the assay was calculated as the sum of the mean fluorescence intensity of media and three times the standard deviation of the mean. If a measured fluorescence intensity value is below the limit of detection, this intensity represents zero TNF molecules with the standard error of the fluorescence intensity. In contrast, if a measure fluorescence intensity is above the limit of detection, the intensity represents the maximum likelihood number of TNF molecules and standard error for that intensity.

2.8.5 Cell culture

Cell culture of the RAW 264.7 cells was previously described (Junkin et al., 2016). No further changes to this protocol were made. The number of cells seeded into a cell culture chamber is controlled by (1) the concentration of cells flowed into the device, (2) the amount of time cells are flowed into the device, and (3) the presence of a cell trap. The cell trap has the same design as the trap used in our previous paper (Junkin et al., 2016). With the trap, and certain loading densities, we could achieve single cell resolution in our chip (Figure S7). The secretion of the single cell reported is within an order of magnitude of single cell secretion measured in our previously published device (Junkin et al., 2016). Specifically, to seed cells into the chip, a solution of 10^5 cell mL^{-1} was prepared. After flowing fresh media through the cell chambers to wash out unbound fibronectin, the cell solution was flowed into the cell chambers. A video showing the flow of cell through the cell chamber, and eventual trapping of two cells is shown in Movie S3. Cells were flowed into the chip for around 10 minutes or until the desired confluency of cells in each cell chamber was achieved. Then, flow was stopped, and cells outside of the cell chamber were washed away with media.

Throughout experiments, cell viability was tracked by looking at membrane integrity by imaging the cells every 5 minutes. From these videos, we could determine the viability of cells as cells having intact membranes. We identified a cell as dead if it either (1) no longer had an intact membrane or (2) had no change in shape for at least 30 minutes. An example image of cells at the beginning and end of the experiments is shown in Figure S7.

2.9 SUPPLEMENTARY FIGURES

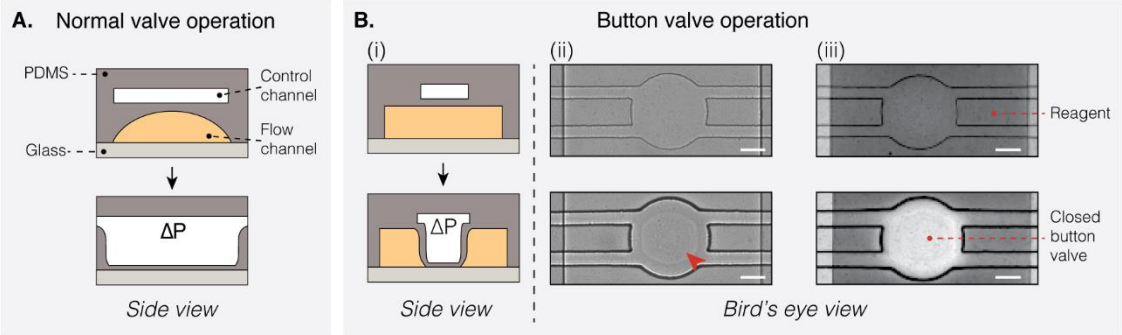

Figure S1. *Differences in conventional and button PDMS valve operation. (A) In a traditional pneumatic PDMS valve, the control channel is at least the same width as the flow channel. When the control line is pressurized, the thin PDMS membrane between the control and flow layers is defected to the bottom of the flow channel. Thus, reagent flow through the flow channel is stopped. (B) (i) In button valve operation, the control channel is narrower than the flow channel (Garcia-Cordero and Maerkl, 2013; 2014; Garcia-Cordero et al., 2013; Maerkl and Quake, 2007). Thus, when the control line is pressurized, only a small surface of the flow channel is blocked from the reagent. (ii) An image of an open (top) and closed (bottom) microfluidic button valve. The surface blocked by the valve is indicated with an arrow. In these images, the flow channel is filled with a transparent reagent (PBS). (iii) The flow channel is filled with food dye (dark regions in image). When the button valve is open (top) food dye can flow below the valve. In contrast, when the button valve is closed, the food dye is pushed away, and the surface below the valve is absent of food dye. Thus, the light patch shows where the button valve is closed. Scale bar is 50 μm.*

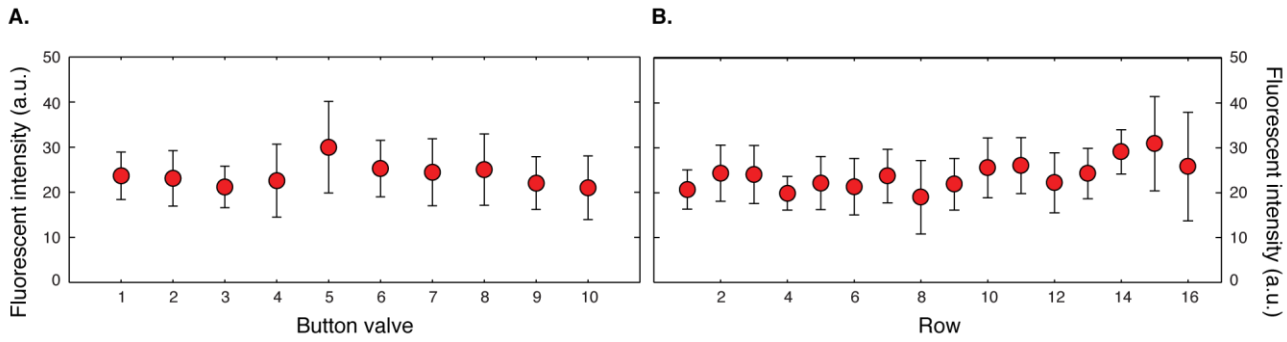

Figure S2. *Variation in capture antibody density on antibody spots. Capture antibodies were patterned on the chip. After patterning, a fluorescent antibody against the capture antibody was added to visualize how much capture antibody was present on each spot. No significant difference in capture antibody density was observed between button valves or rows. (A) The variation in capture antibody density across the 10 button valve control lines. Button valve 1 refers to the antibody spots closest to the cell chamber (left most spots Figure 2a), whereas antibody spot 10 refers to the spots closest to the waste outlet (right most spots Figure 2a). (B) The variation in capture antibody density across the 16 rows in the chip. Row 1 refers to the top row close to high density of control line inlets (top of chip in Figure 2a), whereas row 16 refers to the row closest to the input inlets (bottom of chip in Figure 2a). Error bars indicate standard deviation.*

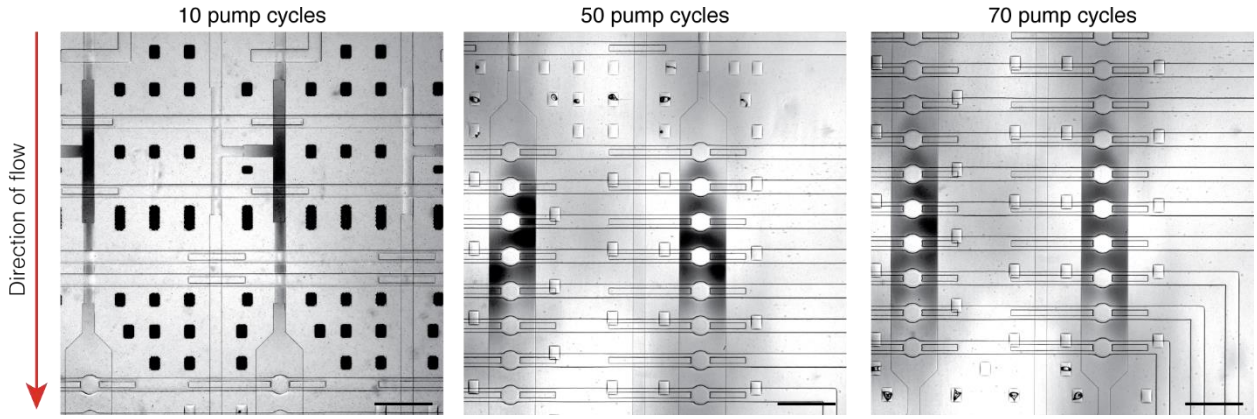

Figure S3. *Variation in peristaltic media transfer pump parameters. Steps 1 and 2 of the fluid transfer steps shown in Figure 4a were tested using different parameters for the media transfer pumping. Cytokine media was represented with food dye (dark fluid in channels). Fresh media was represented with PBS (clear fluid in channels). A pump cycle is defined as the actuation of one 120° pattern, as defined in Unger et al (2000). In brief, a pattern of 6 valve configurations was used over 3 valves. Specifically, the pattern 010, 011, 001, 101, 100, 110 was used. Here, 0 refers to a closed valve, and 1 refers to an open valve. The total pattern (one*

pump cycle) in the left-most picture was repeated 10 times. An image was taken at the end of each pumping script with the specified number of pump cycles above each photo. The pumping parameter used for cell and calibration experiments was 50 pump cycles. Scale bar is 500 µm.

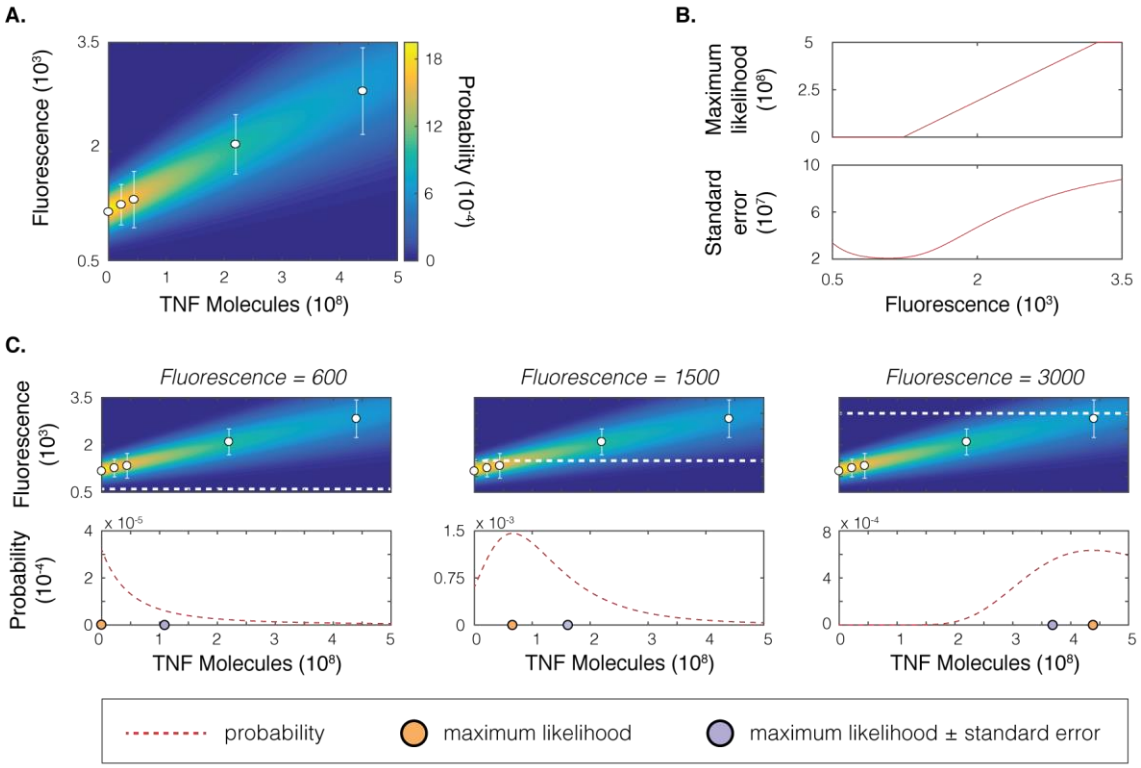

Figure S4. *Quantification of TNF secretion. (A) The normalized probability function is plotted as a heat map. The function is derived from the mean and standard deviation of the calibration curve. The calibration curve is plotted as white circles. Error bars represent standard deviation. (B) The maximum likelihood and standard error for fluorescence values are calculated. (C) For three different fluorescence values, the probability is plotted. These examples show how the maximum likelihood and standard error values in (B) were calculated. The maximum likelihood was calculated as the number of TNF molecules with the maximum probability, for a given fluorescence value.*

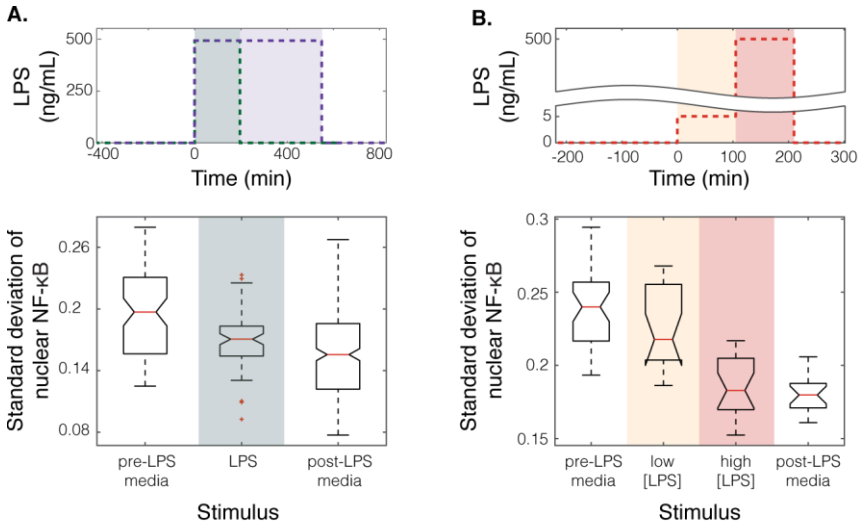

Figure S5. *Variability in macrophage cellular NF-κB response. The top plots show the stimulus conditions the cells were exposed to. The graph plots the standard deviation of nuclear activity of all single cells during each indicated simulation condition. A high standard deviation indicates higher cell-to-cell variability. Specifically, a higher standard deviation indicates higher variability around the average cellular NF-κB response plotted in Figures 6a and 6b. The notches in the bar plots represent the 95% confidence interval the standard deviation of the cellular NF-κB response during each stimulus. (A) The standard deviation of the cellular NF-κB response due to a single LPS pulse. This stimulus mimics a chronic inflammatory response. The cellular variability of cells exposed to a 3 hour (green dashed line) and 9 hour (purple dashed line) were studied as a single group. Cellular variability was highest in during the first media stimulation, and decreased during the first LPS stimulation. (B) The standard deviation of the cellular NF-κB response due to LPS ramp (orange dashed line). This stimulus mimics and increasing inflammatory condition. Variability was highest during the first media stimulation, and decreased during the stimulation with a high concentration of LPS.*

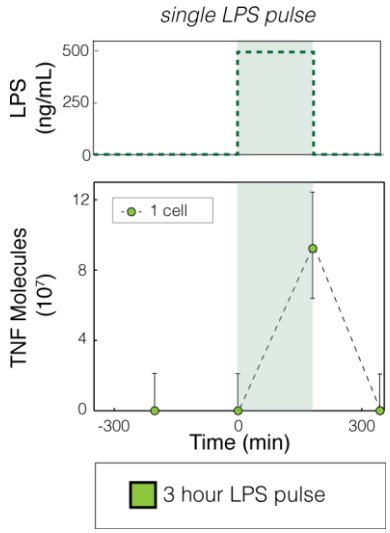

Figure S6. *The TNF secretion response of a single RAW 264.7 cell to a 3 hour LPS pulse. The white and green background indicates when the cell was exposed to media and 500 ng/mL LPS, respectively.*

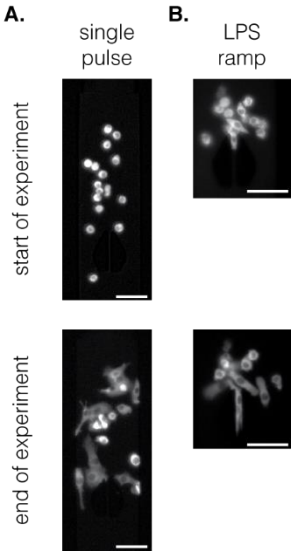

Figure S7. *Morphology of RAW 264.7 cells at the start and end of an experiment. (A) The morphology of RAW 264.7 cells at the start of a single pulse 500 ng/mL LPS experiment. The cellular NF-κB response is shown in Figure 5d. (B) The morphology of RAW 264.7 cells at the start of an LPS ramp experiment. The cellular NF-κB response is shown in Figure 5e. The scale bar is 50 μm.*

Movie S1. *Mixing of food dye in an antibody spot chamber. This movie illustrates step 3 of Figure 4a. Here, the antibody spot chamber is filled with cytokine filled media, represented by food dye (dark liquid) and PBS. The mixing pump is used to mix the contents of the antibody*

spot chamber. A button valve is open, and thus the cytokine media is in contact with an exposed antibody spot. Scale bar is 500 µm.

Movie S2. *Time needed to introduce a new reagent in the cell chamber. The movie shows the time needed to introduce a new stimulus into the cell chamber. The cell chambers were filled with water, and food dye was flowed into the chip from an inlet port. It took ~3.5 seconds for the food dye to travel from the input port to the cell chamber. Scale bar is 500 µm.*

Movie S3. *Cells being seeded into the cell chamber. Cells are flowed into the cell chamber until the desired confluency is reached. Cells are trapped by a cell trap. The valves surrounding the cell trap were closed at time 20.6 seconds. The scale bar is 20 µm.*

2.10 Acknowledgements

We would like to thank Erica Montani and Thomas Horn from the ETH D-BSSE Single Cell Facility for help with the microscopy involved in the project. Further, we would like to thank Felix Franke for help with the statistical analysis, and Tino Frank and Sebastian Bürgel for a critical review of the manuscript. An ERC Starting Grant (SingleCellDynamics) to ST funded this research.

2.11 References

1. Q. Xue, Y. Lu, M. R. Eisele, E. S. Sulistijo, N. Khan, R. Fan and K. Miller-Jensen, *Science Signaling*, 2015, **8**, ra59–ra59.
2. G. A. Duque and A. Descoteaux, *Front Immunol*, 2014, **5**, 1–12.
3. D. K. Ryugo, *Science*, 2005, **310**, 1490–1492.
4. C. A. Klebanoff, S. A. Rosenberg and N. P. Restifo, *Nat Med*, 2016, **22**, 26–36.

3 Leukemia-on-a-chip: a flow-and metabolism-based drug screening platform for patient-derived leukemia samples

Alicia J. Kaestli [a*], Martina A. de Geus [a*], Brice Mouttet [b], Christian Lohasz [a], Nassim Rousset [a], Flavio Bonanini [a], Yun Huang [b], Jean-Pierre Bourquin [b], Beat Bornhauser [b], Andreas Hierlemann [a], and Kasper Renggli [a]

a. ETH Zürich, Department of Biosystems Science and Engineering, Basel, Switzerland

b. University Children's Hospital Zürich, Department of Oncology, Zürich, Switzerland

[*] These authors contributed equally

In preparation for submission.

3.1 AUTHOR CONTRIBUTIONS

AJK*: Conceived project. Designed chip. Ran PDX experiments.

MAdG*: Designed chip. Characterized culturing media. Ran PDX experiments.

BM: Conceived project. Provided PDX samples, protocols, and clinical advice.

CL: Provided training on how to use a tilting platform. Provided advice on tilting chip designs.

NR: Developed tilting chip model.

FB: Advised and helped conduct on-chip CYP assay.

YH: Conceived project. Provided PDX cell culture advice.

JPB: Provided biobank samples.

BB: Conceived project. Provided cell culture and clinical advice.

AH: Provided experimental advice and edited manuscript.

KR: Conceived project. Provided experimental advice. Ran well-based CYP assay.

3.2 ABSTRACT

Although the survival rate of pediatric leukemia has greatly increased over the past 50 years, the outcome of some leukemia subtypes has remained dismal. Drug sensitivity and resistance testing on leukemia samples could provide important functional information to tailor treatment for high-risk patients. However, current well-based leukemia drug screening platforms are unable to integrate multi-tissue cultures, and thus cannot predict the effects of prodrugs, which require hepatic bioactivation. To address this limitation, we created a novel microfluidic drug screening platform, called leukemia-on-a-chip, that enables to culture patient-derived leukemia samples and liver microtissues within the same channel, while at the same time limiting physical interaction between the diverse cell types. We ran proof-of-concept experiments to test the susceptibility of a patient-derived sample to the prodrug cyclophosphamide. We found that the efficacy of cyclophosphamide against a patient-derived sample could be measured in our leukemia-on-a-chip platform, whereas it could not be assessed in a traditional well plate assay. Through the simplicity of the platform and ability to mimic physiologically relevant conditions on the device, the chip has the potential to be translated into the clinic for personalized therapy.

3.3 INTRODUCTION

Over the past 70 years, the drug screening process in leukemia has remained largely the same. Since the initial tests of Sidney Farber in the 1940s[1], to the tests by Emil Frei and Emil Freireich at the National Cancer Institute in the 1960s[2], drug screening processes have relied on high-throughput, brute-force testing of a library of compounds on patient leukemia samples *ex vivo*. This technique has been widely successful, and its use has been largely responsible for the massive decrease in leukemia mortality from over 90% mortality in the 1960s to 10% mortality nowadays[3]. The same high-throughput drug testing technique is still being used today to identify treatments for patients[4,5]. Currently, a focus of high-throughput drug tests is drug-repurposing studies. In such studies, new combinations and applications of previously approved drugs are identified as novel therapies[4,5]. Drug exposure experiments today are typically executed robotically in order to achieve a throughput that is impossible by manual techniques[4,5]. Nevertheless, the overall strategy remains the same in that many combinations of drugs and patient samples are tested in static well plates with the goal of finding a treatment that kills the leukemia samples.

A major pitfall of well-based experiments is that they fail to recapitulate multi-tissue interactions that exist in patients[6]. In a well-based assay, only the interaction between a patient leukemia sample and a drug are studied. In contrast, when drugs are administered in patients, a drug interacts with many tissues besides the cancerous tissue. As an example, intravenously administered drugs need to be distributed throughout the body (e.g., via blood flow), metabolized (e.g., via enzymes in the liver), excreted (e.g. via the kidney), and finally may cause organ-specific toxicity[6]. In particular, some drugs, referred to as prodrugs, require hepatic bioactivation in order to be efficacious. It is essential to include prodrugs in repurposing studies for pediatric leukemia, as one of the key compounds in treatment protocols, cyclophosphamide, is a prodrug[7,8]. Prodrugs require hepatic bioactivation by cytochrome P-450 (CYP450) enzymes in order to be efficacious[8,9]. In cancer treatment, CYP450 enzymes are necessary for the activation and inactivation of both, anticancer drugs and supportive treatment drugs[8]. For instance, epipodophyllotoxins and cyclophosphamide are anticancer drugs that require CYP450 enzymes to be activated; whereas, glucocorticoids and vincristine are anticancer drugs that require CYP450 enzymes to be inactivated[3]. Clearly, it is important to include a hepatic bioactivation compartment in platforms engineered with the goal of identifying new treatment modalities for leukemia.

Creating multi-tissue systems is possible by designing microphysiological systems (MPSs). MPSs are aimed at more closely reproducing the physiology of the human body by combining cell culture models with microfluidics[6,10–19]. MPS models can be used to achieve co-culturing of multiple cell and tissue types within the same device[6]. Furthermore, MPSs offer to mimic aspects of organ architectures, such as shape, stiffness, and surface patterns by using three-dimensional (3D) cell cultures[6]. The additional incorporation of flow allows for relevant physiological factors to be provided in a controlled manner, e.g. biochemical gradients, nutrient supply, and shear stress as it arises from blood flow. Further, MPSs enable *in vitro* drug screening with reduced volumes of biological material and reagents, and, therefore, reduced costs.

In order to design a MPS to test the effect of prodrugs on patient leukemia samples, it is important to culture leukemia cells adjacent to a metabolic compartment, so that leukemia cells can be directly exposed to both, the intermediary and final stable metabolites of a prodrug. For drug exposure studies, the leukemia cell culture and hepatic bioactivation compartments must be separated in order to avoid the cofounding effects of direct physical interaction between the various cell types in the studies. Moreover, it is essential that the MPS platform has continuous flow of media in a closed-loop system in order to prevent the dilution of liver metabolites. Nonetheless, few MPSs feature continuous circulation of media between tissues, despite its vital role in connecting organs *in vivo*[20,21]. Typically, media are pumped into one side of the chip and removed from the other, thus diluting analytes[6]. However, in order to study tissue-blood interactions, e.g., to model blood diseases or the immune system, a liquid-phase transport system with continuously circulating fluid flow is needed. Creating such a system is not trivial, as it requires maintaining the necessary humidity conditions to avoid up-concentrating salts in the on-chip media.

In the following paper, we present the first MPS platform with the ability to test prodrugs on leukemia samples. The platform improves on existing technology through its ability to (1) culture leukemia samples and 3D livers in the same system with limited physical interaction, (2) perfuse media continuously between various on-chip cell cultures without a pump, and (3) run experiments using a simple setup.

Our MPS platform, termed the leukemia-on-a-chip platform, was used to study high-risk cytogenetic subtypes of pediatric acute lymphoblastic leukemia (ALL), where there is a particularly large need for new therapies. It remains particularly difficult to find new therapies for high-risk cytogenetic subtypes of ALL due to a lack of both, robust mouse models and

patients with the disease[22,23]. Further, cell lines are not a valid model for studying ALL due to a varied genetic landscape of clinical models[23]. Because the genetic landscape of ALL is essential to characterize the prognosis of the disease, it is important to study ALL using a method that recapitulates the state of the disease in patients. For these reasons, the following paper uses a patient-derived xenograph (PDX) model as patient leukemia samples. Using the leukemia-on-a-chip platform, we achieved the first efficacy test of a prodrug against a PDX leukemia sample in a microphysiological system.

3.4 RESULTS

3.4.1 Device design

We designed a platform with the ability to test the efficacy of both, standard drugs and prodrugs, on PDX samples. In general, the platform is used to run drug exposure experiments by first generating PDX cells through xenotransplantation in mice (Fig. 1). Next, PDX samples and a drug of interest were added to the platform. Lastly, the efficacy of the drug against the PDX sample was evaluated using flow cytometry. Tissue traps were used to create a metabolic compartment for culturing primary human liver spheroids, whereas the microfluidic channel was used to culture PDX cells and a feeder layer (Fig. 2).

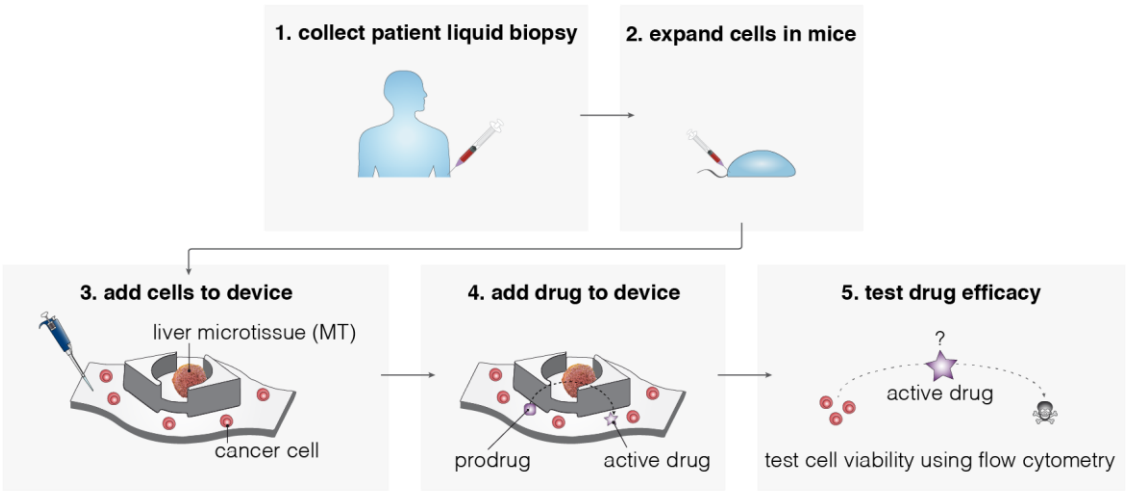

Figure 1. *Overview of drug exposure experiments using the leukemia-on-chip platform. (1) ALL samples were collected from patients. (2) Patient samples were expanded in mice, collected, and stored in a PDX ALL biobank. (3) PDX cells from the biobank were added to a chip with liver microtissues. (4) A drug was added to the device. (5) The efficacy of the drug against the PDX sample was measured using flow cytometry.*

More specifically, the platform is composed of a combination of microfluidics for cell culture and drug exposure as well as water pools for on-chip humidity control (Fig. 2A). The platform is highly modular in that it contains a single channel that connects 10 tissues traps and two media reservoirs (Fig. 2A-C). The simplicity of the platform allows users to culture both, adherent cells, such as a mesenchymal stromal cell (MSC) feeder layer, and suspension cells, such as the leukemia THP-1 cell line (Fig. S1) or PDX ALL cells. Furthermore, the modular design of the tissue traps allows any dense spheroid tissue with less than 500 µm diameter to be loaded into the chip. For instance, besides liver spheroids, we have also cultured colon-cancer-cell-line-HCT-116 and MSC spheroids on the chip, thus demonstrating the modularity of the leukemia-on-a-chip platform design.

The elevated tissue trap (Fig. 2C) is a novel design that can host single 3D spherical microtissues and is optimized to study the interaction between microtissues and cells in the microfluidic channel network. The previous culture chamber designs had semi-circle-shaped barriers at the bottom of the channel [24–26]. The previous design had been used to successfully hold microtissues in place for long term experiments, but was not suitable for use with flowing single cells, as suspension cells accumulated inside the culturing chambers. Therefore, we designed a new elevated tissue trap for the leukemia-on-a-chip platform. The new trap physically separates microtissues from the suspension cells, while still allowing for diffusion between the components. In the new culturing chamber, microtissues are cultured on an elevated platform inside an open culturing chamber (Fig. 2D #1), while suspended single cells settle down to the bottom of the device due to gravity (Fig. 2D #2-3) and then roll along the bottom of the channel. The physical barrier reduces the number of single cells entering the culturing chamber and directly interacting with the microtissues. The design includes flow-focusing structures, intended to direct single cells around the central part of the culturing chamber and to prevent cells from accumulating inside the central compartment. While direct contact between suspension cells and microtissues is limited, tissue-tissue communication (metabolites, signaling molecules) is facilitated through liquid-phase diffusion and the flow of media through the microfluidic culturing chamber.

The elevated tissue trap is essential in preventing the PDX and MSC cells from adhering inside tissue traps during cell seeding. For the PDX drug exposure studies, we cultured a PDX ALL sample and MSC feeder layer in the central microfluidic channel (Fig. 2C-E). A MSC feeder layer is an established method for increasing the viability of ALL cells *ex vivo*[27]. When testing a prodrug, such as cyclophosphamide, 3D primary human spheroid liver microtissues

were added to the chip and cultured in elevated tissue traps (Fig. 2C). During an experiment, MSCs were the first cells added to the platform. After the MSCs had adhered to the channel surface, the PDX sample was added to the chip, followed by the primary human liver spheroids. Through the use of an elevated tissue trap (Fig. 2C), we were able to successfully segregate the MSC and PDX cultures from the liver microtissues. As seen in Fig. 2E, the majority of MSCs (GFP positive) and PDX cells adhered below the tissue trap (referred as position #2 and #3 in Fig. 2D). In contrast, the liver spheroid was cultured on the trap platform (referred as position #1 in Fig. 2D). The PDX sample cells adhered to the MSC feeder layer below the tissue trap (Fig. 2E). Separation of suspension cells and microtissues during seeding and loading, respectively, was achieved through the use of the novel elevated tissue trap.

Similar to our previous devices[24–26], on-chip flow was initiated by tilting the chip. More specifically, the height difference between the two media reservoirs induced a gravity-driven flow in the major microfluidic channel in the chip[26]. For gravity-driven flow, the setup only requires a tilting stage, which can be placed inside an incubator for the duration of the experiment (Fig. S3). Neither a microscope setup nor pneumatic pumps are required. The setup is also easily parallelizable, which is important for high-throughput drug exposure experiments. More specifically, microfluidic chips were placed on a InSphero GravityFlow tilting device with a tilting angle of 2 degrees. According to a model of the effect of tilting on media flow rate, a maximum flow rate of 1.5 uL/s was estimated in the main channel of the chip (Fig. S2).

As a result of closed-loop media perfusion in the leukemia-on-chip platform, robust humidity control is essential to reduce the evaporation of water and up-concentration of analytes in the media. Several measures were taken to ensure on-chip humidity control. First, water pools were added directly to the chip (Fig. 2). On-chip liquid pools have been previously established to increase on-chip cell viability[28]. Viability was further increased through the application of a custom-designed polyester foil sticker on the top of the chip (Fig. 2B-C). Small 1-mm holes in the polyester foil promoted air-exchange between the chip and incubator environment, while simultaneously reducing water evaporation from the chip. Additionally, chips were positioned in a four-well multi-dish plate, which was placed on a tilting machine inside of a cell culture incubator (Fig. S2). Each multi-dish plate was filled with a maximum of three chips (Fig. S3). At least one well of the multi-dish was always left filled with water-saturated sodium polyacrylate gel in order to maintain a humid environment inside the multi-dish wells (Fig. S2). Through a combination of humidity control methods, we were able to

achieve comparable baseline viability of a cell line in both, a leukemia-on-a-chip device and a well plate (Fig. S1).

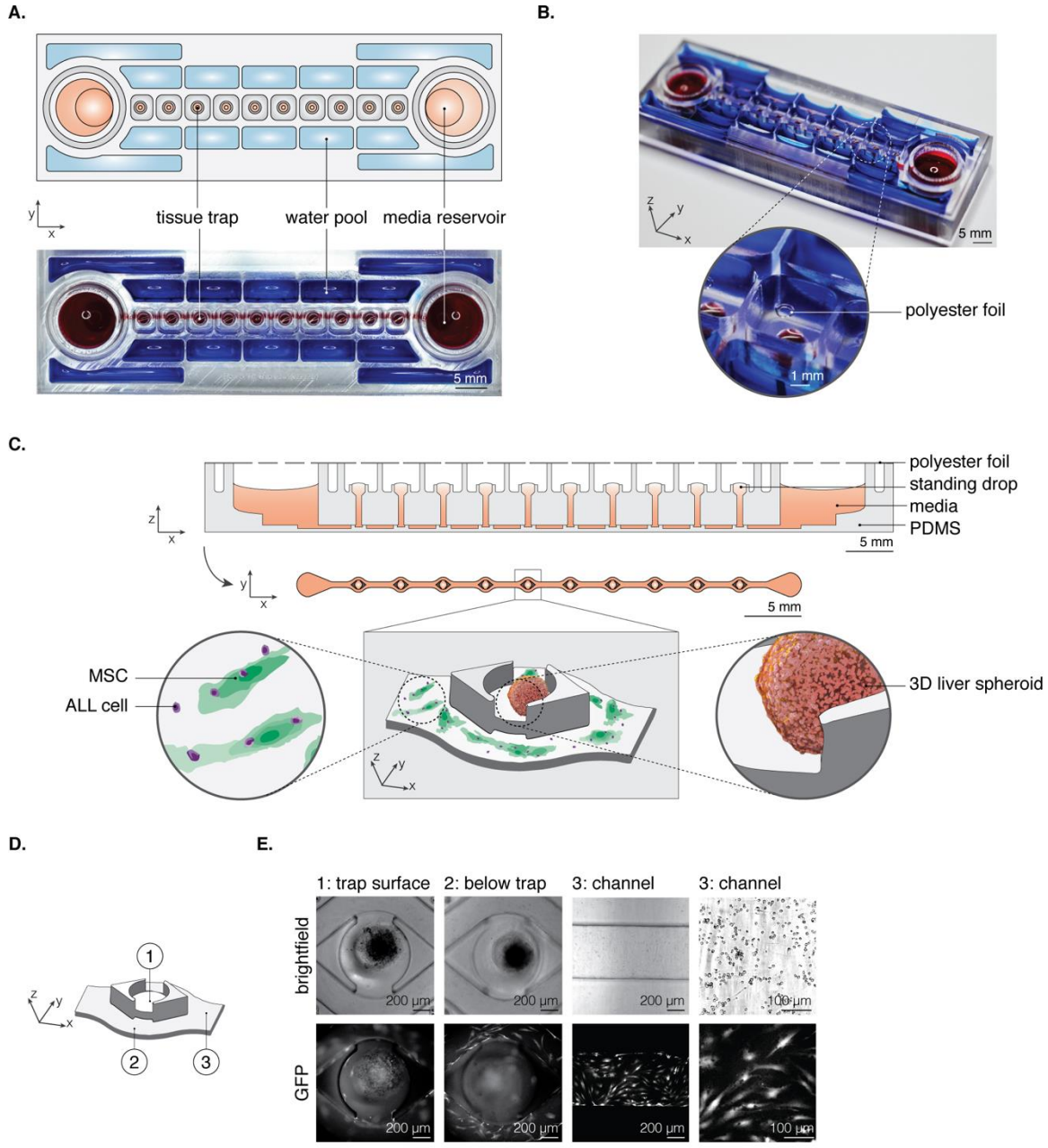

Figure 2. *Chip design overview. (A) The chip consists of two media reservoirs, 10 tissue traps, and 14 water pools. (B) The chip was operated with a polyester foil, attached to the top surface of the chip to help maintain on-chip humidity. One of the 16 custom-designed polyester-foil holes is highlighted with an arrow. (C) The chip as viewed from various sliced angles. A close-up of an elevated trap is illustrated. 3D liver spheroids were cultured on top of the elevated trap platform, whereas MSCs and PDX ALL cells were cultured directly at the bottom of the channel, below the elevated trap platform. (D) #1 points to the top of trap platform. #2 points*

to the surface below the trap. #3 points to the bottom of the channel connecting the various traps. (E) Images of the #1 elevated trap surface, #2 below the trap, #3 the channel, and #4 zoomed in photo of the channel. Both bright-field and green fluorescent protein (GFP) images are shown. MSC cells are GFP positive.

3.4.2 Characterization of cell viability in the device

One of the major challenges in creating an MPS is to identify a medium that is suitable for all tissue types in the system[29]. The medium must supply the necessary nutrients, growth factors, and hormones, required by each tissue, while, at the same time, not impairing the viability or functionality of any component. As of yet, no common universal medium has been established for culturing PDX leukemia samples, MSCs, and primary human liver spheroids together. Consequently, it was necessary to verify that the standard PDX ALL media can be used for primary human liver culture[30]. As this medium was intended to be used for prodrug experiments, it was important to verify that the liver would not only remain viable, but also remain metabolically active.

Liver viability and functionality were initially evaluated in well-plates using the traditional PDX leukemia media, AIM-V, compared to the standard human liver maintenance media, HLiMM AF. Liver viability was assessed by measuring the amount of ATP in each liver microtissue using an ATP assay. This assay has been previously used to characterize primary human hepatocyte spheroids and to assess liver toxicity in response to drugs[31,32]. Low ATP content would indicate a negative effect of the medium on liver viability. Based on ATP content, there is no significant difference in liver viability between the AIM-V and HLiMM AF media ($p > 0.05$, welch two sample t-test) (Fig. S3). Metabolic competence was evaluated in AIM-V and compared to the HLiMM AF control by measuring CYP450 activity[31]. CYP3A4, one of the members of the CYP450 family, was measured as an indicator of general CYP induction of the liver spheroids. CYP3A4 is involved in cyclophosphamide activation[33]. The equivalent CYP3A4 in both, basal and induced livers, indicated that there was no significant difference between the metabolic competence of primary human liver spheroids in AIM-V and HLiMM AF media ($p > 0.05$, welch two sample t-test) (Fig. S3). As a result, AIM-V was used in PDX ALL exposure experiments, because AIM-V medium (1) does not have a detrimental effect on liver viability, (2) does not inhibit liver functionality or metabolism, and (3) allows for direct comparison to the previously performed well-based PDX ALL experiments[5].

Liver viability and functionality were additionally validated after three days of culturing in the leukemia-on-a-chip platform. On-chip cultured livers spheroids were compared to well-plate-cultured liver spheroids. Based on a propidium iodide staining, there was no significant difference in viability between livers, cultured on-chip in medium or in the presence of cyclophosphamide and a liver cultured in medium in a well ($p > 0.05$, one way Anova test) (Fig. S4C). In contrast, a significant difference was measured between livers cultured on-chip in medium or the presence of cyclophosphamide and a dimethyl-sulfoxide (DMSO)-injured liver, cultured in a well ($p < 0.001$, one way Anova test) (Fig. S4C). A DMSO-injured liver was incubated in 50% DMSO in medium for 5 minutes in order to create a dead liver control condition. The CYP3A4 activity of livers, cultured on-chip, was not significantly different in n-fold change of metabolic activity from that of livers cultured in a traditional well-control ($p > 0.05$, welch two sample t-test) (Fig. S4B)[5]. Both livers cultured on-chip and in well-plates were metabolically active, based on a positive n-fold change in CYP3A4 activity after a three-day incubation with cyclophosphamide (Fig. S4B).

PDX ALL samples were tested for on-chip versus well-based viability. PDX samples were collected by pipetting 5 µL from the bottom of each chip reservoir (Fig. 3A). On average, 1.3% ± 0.01% of seeded PDX cells and 0.3% ± 0.003% of seeded MSCs were collected from each chip, and 0.5% ± 0.005% of seeded PDX cells and 0.1% ± 0.001% of seeded MSCs were collected from each well (average ± standard error). PDX sample viability was determined by staining cells with propidium iodide, and measuring fluorescence using flow cytometry. Using this method, we were able to achieve robust separation between live and dead cultures (Fig. S5). PDX ALL cells and MSCs were separated by their ~10-fold difference in size (Fig. 2E) using forward and side-scatter parameters. Percent viability of PDX ALL cells varies widely between patient samples. In the patient-derived ALL sample set, used by Frismantas et al., viability ranged from 69 to 94% after 96 h in culture together with an MSC feeder layer. Without the feeder, viability was between 1 and 45%[5].

Due to the high variability in PDX ALL sample viability[5], the leukemia-on-a-chip viability standards were established using a THP-1 leukemia cell line. Viability of the THP-1 cells were generally consistent, with cells cultured on-chip having a viability of 86% ± 1% and cell cultured in wells having a viability of 78% ± 2% (average ± standard error) (Fig. S1). Lastly, we evaluated the viability of PDX ALL cells on-chip versus that in standard well plates. Overall, we observed that the viability of PDX samples on-chip was lower than in a well-plate ($p < 0.05$, welch two sample t-test), with PDX samples cultured on-chip and in a well having a

viability of 50.3% ± 5.8% (n = 5) and 92.8% ± 0.4% (n = 6), respectively, after three days of culture (average ± standard error). This is likely due to the fact that the PDX culturing protocols were optimized for culturing cells under static conditions[27]. In contrast, in the leukemia-on-a-chip platform, PDX cells were cultured under flow, which is more similar to physiological conditions.

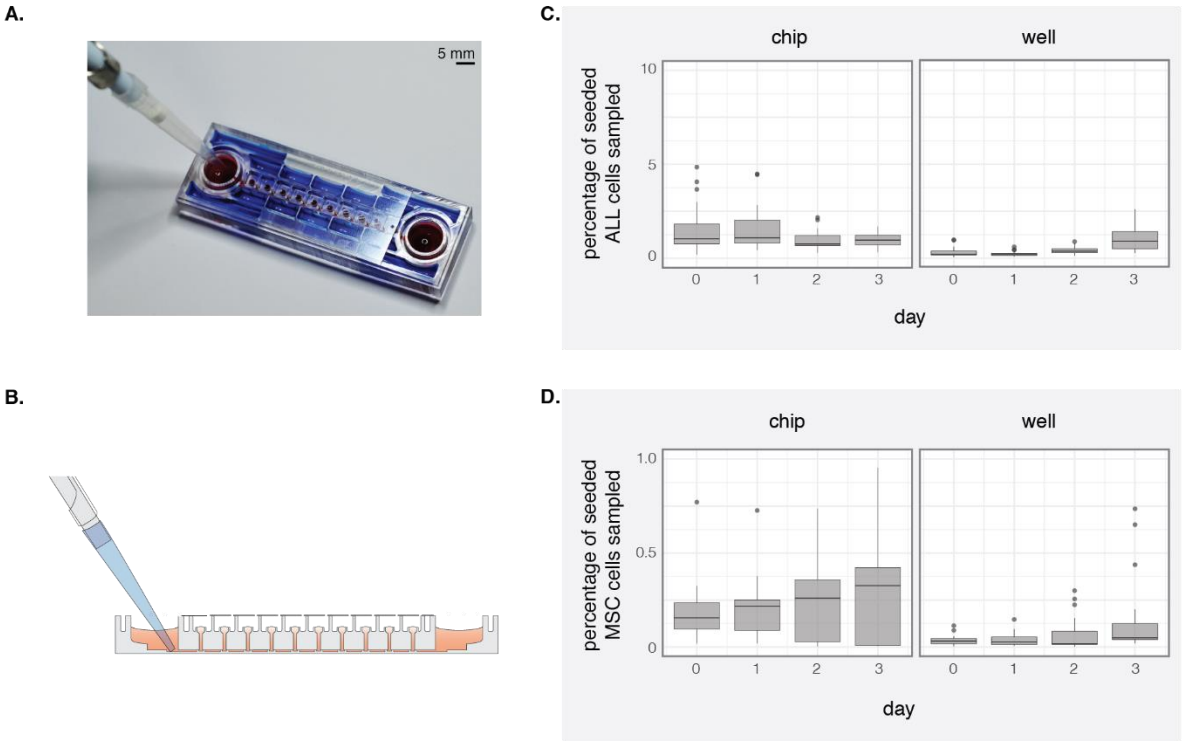

Figure 3. *Chip sampling characterization. (A) Cells were sampled from the chip by pipetting cells out of the media reservoirs. Typically, 5 µL solution was removed from each reservoir for sampling. During sampling, the polyester foil over the reservoirs was removed, and the polyester foil over the tissue traps remained on the chip. (B) When sampling cells, the pipette touched the bottom of the chip. (C) The percentage of seeded ALL cells sampled from a chip (n = 84) or a well (n = 96). (D) The percentage of seeded MSC cells sampled from a chip (n = 84) or a well (n = 96).*

3.4.3 Drug exposure tests using a non-metabolized drug compound

Next, the leukemia-on-a-chip platform was used to run a baseline drug exposure experiment with a non-metabolized drug. Doxorubicin was chosen given both, its wide application in clinics in for hematological and solid malignancies, as well as the fact that recent drug profiling experiments allow[5] for comparison with our leukemia-on-a-chip platform. Experiments were run by adding MSCs on day -2, adding ALL cells on day -1, and starting a drug exposure experiment to doxorubicin (DOX) on day 0 (Fig. S6A). Drug exposure experiments were run

both, on-chip and in a well (Fig. S6B). Doxorubicin was cultured with the ALL cells for three days. The same amount of doxorubicin was added to the chip each day; on day 0, 1, and 2, the concentration of doxorubicin was increased from 10 µM, to 20 µM and 30 µM. A baseline viability measurement was made on day 0, followed by viability measurements after each day of drug exposure, until day 3 (Fig. S6A). Similar results were obtained in both, the on-chip and well-based experiments. Specifically, the medium negative-control condition was found to have statistically significant higher ALL viability than the DOX experimental condition on day 3 in both the on-chip and well-based experiments ($p < 0.05$, Welch two sample t-test). In conclusion, we achieved similar drug exposure results in both, the on-chip and well-based drug exposure tests.

3.4.4 Drug exposure tests using a metabolized drug compound

After the chip system was validated for use with a non-metabolized drug compound, we tested the chip with a prodrug exposure experiment. In recent years, platforms have been established in hemato-oncology to profile the efficacy of drugs *ex vivo* and have helped to identify novel treatment options for patients. We chose to test the alkylating agent cyclophosphamide (CP) for a prodrug exposure experiment, given its paramount importance in the treatment of ALL. In particular, high-risk leukemias are treated with cyclophosphamide, which occur in a patient subpopulation urgently in need of personalized treatment[8]. Similar to the doxorubicin experiments, MSCs were added on day -2, and PDX ALL cells were added on day -1 (Fig. 4A). On day 0, we added 1 liver spheroid per 50 µL to both, the chip and well plates. After the livers were loaded, cyclophosphamide was added to the platforms. The same amount of cyclophosphamide was added to the platforms each day. Thus, the concentration of cyclophosphamide on day 0, 1, and 2, was 1 mM, 2 mM and 3 mM, respectively. In the on-chip experiment, perfusion occurred via tilting, and there was an exchange of cyclophosphamide metabolites via diffusion between the trap compartment and channel culturing the PDX ALL cells (Fig. 6B). In contrast, in the well-based experiments, livers and PDX ALL cells were cultured in different wells, and conditioned medium was transferred (Fig. 2B). This was done to prevent the MSCs, ALL PDX cells, and liver spheroids from physically interacting with each other. Such a control was also used in the characterization of our previously designed MPS[9]. Here, we transferred media from the liver well to the PDX well each day (Fig. 2B).

In total, four culturing conditions were tested: (1) medium, (2) medium with cyclophosphamide, (3) medium with liver tissue, and (4) medium with cyclophosphamide and

liver tissue. No significant difference was measured between conditions in the well plate ($p>0.05$, one-way Anova test). In the on-chip experiments, (1) the medium, (2) medium with cyclophosphamide, and (3) medium with liver tissue tended to have higher viability of 75% ± 7%, 66% ± 8%, and 72% ± 7%, respectively (mean ± standard error), on day 3 of the experiment. We measured a decrease in viability for the fourth condition, where cyclophosphamide was cultured with liver spheroids. In this condition, the CYP enzymes in the liver metabolize cyclophosphamide to an active form, phosphor amide mustard. In the on-chip experiment, a lower viability of 38% ± 7% was measured (mean ± standard error), and on-chip PDX ALL viability was lower than well-based PDX ALL viability (Fig. 4). This important finding is likely due to the fact that the active cyclophosphamide metabolites that act on the cancer cells are chemically not stable[34]. As the medium transfer takes some time and happened only once per day, the PDX samples in the well-based experiments were only exposed to stable metabolites of cyclophosphamide. In contrast, in the chip-based experiments, the PDX sample was continuously exposed to the full spectrum of both, unstable and stable prodrug metabolites, as PDX sample and liver were in the same liquid-phase environment. The liver microtissues, cultured in the presence of just media and media with cyclophosphamide, both on-chip and in a well, were confirmed to be viable via propidium iodide staining and metabolically active via quantification of CYP3A4 activity (Fig. S4). Thus, using the leukemia-on-a-chip platform, we achieved the first *in vitro* measurement of a prodrug, cyclophosphamide, acting on a PDX ALL sample.

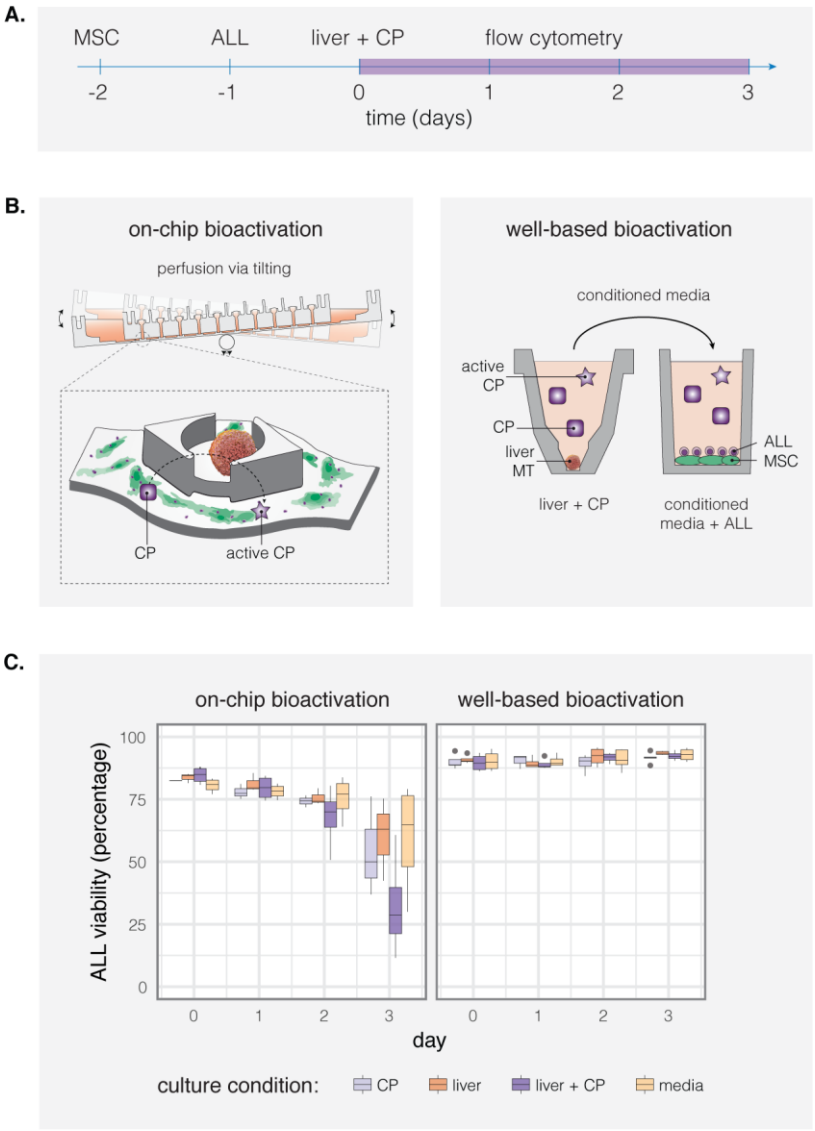

Figure 4. *The effect of cyclophosphamide (CP) on the viability of a PDX ALL sample in both, the leukemia-on-a-chip platform and a well plate. (A) On day -2, MSCs were seeded into the chip. On day -1, PDX ALL samples were seeded into the chip. Lastly on day 0, the liver microtissues were added to the cell traps, and CP was added to the chip. Viability of PDX ALL cells was measured on day 0, 1, 2, and 3 by using flow cytometry. (B) On-chip bio-activation experiments had constant perfusion via tilting. There was continuous mixing of the CP metabolites and PDX ALL sample. In contrast, in the well-based bio-activation experiment, the liver microtissues and PDX ALL samples were cultured separately to avoid physical contact. CP was added to the liver well. Once a day, medium was transferred from the liver well to the PDX ALL well. (C) ALL viability measurements for the on-chip and well-based bio-activation experiments. Specifically, the viability of PDX cells cultured with (1) media and CP (n = 3),*

(2) media and liver (n = 3), (3) media, liver and CP (n = 4), and (4) media (n = 4), were evaluated.

3.5 DISCUSSION

We developed the first microphysiological system with the ability to measure the effect of prodrugs on PDX ALL samples. The ability to culture both, PDX ALL samples and liver microtissues inside the same channel, while those remained, at the same time, physically separated, was critical to the success of our platform. In contrast to standard drug-exposure experiments, run in well plates, the leukemia-on-a-chip platform enabled to measure a decrease in PDX ALL viability in the presence of both, a prodrug and a liver microtissues.

The leukemia-on-a-chip device is a substantial improvement over existing state-of-the-art technologies in both, the MPS and PDX drug exposure fields. Previously, platforms to study how prodrugs affect cell-line tumor models were designed [9,24,25]. We even have optimized robotic systems to run high-throughput drug exposure experiments on over 60 different patient samples in one experiment[4,5]. However, these systems and the respective chips lacked the tissue trap platform architecture, needed to culture liver microtissues, PDX ALL samples, and MSC feeder layer cells, all within the same system. In other words, they lacked the metabolic competence and could not be used for experiments with prodrugs. Other published MPS have incorporated a metabolic compartment with the objective of measuring drug metabolism, but these platforms are either highly complex and thus difficult to translate into a clinic setting, and/or have not been tested using primary human tumor and liver tissues[6,35,36].

For future applications, the leukemia-on-a-chip device can be used to study not only drug metabolism and efficacy, but also tissue-specific toxicity. Our platform is highly modular in the types of cells and tissues that can be cultured in the system. The platform consists of 10 tissue traps that can hold any dense tissue spheroid of less than 500 µm diameter (Fig. 2C), and a simple channel that can culture both, suspension and adherent cell types. In this proof-of-concept study, we used the leukemia-on-a-chip device to measure the efficacy of prodrugs on PDX ALL samples. Consequently, the tissue traps were filled with primary human liver spheroids. In the future, the system can be repurposed to evaluate other types of cell and tissue interactions, in addition to drug metabolism and efficacy studies. For instance, cardiac spheroids[37] could be cultured in the platform in order to study drug efficacy, metabolism, and cardiotoxicity.

The leukemia-on-a-chip device demonstrates a breakthrough in both, MPS and PDX drug exposure technology, by enabling to measure the effect of a prodrug on a PDX sample. The simplicity and modularity of the platform makes the leukemia-on-a-chip platform suitable for transfer into clinical settings. Nevertheless, before the platform can be used to advise treatment decisions, it is essential that the throughput of the device is increased in order to improve statistical confidence in the measured results. Currently, only 12 chips can be run simultaneously due to manual constraints, caused by the multiple pipetting steps needed to operate each device. Further, PDMS as chip material has a well-established history of ad/absorbing hydrophobic compounds[38,39]. Thus, before creating devices for the clinic, it is necessary to manufacture the devices from a more inert material, such as polystyrene or polycarbonate, in order to run drug exposure experiments on both hydrophobic and hydrophilic compounds[38,39].

Drug profiling helps to identify patients benefiting from new drugs[5]. However, it was yet impossible to test prodrugs with the current systems. We have shown compelling evidence that we can predict the sensitivity of PDX samples against cyclophosphamide using the leukemia-on-a-chip platform. Given the broad use of cyclophosphamide in many subtypes of ALL, such as the difficult to treat T-cell ALL, identifying patients benefiting from cyclophosphamide is of particular interest and can have clinical implication. At the same time, given the side effect profile of cyclophosphamide, patients that are not sensitive to the drug can be treated with an alternative drug regimen.

The simple experimental setup of the leukemia-on-a-chip platform gives it the potential to be translated into the clinic with a minimally changed protocol. The only equipment needed is a tilting machine, a cell-culture incubator, and a flow cytometry machine. These are all standard equipment that can be found in large hospitals. Given the growing interest of clinicians in *ex vivo* drug profiling and its clinical application, our platform represents an important milestone in expanding the scope of possible drugs to test.

3.6 METHODS

3.6.1 Device Fabrication

3.6.1.1 Top mold design and manufacturing procedure

3D printed molds were designed using Autodesk Inventor 2018 software. The molds were printed by Protolabs (Feldrichen, Germany) using Accura SL 5530 material and a natural finish. A post-processing thermal bake was used. The mold design is shown in Figure S7.

3.6.1.2 Bottom mold design and manufacturing procedure

Bottom molds were designed using AutoCAD Mechanical 2015. Transparency masks were printed by Selba SA (Versoix, Switzerland) with a resolution of 50,800 dpi. Two masks were used. Mask #1 contained the outline of the cell traps, platform inside the cell trap, and channel. Mask #2 contained the channel and the rim of the cell traps. Photolithography was used to produce the bottom mold on 4-inch silicon wafers. The bottom mold was made with SU-8 100 (MicroChem, Westborough, MA USA). The SU-8 100 was spun at a final speed of 1500 rpm for a 250 μm height of SU-8. The wafers were then prebaked at 65º C for 30 min and soft-baked at 95º C for 90 minutes. Subsequently, the wafers were exposed using mask #1, and then baked in a post-exposure bake of at 65º C for 5 min and then 95º C for 30 minutes. Next, a similar process was repeated for the second SU-8 layer of the wafer. The SU-8 100 was spun at a final speed of 2000 rpm for a 150 μm height of SU-8. The wafers were then prebaked at 65º C for 30 min and soft-baked at 95º C for 90 minutes. Subsequently, the wafers were exposed using mask #2, and then underwent a post exposure bake at 65º C for 5 min and 95º C for 30 minutes. Lastly, the wafers were developed using MR Dev 600 Developer (Micro Resist Technology GmbH, Berlin, Germany).

3.6.1.3 PDMS device production

Before using the top and bottom molds for the first time, the molds were silanized using 20 μL of silane (Trichloro(1H,1H,2H,2H-perfluorooctyl) silane) in a vacuum for 2 hours. Next, scotch magic tape (4.977.763, Lyecro, Dietikon, Switzerland) was taped around the outside of the top mold. Subsequently, 25 g of 1:10 Sylgard PDMS (Sylgard® 184, Sigma-Aldrich, Buchs, Switzerland) were cast onto each top mold. 12 g of 1:10 PDMS were cast onto each bottom mold. The PDMS top and bottom molds were then degassed in a dedicator for at least 1 hour. The chips were cured in an 80º C oven overnight. After curing, the PDMS chips were carefully removed from the molds. The tissue trap columns and reservoirs of the top mold were

then punched with a 0.5 mm and 6 mm biopsy punch, respectively. The top and bottom molds were aligned and bonded after plasma treatment for 20 seconds at 45W (Femto #112296, Diener electronic GmbH + Co. KG, Ebhausen, Germany), and baked overnight at 80°C.

3.6.2 Device preparation

3.6.2.1 Chip setup

Before starting an experiment, the chips were UV-treated for 1 hr. The chips were then placed in a sterile Thermo Scientific™ Nunc™ cell-culture-treated 4-well multidish box (#167063, ThermoFisher Scientific, Reinach, Switzerland). One well of each box was filled with humidity gel (sodium polyacrylate; Sigma-Aldrich, Buchs, Switzerland), mixed with autoclaved DI water. The leukemia-on-a-chip devices were placed in the other three wells of the box (Fig. S2).

3.6.2.2 Chip biolipidure coating for THP-1 suspension cell culture

For experiments without an MSC feeder layer at the bottom of the channel, the chip was treated with Biolipidure (NOF America Corp., White Plains, New York, USA). Biolipidure is used to block cells from adhering to PDMS. The chip was first treated with oxygen plasma for 45 s at 50 W, 0.5 bar O_2. 100 µL of biolipidure were then added to the reservoir of each chip. After a 30 min incubation at room temperature, the biolipidure was aspirated from the chip, and the chip was left to dry overnight in the sterile cell-culture hood.

3.6.2.3 Chip fibronectin coating for MSC and PDX adherent cell culture

For experiments requiring a MSC feeder layer, the chip was first treated with oxygen plasma for 45 s at 50 W, 0.5 bar O_2 to render the surface hydrophilic, and, then, the chip was coated with fibronectin to improve MSC adhesion to the PDMS. Fibronectin (FC010, Milipore, Zug, Switzerland) was diluted in DPBS +Ca +Mg (Thermo Fisher Scientific, Reinach, Switzerland) to a final concentration of 50 µg/mL. The solution was mixed gently, avoiding any vortexing or spinning due to fibronectin's susceptibility to shear stress. 100 µL of fibronectin solution were added to each reservoir of the chip. The chip was incubated for 90 min at 37°C, 95% humidity, and 5% CO_2 in a cell culture incubator. After the incubation, the excess fibronectin was flushed out with fresh media by adding 100 µL to one reservoir and removing the same volume from the other reservoir, until the entire contents had been replaced. The washing of media through the chip was repeated three times.

3.6.2.4 MSC seeding for chip-and well-based experiments

45,000 and 52,000 MSC cells were seeded per chip and well, respectively. To seed MSC cells into the chip, cells were re-suspended in a solution of 320,000 MSC cells/mL AIM-V media (Thermo Fischer Scientific, Reinach, Switzerland), and 5 μL of this solution was added to each of the two chip reservoirs.

After the MSC cells were added to the chip, the water pools were filled with 1 mL sterile diH_2O per chip. Then, three pieces of custom-designed polyester film were attached to each chip (Fig. 2) in order to prevent evaporation of water from the chip. The chip was then tilted back and forth to mix the cells in the channel. The chip was afterwards placed on a flat surface in a cell culture incubator at 37°C, 95% humidity, and 5% CO_2 for 24 hours.

To seed MSC cells in a well plate, 100 μL of a 520,000 MSC cells/mL MSC cell solution were added to each well (237105, Thermo Scientific Nunc™ F96 MicroWell™ Polystyrene Plate, Thermo Fisher Scientific, Reinach, Switzerland). The chip was then placed on a flat surface in a cell culture incubator at 37°C, 95% humidity, and 5% CO_2 for 24 hours.

3.6.2.5 PDX ALL seeding for chip-and well-based experiments

PDX ALL cells were not subcultured and were added directly to experiments after thawing. PDX ALL cells were stored in a liquid nitrogen tank until the start of an experiment. To thaw PDX ALL cells, cells were thawed in a cell culture incubator at 37°C for 5 minutes. Next, the contents of the vial were transferred to a 50 mL tube. The old cell vial was washed with 1 mL fresh MSC media (described in the cell culture section), and this 1 mL of media was then slowly added to the 50 mL tube containing the cells at rate of 1 drop per 5 seconds. 5 mL of room temperature MSC media was gently added to the vial with 1 drop of media added every 2 seconds. It is important to add the room temperature media slowly to the PDX ALL cells to avoid osmotic shock. Next, the cells were spun down for 5 minutes at 200g. The supernatant was aspirated, and 1 mL fresh AIM-V media was mixed with the cell pellet. Next, a solution of 100,000 PDX ALL cells/mL was prepared. 20 μL PDX ALL solution were added per reservoir of the chip, and the chip was tilted back and forth briefly to mix the cells in the channel. 10 μL of the PDX ALL solution were added per well. After loading the PDX ALL cells, the chips and well plates were then placed on a flat surface in a cell culture incubator at 37°C, 95% humidity, and 5% CO_2 for 24 hours. After 24 hours, the chip-based tilting protocol began.

3.6.2.6 Liver microtissue on-chip seeding and culture

The protocol for loading liver microtissues into traps was described in detail previously[24,25]. In brief, liver microtissues were rapidly pipetted up from a InSphero GravityTRAP™ Ultra-Low Attachment (ULA) microplate (ISP-09-001, PerkinElmer, USA). After pulling a microtissue into a pipette tip, the microtissue can be been seen by the experimenter, and the microtissue was observed until it sedimented to the bottom of the pipette tip. Subsequently, the pipette tip was placed on a funnel-shaped microtissue loading port in a perpendicular position[24,25]. It is essential to keep the pipette tip in this position for at least 5 seconds, to ensure enough time for the microtissue to fall into the chip. The loading of microtissues was then confirmed using bright-field microscopy.

3.6.2.7 On-chip tilting protocol

One day after loading PDX ALL cells, leukemia-on-chip platforms were moved from an incubator shelf to the InSphero GravityFlow tilting stage (Figure S2). The tilting device was operated with a tilting angle of 2°, a hold time of 5 seconds, and a transition time of 60 seconds.

3.6.2.8 Drug exposure experiment protocol

3.6.2.8.1 On-chip sampling protocol

First, the reservoir foils were removed from each chip. Next, 50 µL of media were removed from each chip. The bottom of the reservoirs was then scratched with a pipette tip. Next, 5 µL of cell solution were sampled from each reservoir and pooled into a single Eppendorf tube. If required, cyclophosphamide or doxorubicin was added to the chip according to the protocol in Section "1.6.2.8.4 experimental drug dosing regimen" below. Lastly, 60 µL of fresh and warmed AIM-V media were added back into the chip. Then, the water pools were filled with sterile diH_2O, new reservoir foils were applied on the top of each chip, and the chips were placed back onto a InSphero GravityFlow tilting stage inside a cell culture incubator at 37°C, 95% humidity, and 5% CO_2.

3.6.2.8.2 Well-based sampling protocol for wells without a liver condition

10 µL media were removed from each well. Next, the bottom of each well was scratched with a pipette tip. Then, 10 µL of cell solution from each well were placed into a separate Eppendorf tube. If required, cyclophosphamide or doxorubicin was added to the chip according to the protocol in Section "1.6.2.8.4 experimental drug dosing regimen" below. Lastly, 20 µL of fresh and warmed AIM-V media were added back into the well. Then, the well plates were placed back into a cell culture incubator at 37°C, 95% humidity, and 5% CO_2.

3.6.2.8.3 Well-based sampling protocol for wells with a liver condition

80 µL media were removed from each well. Next, the bottom of each well was scratched with a pipette tip. Then, 10 µL of cell solution from each well were placed into a separate Eppendorf tube. 70 µL media from the liver microtissues, cultured in a InSphero GravityTRAP™ Ultra-Low Attachment (ULA) microplate, were added to the well. The 70 µL AIM-V media in the InSphero GravityTRAP™ Ultra-Low Attachment (ULA) microplate were then replaced with fresh AIM-V media. If required, cyclophosphamide or doxorubicin was added to the chip according to the protocol in Section "1.6.2.8.4 experimental drug dosing regimen" below. Lastly, 20 µL of fresh and warmed AIM-V media were added back into the chip. Then, the well plates were placed back into a cell culture incubator at 37°C, 95% humidity, and 5% CO_2.

3.6.2.8.4 Experimental drug dosing regimen

When required, cyclophosphamide (cyclophosphamide monohydrate ISOPAC, C7397, Sigma-Aldrich, Buchs, Switzerland) was added to each reservoir and/or well. A 143 mM solution of cyclophosphamide in diH_2O was prepared, and 0.7 µL and 1.4 µL of the solution were added to each reservoir of the chip and each well, respectively. When required, doxorubicin (doxorubicin hydrochloride, D1515, Sigma-Aldrich, Buchs, Switzerland) was added to each reservoir and/or well. A 10 mM doxorubicin solution in DMSO was prepared, and further diluted to 100 µM using AIM-V media. Then, 20 µL and 10 µL of 100 µM doxorubicin were added to each reservoir of a chip and each well, respectively.

3.6.2.9 Flow cytometry

Directly before beginning flow cytometry analysis, propidium iodide solution (P4864, Sigma-Aldrich, Buchs, Switzerland) was added to prepared Eppendorf tubes containing cell samples at a concentration of 1 µg/mL, diluted in a total volume of 200 µL AIM-V media. Flow cytometry was performed on a BD LSRFortessa™ cell analyzer (BD Biosciences, Allschwil, Switzerland). PI was assessed with the 561 nm (yellow/green) laser, with a 600 nm long pass filter, and a 610/620 nm band pass filter. Analysis was completed using FlowJo software (FlowJo, LLC, Ashland, Oregon, USA), with further downstream analysis completed with custom scripts in R.

3.6.2.10 Chip cleaning protocol after each experiment

After an experiment, the chip could be cleaned and re-used for a new experiment. First, all cells and media were removed, then the channel was washed with PBS. 500 µL trypsin were added via the inlet ports, and the chip was incubated at 37°C for approximately 30 min. The trypsin

was removed, and the chip was rinsed twice with EtOH, followed by a 10-minute sonication in diH_20. Before using the chip again, it was treated with UV-light and re-coated with either biolipidure or fibronectin.

3.6.3 Cell culture

3.6.3.1 THP-1

THP-1 (TIB-202; ATCC, Manassas, VA, USA) cells were cultured according to standard American Type Culture Collection (ATCC) protocols, and maintained in RPMI-1640 (RPMI; PAN-Biotech GmbH, Aidenbach, Germany), supplemented with 10% (v/v) fetal bovine serum (FBS; Sigma-Aldrich, Buchs Switzerland), 100 µg/mL Penicillin, 10 µg/mL Streptomycin (Sigma-Aldrich, Buchs, Switzerland), and 0.05 mM 2-mercaptoethanol (Life Technologies, Carlsbad, CA, USA). The medium was passed through a 0.2 µm filter (Thermo Fisher Scientific, Reinach, Switzerland) to remove any protein aggregates or contaminants. The cells were also cultured in AIM-V (Thermo Fischer Scientific, Reinach, Switzerland) by the same methods. In both cases, cells were kept in non-adherent flasks (Greiner Bio-One, Frickenhausen, Germany) at 37 °C, 5% CO_2, and 95% humidity. The cells were subcultured every 2 to 3 days at a ratio of 1-3:5 to maintain a density of 2 x 10^5 to 1 x 10^6 cells/mL.

For long term-storage, cells were frozen in complete growth medium, supplemented with 10% (v/v) dimethyl sulfoxide (DMSO; Sigma-Aldrich, Buchs, Switzerland) at a concentration of 2 x 10^6 cells/mL. Cells were first cooled down to -80 °C at a controlled rate of -1 °C/min using a Mr. Frosty freezing container (Thermo Fisher Scientific, Reinach, Switzerland), filled with isopropyl alcohol, then transferred to liquid-nitrogen storage after 24 hr.

THP-1 could be counted by hand with a hemocytometer or with a TC20 Automated Cell Counter (Bio-Rad, Hercules, CA, USA). In both cases, Trypan blue (Invitrogen, Carlsbad, CA, USA) was used to assess viability.

3.6.3.2 MSCs

GFP-tagged h-TERT immortalized human bone marrow-derived mesenchymal stromal cells (MSCs) were used as a feeder layer for the patient-derived ALL samples. MSCs were thawed and cultured according to standard cell-culture protocols. MSCs were maintained in RPMI-1640 w/o L-glutamine (Bioconcept AG, Allschwil, Switzerland), supplemented with 10% heat-inactivated fetal bovine serum (hiFBS; Invitrogen, Carlsbad, CA, USA), 2mM L-glutamine (Glutamax; Thermo Fisher Scientific, Reinach, Switzerland), and 100 IU/ml P/S. For long-

term culture maintenance, 1 μM hydrocortisone (HC; Sigma-Aldrich, Buchs, Switzerland) was added fresh to each flask. The cells were maintained at 37 °C, 5% CO_2, and 95% humidity.

For long-term storage, cells were frozen in heat inactivated fetal bovine serum (hiFBS) with 10% (v/v) DMSO at a concentration of 2 x 10^6 cells/mL. Cells were first cooled down to -80 °C at a controlled rate of -1 °C/min using a Mr. Frosty freezing container, filled with isopropyl alcohol, then transferred to liquid nitrogen storage after 24 hrs.

3.6.3.3 ALL PDX cells

ALL PDX cells were not subcultured and thawed directly before experiments[5]. The protocol for thawing ALL PDX cells is described in the material and methods section titled "device preparation."

3.6.3.4 Liver spheroids

3D InSight™ Human Liver Microtissues (multi-donor hepatocytes, co-culture with Kupffer cells and LECs, MT-02-302-04, InSphero AG, Schlieren, Switzerland) were cultured using 3D InSight™ Human Liver Maintenance Media - AF (HLiMM AF; InSphero AG, Schlieren, Switzerland) in GravityTRAP Ultra-Low Attachment (ULA) plates (InSphero AG, Schlieren, Switzerland) at 37 °C, 5% CO_2, and 95% humidity. Media were changed every 2-3 days.

3.6.4 Modeling

The finite element method (COMSOL Multiphysics® Version 5.3a; COMSOL, Inc., Burlington, MA, USA) was used to model the hanging-drop network. The laminar-flow-rate module and parametric sweeps were used to find the net forces on spherical samples at the air liquid interface. The flow-rate model for the tilting platform was made using MATLAB Version R2016a (MathWorks, Natick, MA, USA).

3.7 SUPPLEMENTARY MATERIALS AND METHODS

3.7.1 Modeling flow rates in the tilting chip

Flow in the tilting chip is driven by gravity and depends on a number of factors, including tilting angle (θ), hold time (t_{HOLD}), transition time (t_{TRANS}), and the channel dimensions. Changing the flow rates in the chip can be done by changing the design, specifically, changing the resistance in the chip, or adjusting the tilting protocol. Flow rates in the tilting chip were modeled to optimize the tilting protocol and better understand the motion of flowing single cells in the channel.

The chip was modeled as a channel of rectangular cross section with a reservoir of circular cross section at each end. The channel and the reservoirs were connected by punched holes of circular cross section. Resistance through each part was calculated.

Hydraulic resistance for channel of circular cross section with length L and radius r:

$$R_{hyd} = \frac{8\mu L}{\pi r^4}$$

Hydraulic resistance for channel of rectangular cross section with length L, width w, and height h, where h<w (μ is the viscosity of water at 37°C):

$$R_{hyd} = \frac{12\mu L}{wh^3(1 - \frac{0.630h}{w})}$$

Since the channels and reservoirs are connected in series, the total hydrodynamic resistance through the chip was the sum of the resistance through each part.

$$R_{hyd} = R_{reservoir1} + R_{inlet} + R_{channel} + R_{outlet} + R_{reservoir2}$$

Since the inlet and outlet have the same resistance, and since any change in height Δh of one reservoir is equal to $-\Delta h$ the other reservoir, this can be rewritten as:

$$R_{hyd}(t) = 2R_{res} + 2R_{inlet} + R_{channel}$$

Flow rate Q is defined as a function of pressure and resistance over time.

$$Q(t) = \frac{\Delta P(t)}{R_{hyd}(t)}$$

In the tilting chip, the reservoirs are open to atmospheric pressure on both sides. The difference in pressure comes from the difference in height of the liquid in the reservoirs. This is affected by both, the tilting angle and the flow of liquid from one reservoir to the other.

$$\Delta P(t) = \rho g \Delta h$$

If the chip is tilted from -θ to +θ over a non-zero transition time, the flow rate must be solved for numerically. Figure S2C shows the flow rates for one period of the tilting protocol with a tilting angle of 2°, hold time of 5 s, and transition time of 5 s.

3.8 SUPPLEMENTARY FIGURES

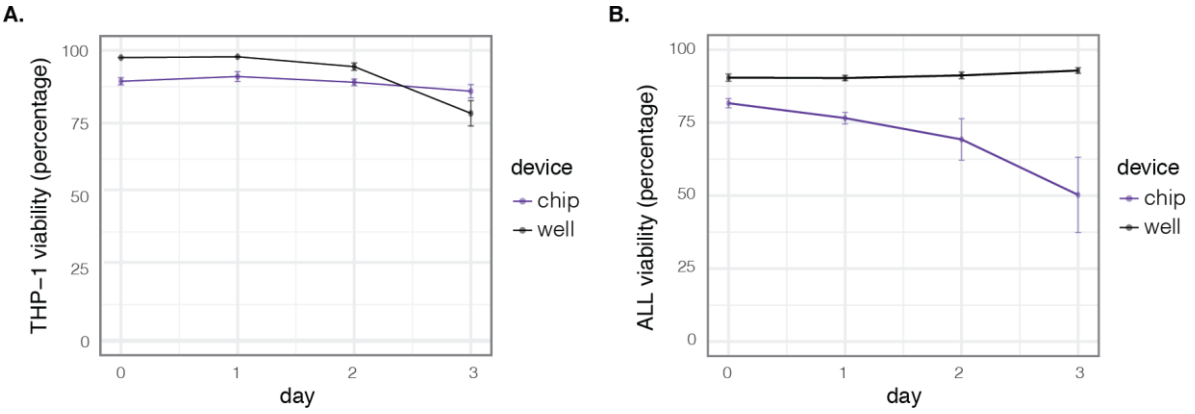

Figure S1. *Baseline THP-1 cell line and PDX ALL viability. (A) THP-1 cells were cultured on the leukemia-on-a-chip platform (n = 4) or in a well plate (n = 6) for three days. The viability of cells was measured each day using a propidium iodide staining and flow cytometry. (B) PDX ALL cells were cultured on the leukemia-on-a-chip platform (n = 5) or in a well plate (n = 6) for three days. The viability of cells was measured each day using a propidium iodide staining and flow cytometry. Error bars indicate standard deviations.*

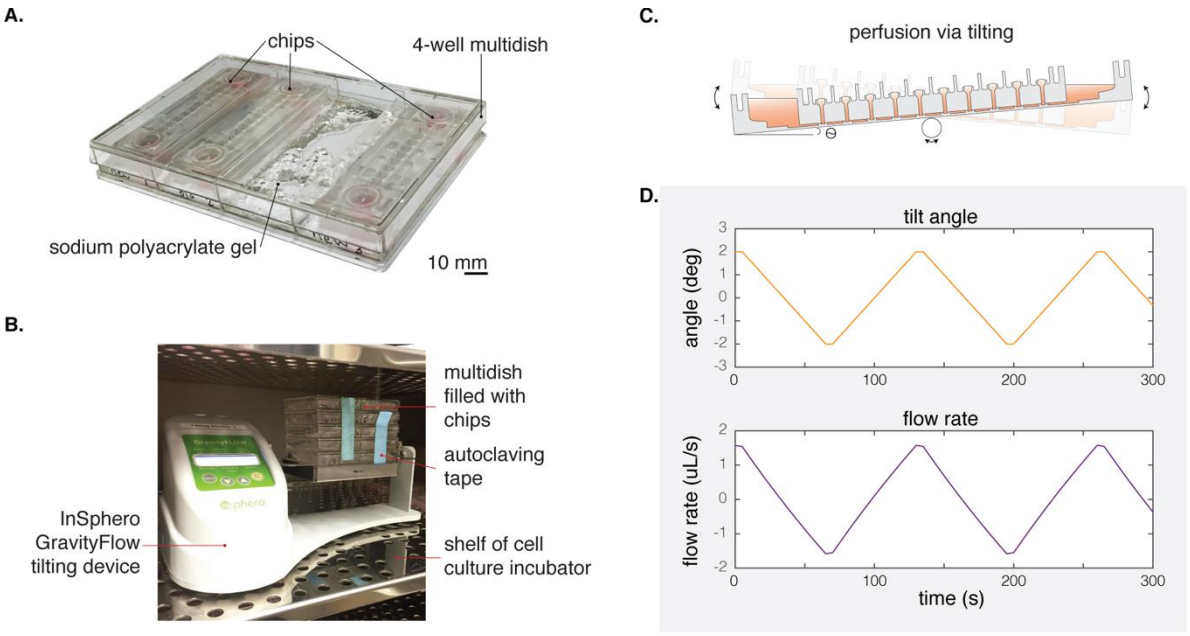

Figure S2. *Experimental setup and perfusion method. (A) For an experiment, three chips were added to a 4-well multidish plate. One well of the multidish plate was always filled with water-saturated sodium polyacrylate gel for humidity control. (B) Chip-filled multi-dish plates were kept on an InSphero GravityFlow tilting device inside of a cell culture incubator for the duration of experiments. (C) The leukemia-on-a-chip platform featured medium perfusion by means of tilting the chip. (D) A model of the effect of a tilting protocol on the flow rate of medium through the central channel of the chip. The tilting chip model is described in the Supplementary Methods.*

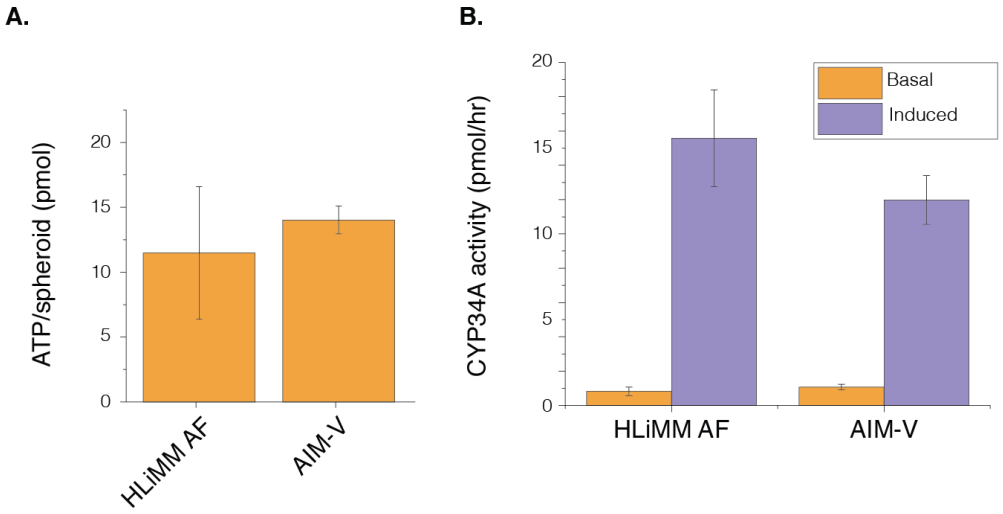

Figure S3. *Liver viability and functionality in common media. (A) Liver spheroid ATP content after 8 days in liver maintenance media, HLiMM AF, or PDX standard media, AIM-V (n=3). The error bars represent standard deviations. (B) CYP3A4 after induction with 10 µM Rifampicin on liver spheroids, cultured in either HLiMM AF or AIM-V for 5 days (n=16). The error bars represent standard errors of the mean.*

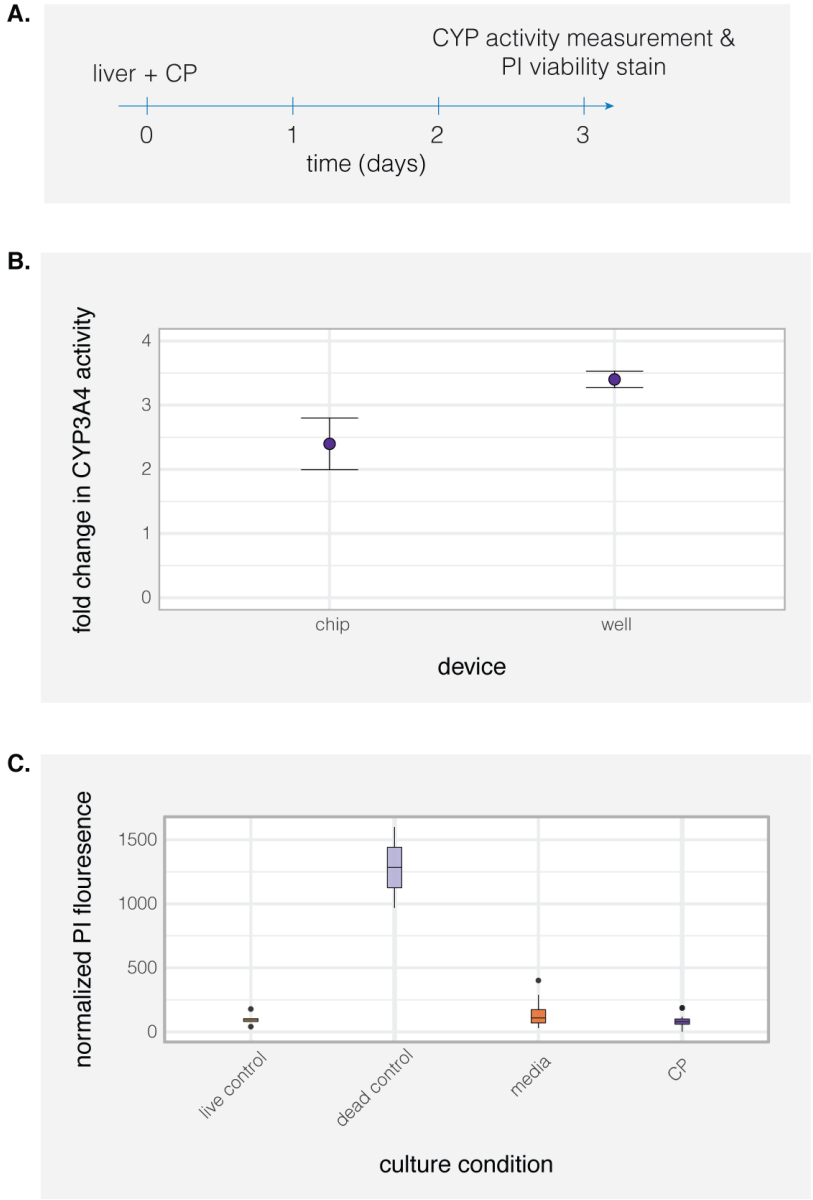

Figure S4. *On-chip cultured livers are metabolically active and viable. (A) On day 0, livers were loaded into the chip tissue traps or into well plates. Cyclophosphamide (CP) was added to the chips and wells. After three days of culture, the functionality and viability of the livers were assessed through (B) CYP3A4 and (C) propidium iodide (PI) staining, respectively. In (B) bars indicate standard deviations.*

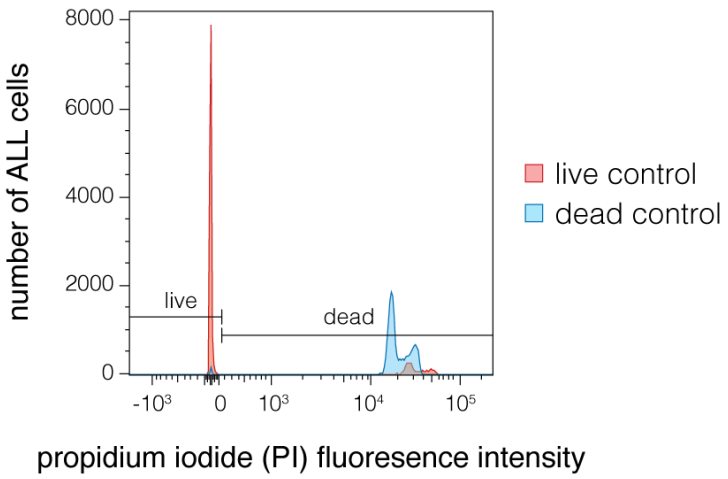

Figure S5. *Flow cytometry propidium iodide (PI) viability gating. Freshly thawed PDX ALL cells (live control) or DMSO-incubated PDX ALL cells (dead control) were stained with PI. Florescence was measured using flow cytometry.*

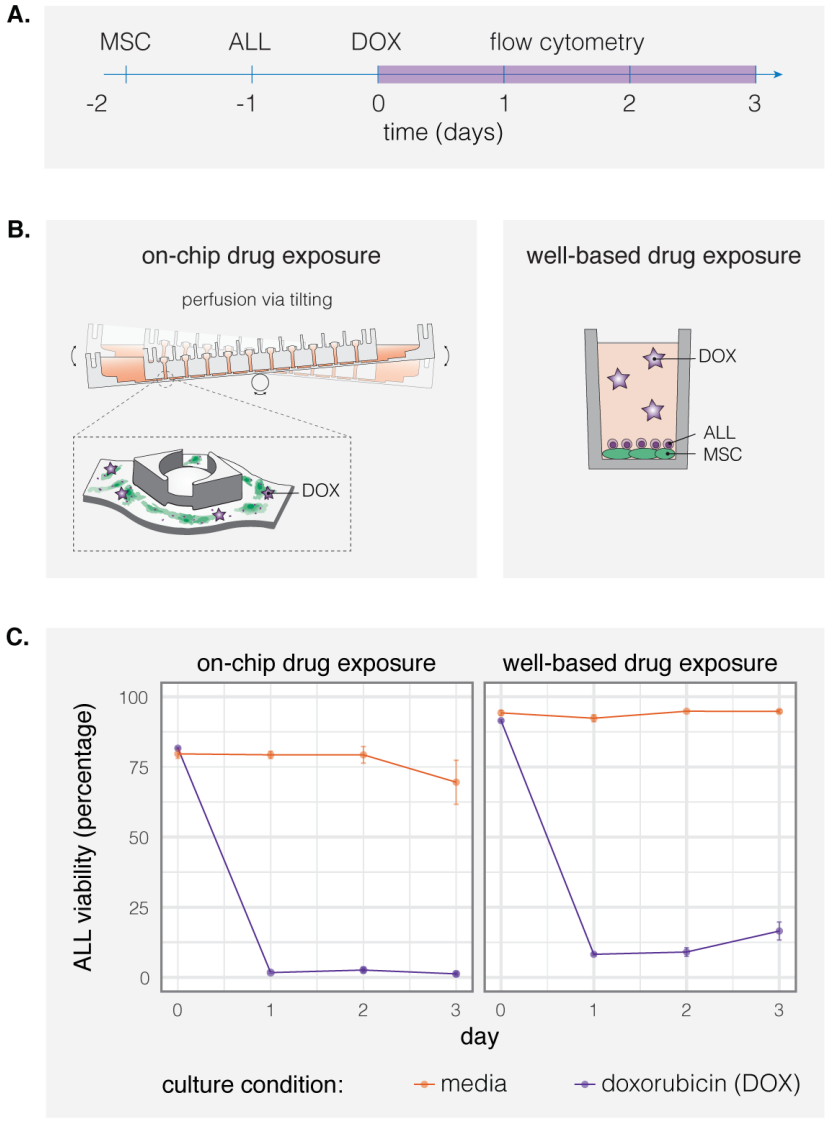

Figure S6*. The effect of doxorubicin (DOX) on the viability of a PDX ALL sample in both, the leukemia-on-a-chip platform and a well plate. (A) On day -2, MSCs were seeded into the chip. On day -1, PDX ALL samples were seeded into the chip. Lastly on day 0, DOX was added to the chip. Viability of PDX ALL cells was measured on day 0, 1, 2, and 3 using flow cytometry. (B) On-chip experiments had constant perfusion via tilting. In contrast, the well-based experiment was run statically. (C) ALL viability measurements for the on-chip and well-based experiments. Specifically, the viability of PDX cells, cultured with (1) media, and (2) media and DOX, were evaluated. Bars indicate standard deviations.*

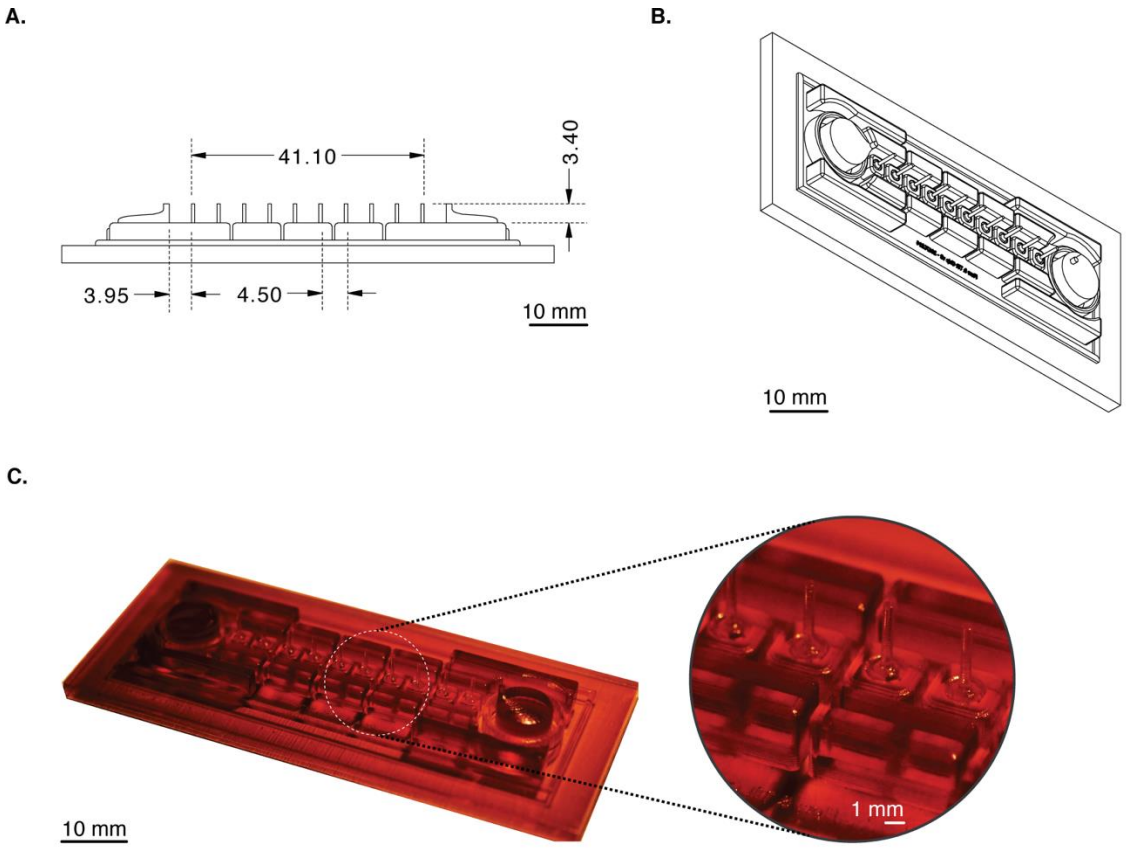

Figure S7. *3D-printed mold used for tissue trap and reservoir production. (A) A CAD drawing of the design of the mold used to produce the tissue traps and reservoirs. (B) A side-view of the mold. (C) A photo of the mold. The zoomed-in photo shows long columns that were produced to connect the tissue loading ports to the tissue traps inside the chip.*

3.9 ACKNOWLEDGEMENTS

We would like to thank Dr. Olivier Frey from InSphero AG for advice on the on-chip liver activity. Dr. Mario Modena and Ketki Chawla from ETH Zurich provided advice on experimental design. Further, we would like to Verena Jäggin, Dr. Gumienny Aleksandra, Telma Lopes, and Dr. Tom Lummen from the D-BSSE Single-Cell Facility for help with flow cytometry analysis and microscopy. An ERC Advanced Grant (AdG 694829 “neuroXscales”) and Personalized Health and Related Technologies Grant (PHRT-309) contributed to funding this research.

3.10 REFERENCES

1. Farber, S., Diamond, L. K., Mercer, R. D., Sylvester, R. F. J. & Wolff, J. A. Temporary remissions in acute leukemia in children produced by folic acid antagonist, 40aminopteroyl-glutamic acid (aminopterin). *N. Engl. J. Med.* **238,** 787–793 (1943).

2. Chabner, B. A. & Roberts, T. G. Timeline: Chemotherapy and the war on cancer. *Nat. Rev. Cancer* **5,** 65–72 (2005).

3. Hunger, S. P. & Mullighan, C. G. Acute Lymphoblastic Leukemia in Children. *N. Engl. J. Med.* **373,** 1541–1552 (2015).

4. Peirs, S. *et al.* Targeting BET proteins improves the therapeutic efficacy of BCL-2 inhibition in T-cell acute lymphoblastic leukemia. *Leukemia* **03,** 3 (2017).

5. Frismantas, V. *et al.* Ex vivo drug response pro fi ling detects recurrent sensitivity patterns in drug-resistant acute lymphoblastic leukemia. *Blood* **129,** e26–e38 (2017).

6. Bhatia, S. N. & Ingber, D. E. Microfluidic organs-on-chips. *Nat. Biotechnol.* **32,** 760–772 (2014).

7. Chang, J. E. *et al.* Augmented and standard Berlin-Frankfurt-Münster chemotherapy for treatment of adult acute lymphoblastic leukemia. *Leuk. Lymphoma* **49,** 2298–2307 (2008).

8. Pui, C.-H. & Evans, W. E. Acute Lymphoblastic Leukemia. *N. Engl. J. Med.* **339,** 605–615 (2004).

9. Frey, O., Misun, P. M., Fluri, D. A., Hengstler, J. G. & Hierlemann, A. Reconfigurable microfluidic hanging drop network for multi-tissue interaction and analysis. *Nat. Commun.* **5,** 1–11 (2014).

10. Park, T. H. & Shuler, M. L. Integration of cell culture and microfabrication technology. *Biotechnol. Prog.* **19,** 243–253 (2003).

11. Benam, K. H. *et al.* Engineered In Vitro Disease Models. *Annu. Rev. Pathol. Mech. Dis. Vol 10* **10,** 195–262 (2015).

12. El-Ali, J., Sorger, P. K. & Jensen, K. F. Cells on chips. *Nature* **442,** 403–411 (2006).

13. Ebrahimkhani, M. R., Young, C. L., Lauffenburger, D. A., Griffith, L. G. & Borenstein, J. T. Approaches to in vitro tissue regeneration with application for human disease

modeling and drug development. *Drug Discov. Today* **19,** 754–762 (2014).

14. Marx, U. *et al.* Biology-inspired microphysiological system approaches to solve the prediction dilemma of substance testing. *ALTEX* **33,** 272–321 (2016).

15. Rebelo, S. P. *et al.* Validation of Bioreactor and Human-on-a-Chip Devices for Chemical Safety Assessment. *Adv. Exp. Med. Biol.* **856,** 299–316 (2016).

16. Sung, J. H. *et al.* Using physiologically-based pharmacokinetic-guided "body-on-a-chip" systems to predict mammalian response to drug and chemical exposure. *Exp. Biol. Med.* **239,** 1225–1239 (2014).

17. Frisk, T., Rydholm, S., Andersson, H., Stemme, G. & Brismar, H. A concept for miniaturized 3-D cell culture using an extracellular matrix gel. *Electrophoresis* **26,** 4751–4758 (2005).

18. Kim, M. S., Yeon, J. H. & Park, J.-K. A microfluidic platform for 3-dimensional cell culture and cell-based assays. *Biomed. Microdevices* **9,** 25–34 (2007).

19. Tan, W. & Desai, T. A. Layer-by-layer microfluidics for biomimetic three-dimensional structures. *Biomaterials* **25,** 1355–1364 (2004).

20. Ryu, H. *et al.* Engineering a Blood Vessel Network Module for Body-on-a-Chip Applications. *J. Lab. Autom.* **20,** 296–301 (2015).

21. Yasotharan, S., Pinto, S., Sled, J. G., Bolz, S. S. & Günther, A. Artery-on-a-chip platform for automated, multimodal assessment of cerebral blood vessel structure and function. *Lab Chip* **15,** 2660–2669 (2015).

22. Duque-Afonso, J., Smith, K. S. & Cleary, M. L. Conditional expression of E2A-HLF induces bcell precursor death and myeloproliferative-like disease in knock-in mice. *PLoS One* **10,** 1–14 (2015).

23. Fischer, U. *et al.* Genomics and drug profiling of fatal TCF3-HLF-positive acute lymphoblastic leukemia identifies recurrent mutation patterns and therapeutic options. *Nat. Genet.* **47,** 1020–9 (2015).

24. Kim, J.-Y. *et al.* 3D spherical microtissues and microfluidic technology for multi-tissue experiments and analysis. *J. Biotechnol.* **205,** 24–35 (2015).

25. Kim, J.-Y., Fluri, D. A., Kelm, J. M., Hierlemann, A. & Frey, O. 96-Well Format-Based

Microfluidic Platform for Parallel Interconnection of Multiple Multicellular Spheroids. *J. Lab. Autom.* **20,** 274–282 (2015).

26. Lohasz, C., Frey, O., Renggli, K. & Hierlemann, A. A Tubing-Free, Microfluidic Platform for the Realization of Physiologically Relevant Dosing Curves on Cellular Models. *Proceedings* **1,** 497 (2017).

27. Schmitz, M. *et al.* Xenografts of highly resistant leukemia recapitulate the clonal composition of the leukemogenic compartment. *Blood* **118,** 1854–1864 (2011).

28. Lecault, V. *et al.* High-throughput analysis of single hematopoietic stem cell proliferation in microfluidic cell culture arrays. *Nat. Methods* **8,** 581–586 (2011).

29. Perestrelo, A. R., Águas, A. C. P., Rainer, A. & Forte, G. Microfluidic organ/body-on-a-chip devices at the convergence of biology and microengineering. *Sensors (Switzerland)* **15,** 31142–31170 (2015).

30. Esch, E. W., Bahinski, A. & Huh, D. Organs-on-chips at the frontiers of drug discovery. *Nat. Rev. Drug Discov.* **14,** 248–260 (2015).

31. Nguyen, D. G. *et al.* Bioprinted 3D primary liver tissues allow assessment of organ-level response to clinical drug induced toxicity in vitro. *PLoS One* **11,** 1–17 (2016).

32. Bell, C. C. *et al.* Characterization of primary human hepatocyte spheroids as a model system for drug-induced liver injury, liver function and disease. *Sci. Rep.* **6,** 25187 (2016).

33. Huang, Z., Roy, P. & Waxman, D. J. Role of human liver microsomal CYP3A4 and CYP2B6 in catalyzing N-dechloroethylation of cyclophosphamide and ifosfamide. *Biochem. Pharmacol.* **59,** 961–972 (2000).

34. Borch, R. F. & Millard, J. A. The Mechanism of Activation of 4-Hydroxycyclophosphamide. *J. Med. Chem.* **30,** 427–431 (1987).

35. Tatosian, D. A. & Shuler, M. L. A novel system for evaluation of drug mixtures for potential efficacy in treating multidrug resistant cancers. *Biotechnol. Bioeng.* **103,** 187–198 (2009).

36. Sung, J. H., Kam, C. & Shuler, M. L. A microfluidic device for a pharmacokinetic – pharmacodynamic (PK – PD) model on a chip †. *Lab Chip* **10,** (2010).

37. Schmid, Y. R. F., Bürgel, S. C., Misun, P. M., Hierlemann, A. & Frey, O. Electrical Impedance Spectroscopy for Microtissue Spheroid Analysis in Hanging-Drop Networks. *ACS Sensors* **1,** 1028–1035 (2016).

38. Meer, B. J. Van *et al.* Biochemical and Biophysical Research Communications Small molecule absorption by PDMS in the context of drug response bioassays. *Biochem. Biophys. Res. Commun.* **482,** 323–328 (2017).

39. van Midwoud, P. M., Janse, A., Merema, M. T., Groothuis, G. M. M. & Verpoorte, E. Comparison of Biocompatibility and Adsorption Properties of Different Plastics for Advanced Microfluidic Cell and Tissue Culture Models. *Anal. Chem.* **84,** 3938–3944 (2012).

This page is intentionally left blank.

4 Conclusion and outlook

4.1 Conclusion

In conclusion, this thesis presents novel strategies for studying how small populations of cells and tissues communicate with one another. Two different types of microfluidic devices were developed in order to (1) understand how immune cells respond to dynamic stimuli, and (2) predict the susceptibility of patient derived leukemia cells to prodrugs.

4.1.1 Cytokine secretion chip

The first half of this thesis focused on the creation of an integrated microfluidic chip with the goal of exploring how immune cells respond to dynamic inputs. Coordinating the dynamics of cytokines released and received by immune cells is essential for understanding the immune system. For instance, a single activated macrophage can transmit a wave of the transcription factor NF-κB activity across a population of cells through cytokine TNF secretion[1]. Moreover, exposing a population of cells to oscillating levels of TNF was found to entrain the cells and increase the robustness of gene transcription[2].

The secretion device, described in chapter 2, was the first published microfluidic device with immunoassay patterning, cell culture, and secretion quantification all automated inside the same chip. This is an impressive achievement, considering that some of the chemicals used in standard immunoassays, such as the detergent mixture PBS Tween, are toxic to cell cultures. The integration of immunoassay patterning, cell culture, and immunoassay quantification all in the same device simplified the immunoassay protocol compared to alternative nanowell-based platforms[3–5]. Using the developed chip, it was possible to run fully automated assays over several days. Through the newly developed cytokine secretion chip, we were able to expand on previous work[6] in order to study how small populations of cells respond to both, an acute and chronically increasing level of infection.

4.1.2 Leukemia-on-a-chip

In the second half of this thesis, a device to measure how patient-derived-xenograph (PDX) leukemia samples respond to prodrugs is described. The platform is able to culture up to 10 human liver microtissues, PDX samples, and a feeder cell line all within the same channel. Liver microtissues are cultured in a patent-pending cell trap, which keeps microtissues separated from PDX and feeder cells. Using this platform, it was possible to study the interaction of prodrugs with PDX leukemia samples. For the first time, a trend of decreased

viability of PDX cells in the presence of both, the prodrug cyclophosphamide and liver tissue was observed. Thus, the platform meets a large clinical need of an easy-to-use device that can measure the effect of prodrugs on PDX leukemia samples.

4.2 OUTLOOK

The major limitations of both, the cytokine secretion chip and leukemia-on-a-chip platforms are their limited throughput. Through increased throughput, the sample size of all experiments can be increased, and stronger statistical conclusions can be made from the platforms. In this thesis, proof-of-concept devices were created. In order to have clinical impact, it is essential that the throughput of the devices will be increased.

4.2.1 Improvements to the cytokine secretion chip

Increasing both, the throughput and multiplexing ability of the cytokine secretion chip is essential in order for the chip to have a clinical impact[6,7]. The current chip was designed to test just 16 cell populations for TNF secretion. In chimeric antigen receptor (CAR)-engineered T cell therapy, polyfunctional T cells are associated with treatment efficacy[8]. Current tests for CAR-T polyfunctionality include up to 42 different cytokines[8]. Further, given the high heterogeneity in the CAR-T cell population, it is important to characterize the cytokine dynamics from hundreds, if not even millions of cells in order to understand the true composition of the population. Clearly, with the increasing investment into CAR-T cell therapy, it is becoming more important to better characterize immune cell dynamics[8,9].

4.2.1.1 Increased temporal resolution

A future goal is to increase the temporal resolution of the on-chip immunoassay. A quicker immunoassay could reduce the time and amount of resources needed to run each experiment. A quicker immunoassay will be achieved through an incubation pump that flows a cytokine-filled solution over antibody coated beads. This results in a convection-dominated system with a minimized depletion region[10]. In this example, a depletion zone is the area around the antibody-coated bead that has a lower cytokine concentration because of cytokine binding to the bead[10]. In future iterations of the project, commercial bead assays will be used in order to save time in optimizing the on-chip immunoassay. The volume of cell- and immunoassay-incubation chambers will be tuned to ensure that the cytokine production of single cells is within the detection range of the bead assay. Specifically, Luminex xMAP beads will be used for the immunoassays. xMAP beads are surface-functionalized 5.6-µm-diameter beads. The beads can be either purchased, pre-coated with an antibody, or functionalized using a standard

Luminex protocol. The beads can be multiplexed with up to 500 different surface proteins. Multiplexing is possible through a unique intensity profile of two dyes for each type of bead. For instance, a bead, coated with an anti-TNF antibody, would have a different intensity profile than a bead, coated with an anti-IL-6 antibody.

4.2.1.2 Increased number of cells measured

In order to increase the throughput of the cell secretion chip, an option would be to use a bead-based immunoassay that relies on diffusion from the cell to the bead chamber in order to measure cytokine secretion. As this chip would have lower time resolution, pumping would no longer be necessary to speed up the immunoassay protocol. Moreover, as diffusion time scales at x^2/D where D is the diffusion constant ($D \sim 10\ \mu m^2/s$ for a protein) and x is the length scale ($x \sim 150\ \mu m$), equilibrium of cytokines in the immunoassay chamber would be reached in about 38 minutes. Diffusion-based immunoassays are frequently used in microfluidic systems[3–5,11–14]. There are chips that can culture cells and measure cytokine secretion from single cells, but these devices lack automation and the ability to expose cells to a dynamic input[3,11,12,15].

4.2.1.3 Increased number of cell types cultured

A new deep-well cell chamber could further be used to culture both, suspension and adherent cells. This is essential for studying how suspended T cells interact with a mixed suspension and adherent dendritic cell line. The deep-well cell chambers were found to be beneficial to cell health by decreasing the shear stress from the flow of media over the cells to a gentle diffusion-based media transfer[16].

4.2.2 Leukemia-on-a-chip

Using patient-derived xenografts of the University Children Hospital Zürich, we have access to over 200 patient genotypes. By culturing circulating PDX ALL cells in a multi-tissue setup with liver microtissues, we will be able to investigate efficacy and toxicology of therapies simultaneously, and to model bioactivation experiments with prodrugs. The long-term goal is to establish a technology pipeline to recognize ALL clinical forms of individual patients and to possibly predict disease evolution and therapy outcome. What is key to implementing the leukemia-on-a-chip platform in a clinical setting is (1) increasing the temporal resolution of the platform, in order to decrease the experiment time and resources used, and (2) increasing the number of samples that can be tested in each experiment, in order to test more drugs at various concentrations to identify the ideal regimen for each patient.

4.2.2.1 Increased temporal resolution

The temporal resolution of the leukemia-on-a-chip device can be increased by replacing its once-per-day flow cytometry readout with a real-time electrical impedance spectroscopy (EIS) readout. The channels of the platform need to be coated with biolipidure[17,18] in order to render the surface non-stick, so that ALL PDX cells can be cultured in suspension. EIS will allow for real-time monitoring of the circulating ALL cells. High-frequency EIS will provide dielectric parameters, such as internal and membrane (tegument) conductivity and dielectric constant, which are expected to change upon death of the ALL cells. To accomplish this, microtissue wells will be arrayed on a glass slide and combined with electrodes for EIS readout (Fig. 1). The chip will rely on the current concept of the tilting the platform to move the ALL-cells across the measuring electrodes. When a circulating cell passes over the electrodes, an impedance recording will be performed. By adding EIS to the leukemia-on-a-chip platform, real-time quantification of the effect of drugs on PDX ALL viability should be possible.

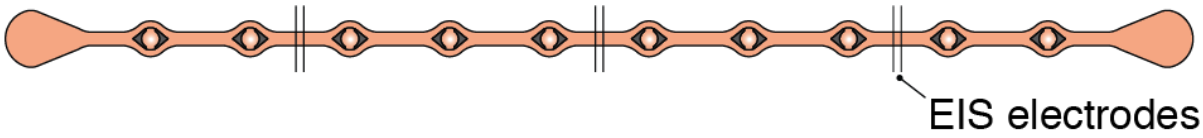

Figure 5: *Possible design of a new leukemia-on-a-chip platform with integrated electrical impedance spectroscopy (EIS) sensors.*

4.2.2.2 Increase number of samples measured

The number of samples, measured in the leukemia chip, can be increased simply by decreasing the size of each leukemia-on-a-chip unit. The overall volume of the chip can be reduced from 400 µL per chip to 50 µL per chip while maintaining the same liver microtissue size, and volume ratio for each cell component. The limiting factor in reducing chip size is the volume needed to culture liver microtissues. Each liver microtissue is roughly 250 µm in diameter and requires 50 µL media. A solution to further decrease the size of each device is to reduce the number of cells in each liver microtissue, thereby decreasing the diameter of the microtissues. By decreasing the size of each device, more chips can be cultured on the tilting device, thus resulting in more samples per experiment.

4.3 REFERENCES

1. Frank, T. & Tay, S. Automated co-culture system for spatiotemporal analysis of cell-to-cell communication. *Lab Chip* **15,** 2192–2200 (2015).

2. Kellogg, R. A. & Tay, S. Noise facilitates transcriptional control under dynamic inputs. *Cell* **160,** 381–392 (2015).

3. Han, Q., Bradshaw, E. M., Hafler, A. & Love, J. C. Multidimensional analysis of the frequencies and rates of cytokine secretion from single cells by quantitative microengraving. *Lab Chip* **10,** 1391–1400 (2010).

4. Han, Q. *et al.* Polyfunctional responses by human T cells result from sequential release of cytokines. *PNAS* **109,** 1607–1612 (2011).

5. Xue, Q. *et al.* Analysis of single-cell cytokine secretion reveals a role for paracrine signaling in coordinating macrophage responses to TLR4 stimulation. *Sci. Signal.* **8,** ra59-ra59 (2015).

6. Junkin, M. *et al.* High-Content Quantification of Single-Cell Immune Dynamics. *Cell Rep.* **15,** (2016).

7. Kaestli, A. J., Junkin, M. & Tay, S. Integrated platform for cell culture and dynamic quantification of cell secretion. *Lab Chip* 4124–4133 (2017). doi:10.1039/C7LC00839B

8. Xue, Q. *et al.* Single-cell multiplexed cytokine profiling of CD19 CAR-T cells reveals a diverse landscape of polyfunctional antigen- specific response. 1–16 (2017). doi:10.1186/s40425-017-0293-7

9. Cho, J. H. *et al.* Universal Chimeric Antigen Receptors for Multiplexed and Logical Control of T Cell Responses Article Universal Chimeric Antigen Receptors for Multiplexed and Logical Control of T Cell Responses. *Cell* **173,** 1426–1431.e11 (2018).

10. Squires, T. M., Messinger, R. J. & Manalis, S. R. Making it stick : convection , reaction and diffusion in surface-based biosensors. **26,** 417–426 (2008).

11. Fan, R. *et al.* Integrated barcode chips for rapid , multiplexed analysis of proteins in microliter quantities of blood. **26,** 1373–1378 (2008).

12. Ma, C. *et al.* Technical Reports A clinical microchip for evaluation of single immune cells reveals high functional heterogeneity in phenotypically similar T cells. *Nat. Med.* **17,** 738–743 (2011).

13. Garcia-cordero, J. L., Nembrini, C., Stano, A., Hubbell, J. A. & Maerkl, S. J. Interdisciplinary approaches for molecular and cellular life sciences. *Integr. Biol.* **5,** 650–658 (2013).

14. Garcia-cordero, J. L. & Maerkl, S. J. A 1024-sample serum analyzer chip for cancer diagnostics. *Lab Chip* 2642–2650 (2014). doi:10.1039/c3lc51153g

15. Lu, Y. *et al.* Highly multiplexed profiling of single-cell effector functions reveals deep functional heterogeneity in response to pathogenic ligands. *PNAS* **112,** 607–615 (2015).

16. Zhang, C. *et al.* Universal Microfluidic System for Analysis and Control of Cell Dynamics. *bioRxiv* (2017).

17. Kim, J.-Y. *et al.* 3D spherical microtissues and microfluidic technology for multi-tissue experiments and analysis. *J. Biotechnol.* **205,** 24–35 (2015).

18. Kim, J.-Y., Fluri, D. A., Kelm, J. M., Hierlemann, A. & Frey, O. 96-Well Format-Based Microfluidic Platform for Parallel Interconnection of Multiple Multicellular Spheroids. *J. Lab. Autom.* **20,** 274–282 (2015).